CAPITAL UNIVERSITY OF SCIENCE AND TECHNOLOGY, ISLAMABAD

The Enhanced Thermal Performance of Prandtl-Eyring Nanofluid under the Effect of Motile Microorganism

by

Mutayba Rafique

A thesis submitted in partial fulfillment for the degree of Master of Philosophy

in the

Faculty of Computing
Department of Mathematics

2023

This thesis is dedicated to my family, teachers and friends.

CERTIFICATE OF APPROVAL

The Enhanced Thermal Performance of Prandtl-Eyring Nanofluid under the Effect of Motile Microorganism

by

Mutayba Rafique

(MMT203022)

THESIS EXAMINING COMMITTEE

S. No.	Examiner	Name	Organization
(a)	External Examiner	Dr. Tanvir Akbar	COMSATS, Islamabad
(b)	Internal Examiner	Dr. Muhammad Sabeel Khan	CUST, Islamabad
(c)	Supervisor	Dr. Dur-e-Shehwar Sagheer	CUST, Islamabad

Dr. Dur-e-Shehwar Sagheer
Thesis Supervisor
February, 2023

Dr. Muhammad Sagheer
Head
Dept. of Mathematics
February, 2023

Dr. Muhammad Abdul Qadir
Dean
Faculty of Computing
February, 2023

Author's Declaration

I, **Mutayba Rafique** hereby state that my MPhil thesis titled "**The Enhanced Thermal Performance of Prandtl-Eyring Hybrid Nanofluid under the Effect of Motile Microorganism**" is my own work and has not been submitted previously by me for taking any degree from Capital University of Science and Technology, Islamabad or anywhere else in the country/abroad.

At any time if my statement is found to be incorrect even after my graduation, the University has the right to withdraw my MPhil Degree.

(Mutayba Rafique)

Registration No: MMT203022

Plagiarism Undertaking

I solemnly declare that research work presented in this thesis titled "**The Enhanced Thermal Performance of Prandtl-Eyring Hybrid Nanofluid under the Effect of Motile Microorganism**" is solely my research work with no significant contribution from any other person. Small contribution/help wherever taken has been duly acknowledged and that complete thesis has been written by me.

I understand the zero tolerance policy of the HEC and Capital University of Science and Technology towards plagiarism. Therefore, I as an author of the above titled thesis declare that no portion of my thesis has been plagiarized and any material used as reference is properly referred/cited.

I undertake that if I am found guilty of any formal plagiarism in the above titled thesis even after award of MPhil Degree, the University reserves the right to withdraw/revoke my MPhil degree and that HEC and the University have the right to publish my name on the HEC/University website on which names of students are placed who submitted plagiarized work.

(Mutayba Rafique)

Registration No: MMT203022

Acknowledgement

I would like to acknowledge **Allah Almighty**, the creator of all things, for providing me with the strength and knowledge to finish this thesis. I would like to thank my supervisor **Dr. Dur-e-Shehwar Sagheer** for her time and guidance during my thesis research. She has been a great helper in reviewing my thesis and giving me valueable feedback. She is always available for the questions i have and she takes the time to explain things thoroughly. I would like to express my gratitude towards my MPhil coursework teachers, **Dr. Muhammad Sagheer, Dr. Rashid Ali, Dr. Shafqat Hussain** and **Dr. Samina Rashid** for their support and guidance. Thankyou to my parents for their incredible support that i have received throughout my life. I would like to thanks my friends for their assistance in my thesis, specially **Rimsha Shehzad** for her support throughout the years.

(Mutayba Rafique)

Abstract

This thesis investigates heat and mass transfer, bio-convection and entropy generation in Prandtl-Eyring hybrid nanofluids (P-EHNF). The flow and thermal transport properties of P-EHNF are examined using a slippery heated surface. In this research, the effects of porous materials, Cattaneo-Christov heat flow, radiative flux, chemical reaction, bio-convection lewis number, brownian motion and thermophoresis have also been investigated. This study investigated single-walled carbon nanotubes (SWCNT) and multi-walled carbon nanotubes (MWCNT) utilizing engine oil (EO) as a base fluid. The PDEs have been converted into ordinary differential equations (ODEs), and then solved using the shooting method. Graphical representation of the flow depicts the temperature, concentration, motile microorganism, and entropy profiles. Variation in drag force and Nusselt number for various dimensionless parameters are shown in tables. It is notable that there is continuously larger rise in temperature when comparing the heat transfer rate of P-EHNF (MWCNT-SWCNT/EO) to nanofluid (SWCNT-EO). As the size of the nanoparticles rises, the entropy of the model increases.

Contents

List of Figures

List of Tables

Abbreviations

CCHFM	Cattaneo Christov Heat Flux Model
EO	Engine Oil
HMC	Hybrid Mixed Convection
HNF	Hybrid Nanofluid
MWCNT	Multi Walled Carbon Nanotubes
MHD	Magnetohydrodynamics
NF	Nanofluid
ODEs	Ordinary Differential Equations
PDEs	Partial Differential Equations
P-EHNF	Prandtl-Eyring Hybrid Nanofluid
P-E	Prandtl-Eyring
RK-4	Runge Kutta Four
SWCNT	Single Walled Carbon Nanotubes

Symbols

A_1^*	Prandtl–Eyring Parameter-I
A_2^*	Prandtl–Eyring Parameter-II
b	Initial Stretching Rate
B_ς	Brinkman Number
H_ς	Biot Number
K_ς	Porous Media Parameter
N_ς	Radiation Parameter
C_f	Drag Force
C_p	Specific Heat Capacity
E_G	Dimensional Entropy
N_G	Dimensionless Entropy Generation
U_w	The Velocity of the Stretching Sheet
S	Suction/Injection Parameter
k_s	Thermal Conductivity of the Surface
E_ς	Eckert Number
P_ς	Prandtl Number
R_e	Reynolds Number
η	Dimensionless Temperature Gradient
V_ς	Vertical Velocity
ϕ	Volume Fraction of the Particles
ρ	Density
ϵ_ς	Relaxation Time
A_ς	Velocity Slip Parameter

h_ς	Heat Transfer Coefficient
k^*	Obsorption Coefficient
k	Thermal Conductivity
N_u	Nusselt Number
q_r	Radiative heat flux
σ^*	Stefan-Boltzman Constant
B_1, B_2	Velocity Components in x, y direction
x, y	Dimensional Space Coordinates
ψ	Stream Function
m	Solid Particle Shape
$\mathcal{T}$	Dimensional Temperature
θ	Dimensionless Temperature
Ω	Independent Similarity Variable
μ	Dynamic Viscosity of the Fluid
ν	Kinematic Viscosity of the Fluid
N_b	Brownian Motion Parameter
N_t	Parameter of Thermophoresis
$\mathcal{L}_e$	Lewis Number
γ	Chemical Reaction Parameter
$\mathcal{L}_b$	Bioconvection Lewis Number
ω	Bioconvection Constant
P_e	Peclet Number
C	Dimensional Concentration
Φ	Dimensionless Concentration
N	Dimensional Motile Microorganism
χ	Dimensionless Motile Microorganism

Chapter 1

Introduction

Fluid mechanics is the branch of physics which studies the forces acting on and within fluids (liquids, gases, and plasmas). There are numerous uses of fluid mechanics in astrophysics, mechanical and chemical engineering, and biological systems. It is an exciting branch of physics that deals with the motion of gases and liquids as well as how they interact with their environment. The principles of fluid mechanics, can be used to comprehend the motion of fish in water and the flight of birds in the air. Such knowledge aids in the design of ships and airplanes. The equations of fluid mechanics can also be used to explain how thunderstorms and hurricanes form.

A thin layer of fluid in adjacent with the surface of pipes and wings of an aircraft defines the limits of liquid mechanics. Shear forces in the boundary layer might harm the liquid. The values of speed exists within the maximum and zero boundary layer speeds because the fluid is in contact with the surface. Prandtl introduced the idea of boundary layers in 1904 to explain how viscous fluid behaves near solid boundries for details one can see [1] by Aziz et al. Prandtl presented the idea of boundary layer in high Reynolds number flows and developed the boundary layer equations by simplifying the Navier Stokes equations to produce approximate solutions. Prandtl's boundary layer equations appear in a variety of physical designs of fluid mechanics. Hussain et al. [2] found that the convective heat transfer has been thicken the thermal boundary layer as a Casson fluid moves in the direction of the expanding porous wedge. The literature contains several studies examining the effects of different physical parameters on boundary layer flow [3, 4] with a variety of liquids. [5, 6].

Many scientists are currently interested in hybrid nanofluid. Hybrid nanofluids are made of two different kinds of nanoparticles combined into one fluid. The hybrid nanofluid's thermal characteristics are superior than those of the main liquid and nanofluids. Hybrid nanofluids are frequently used in solar systems, auto's, and lubricant in machining and production. Suresh et al. [7], presented that copper nanoparticles when mixed at sufficient level with alumina matrix will preserve the strength of the hybrid nanofluids. Alumina nanoparticles have excellent thermal stability and inactivity, while copper nanoparticles have higher thermal conductivity than alumina nano particles.

For the performance of heat transmission in hybrid-nanofluid, Yildiz et al. [8] proposed that the theoretical and experimental results are equivalent for thermal conductivity models. The hybridization of nanoparticles at a lower particle percentage enhanced heat transport than a mono nanofluid. Waini et al. [9] investigated unsteady flow and heat transfer of a hybrid nanofluid in a curved surface. With the change in curve, the involvement of dual solutions increased the volume ratio of Cu nanoparticles. Qureshi et al. [10] depicts the properties of the HMC nanofluid by using a straight obstacle channel. According to their research, expanding the radius of barrier can enhance heat transmission up to 11.9%. Mabood and Akinshilo [11] examined the stability of flowing viscous hybrid nanofluid on a stretching surface under radiation and uniform magnetic effect.

The CCHFM explains the transfer of heat in visco-elastic flows induced by an exponentially stretching sheet. Cattaneo proposed a successful modification to Fourier's model by introducing a important feature of thermal relaxation time. The boundaries of this model may be related to the thermal relaxation time. Dogonchi and Ganji [12] used a CCHFM to study unstable compressing MHD nanofluid flow through parallel plates. They discovered that the thermal relaxation parameter reduced heat transfer process. Muhammad et al. [13] found that fluid temperature decreased as thermal relaxation increased. The Cattaneo-Christov heat flux model has been used by other researchers to analyze flow of fluid and classify the physical aspects that are effected by thermal relaxation. Waqas et al. [14] introduced mathematical modeling for hybrid type nanofluid flow in a rocket engine using the Cattaneo-Christov model. The discovery demonstrated that when thermal relaxation and melting parameters vary, the temperature decreases while the Biot number rises.

It was also necessary to conduct research to identify the non-Newtonian aspect of hybrid nanofluids. Yan et al. [15] investigated the rheological behavior of a powered pump using a non-Newtonian hybrid nanofluid. They stated that the viscosity decreased to less than 21% at the highest volume fraction of hybrid nanofluid. Numerous studies have been done for various non-Newtonian hybrid nanofluids, including MWCNT-Al2O3/5W50 by Esfe et al. [16], and aluminum alloy nanoparticles by Madhukesh et al. [17]. Despite this, there aren't many studies looking into the behavior of viscoelastic hybrid nanofluids. The power-law, the Prandtl fluid, and the P-E are some of the models that can be used to analyze the physical characteristics of the viscoelastic fluid. The non-linear relationship between shear stress and deformation rate is indicated by the power-law model. It has been proposed that shear stress is related to the sine inverse function of the rate of deformation by the Prandtl model and to the hyperbolic sine function of deformation rate by the P-E model.

Hussain et al. [18] examined the physical aspects of MHD Prandtl-Eyring fluid flow and reported that in the flow domain when fluid parameter rised at all positions then significant increase in momentum transportation has been seen. The entropy of the P-E fluid flow model on a rotating cone has been investigated by Li et al. [19] which demonstrates that when the viscosity parameter is increased in magnitude, the behavior of the velocity and temperature changes.

Sahoo [20], investigated that a thermo-hydraulic performance of ternary hybrid nanofluid is significantly influenced by the particle shapes. Meanwhile Rashid et al. [21] have discovered that sphere shaped nanoparticles have more temperature disturbance and heat transfer than the other shapes.

Several studies have been conducted to investigate the effect of porosity materials, viscid dissipative flow, Cattaneo-Christov heat flow, and thermal radiative flow. However, the impact of shape of nanoparticles is still to be addressed. To fill this space, the interest of present study is on the impacts of solid properties of liquid and the choas in the boundary layer using the shooting method.

Shah et al. [22] studied the heat transfer characteristics of a magnetohydrodynamic Prandtl hybrid nanofluid over a stretched surface with the addition of bioconvection and chemical reaction effects. Getting inspiration from this research, in the present research, heat transfer properties of P-EHNF over a stretched surface in presence of bio-convection are discussed. Additionally it is checked how the Lewis number, chemical reaction parameter, Brownian motion, and thermophoresis affect concentration in mono and hybrid nanofluid flow, and determine motile affected by bio-convection Lewis number, and peclet number.

1.1 Thesis Contributions

In this thesis, a detailed review of article [23] by Jamshed et al. is presented. It is observed that no study on Prandtl-Eyring hybrid nanofluid with Cattaneo-Christov heat flux model and bio-convection has yet been done. The aim of this research is to further extend [23] by discussing the mass transfer. For this purpose concentration and motile microorganism equations are added to the previous flow problem. Tables and graphs have been used to discuss the effects of different physical parameters that are relevant.

1.2 Layout of the Thesis

A brief overview of contents of the thesis is provided below.

Chapter 2 includes some fundamental terminologies and definitions that are essential for understanding the concepts discussed later.

Chapter 3 discuss in detail the thermal efficiency of Prandtl-Eyring hybrid nanofluid.

It contains a detailed review of [23]. Numerical technique shooting method is used to obtain the solutions.

Chapter 4 extends the proposed model flow discussed in Chapter 3 by including the concentration and motile equation. PDEs have been transformed into ODEs using the similarity transformations and then solved by shooting method. This new model discuss the bio-convection and mass transfer. The aim of this whole research is to increase the heat transfer.

Chapter 5 provides the thesis concluding remarks.

References used in this thesis are mentioned in **Biblography**.

Chapter 2

Preliminaries

Fluid dynamics is the sub-branch of fluid mechanics that deals with fluid in motion. This chapter contains some basic definitions and governing laws, which are helpful in the study of our main problem.

2.1 Some Basic Terminologies

This section addresses some important properties of fluids.

Definition 2.1.1. (**Fluid**)

"A substance exists in three primary phases: solid, liquid, and gas. (At very high temperatures, it also exists as plasma.) A substance in the liquid or gas phase is referred to as a fluid. Distinction between a solid and a fluid is made on the basis of the substances ability to resist an applied shear (or tangential) stress that tends to change its shape. A solid can resist an applied shear stress by deforming, whereas a fluid deforms continuously under the influence of shear stress, no matter how small. In solids stress is proportional to strain, but in fluids stress is proportional to strain rate. When a constant shear force is applied, a solid eventually stops deforming, at some fixed strain angle, whereas a fluid never stops deforming and approaches a certain rate of strain." [24]

Definition 2.1.2. (**Fluid Mechanics**)

"The fluid mechanics is defined as the science that deals with the behavior of fluids at rest or in motion, and the interaction of fluids with solids or other fluids at the boundaries." [24]

Definition 2.1.3. (**Fluid Dynamics**)

"The study of fluid if the pressure forces are considered for the fluids in motion, is called fluid dynamics." [25]

Definition 2.1.4. (**Fluid Statics**)

"The study of fluid at rest is called fluid statics." [25]

Definition 2.1.5. (**Viscosity**)

"Viscosity is defined as the property of a fluid which offers resistance to the movement of one layer of fluid over another adjacent layer of the fluid. Mathematically,

$$\mu = \frac{\tau}{\frac{\partial u}{\partial y}},$$

where μ is viscosity coefficient, τ is shear stress and $\frac{\partial u}{\partial y}$ represents the velocity gradient." [25]

The SI units of viscosity is $kgm^{-1}s^{-1}$.

Definition 2.1.6. (**Density**)

"Density is defined as the mass per unit volume. that is,

$$\rho = \frac{m}{V}$$

where m and V are the mass and volume of the substance, respectively."[25]

The SI units of density is $\frac{kg}{m^3}$.

Definition 2.1.7. (**Kinematic Viscosity**)

"It is defined as the ratio between the dynamic viscosity and density of fluid. It is denoted by symbol ν called **'nu'**. Mathematically,

$$\nu = \frac{\mu}{\rho}.\text{''} \qquad [25]$$

The SI units of kinematic viscosity is m^2s^{-1}.

Definition 2.1.8. (**Nanofluid**)

"Nanofluids are engineered by suspending nanoparticles with average size below 100 nm in traditional heat transfer fluids such as water, oil, and ethylene glycol. A very small amount of guest nanoparticles, when dispersed uniformly and suspended stably in host fluids, can provide dramatic improvements in the thermal properties of host fluids." [26]

Definition 2.1.9. (**Hybrid Nanofluid**)

"Hybrid nanofluid is a very new type of nanofluids that contains two or more various nanoparticles. The use of hybrid nanofluids is aimed at simultaneously using the physical and chemical properoties of two or more different types of nanoparticles, for improving the base fluid properties." [27]

Definition 2.1.10. (**Hydrodynamics**)

"The study of the motion of fluids that are practically incompressible such as liquids, especially water and gases at low speeds is usually referred to as hydrodynamics." [28]

Definition 2.1.11. (**Magnetohydrodynamics**)

"Magnetohydrodynamics (MHD) is concerned with the flow of electrically conductoing fluids in the presence of magnetic fields, either externally applied or generated within the fluid by inductive action." [28]

Definition 2.1.12. (**Boundary Layer**)

"Viscous effects are particularly important near the solid surfaces, where the strong interaction of the molecules of the fluid with molecules of the solid causes the relative velocity between the fluid and the solid to become almost exactly zero for a stationary surface. Therefore, the fluid velocity in the region near the wall must reduce to zero. This is called no slip condition. In that condition there is no relative motion between the fluid and the solid surface at their point of contact. It follows that the flow velocity varies with distance from the wall; from zero at the wall to its full value at some distance away, so that significant velocity gradients are established close to the wall. In most cases this region is thin (compared to the typical body dimension), and it is called a boundary layer." [29]

Definition 2.1.13. (**Prandtl–Eyring Nanoliquid**)

"Prandtl–Eyring nanoliquid is nonlinear and mixed convection flow of nanofluid with activation energy. So in literature, there are many fluid models that are suggested for non-Newtonian fluid. Prandtl-Eyring fluid (PEF) model is also one of them." [30]

2.2 Types of Flow

Some important types of flow are discussed in this section:

Definition 2.2.1. (**Rotational Flow**)

"Rotational flow is that type of flow in which the fluid particles while flowing along stream-lines, also rotate about their own axis." [25]

Definition 2.2.2. (**Irrotational Flow**)

"Irrotational flow is that type of flow in which the fluid particles while flowing along stream-lines, do not rotate about their own axis then this type of flow is called irrotational flow." [25]

Definition 2.2.3. (**Compressible Flow**)

"Compressible flow is that type of flow in which the density of the fluid changes from point to point or in other words the density (ρ) is not constant for the fluid, Mathematically,

$$\rho \neq k,$$

where k is constant."

For example, air is compressible, which means that you can compress the air and add a little bit more air. [25]

Definition 2.2.4. (**Incompressible Flow**)

"Incompressible flow is that type of flow in which the density is constant for the fluid flow. Liquids are generally incompressible while gases are compressible, Mathematically,

$$\rho = k,$$

where k is constant."

For example, cup of water can be put into a differently shaped cup-sized container, but we would not be able to squeeze that whole cup of water into half cup-sized container. [25]

Definition 2.2.5. (**Steady Flow**)

"Steady flow is defined as that type of flow in which the fluid characteristics like velocity, pressure, density, etc., at a point do not change with time. Thus for steady flow, Mathematically, we have

$$\frac{\partial Q}{\partial t} = 0,$$

where Q is any fluid property." [25]

Definition 2.2.6. (**Unsteady Flow**)

"Unsteady flow is defined as that type of flow in which the fluid characteristics like velocity, pressure, density, etc., at a point do change with time. Thus for Unsteady flow, Mathematically, we have,

$$\frac{\partial Q}{\partial t} \neq 0,$$

where Q is any fluid property." [25]

Definition 2.2.7. (**Laminar Flow**)

"Laminar flow is defined as that type of flow in which the fluid particles move along well-defined paths or stream lines and all the stream-lines are straight and parallel." [25]

Definition 2.2.8. (**Turbulent Flow**)

"Turbulent flow is that type of flow in which the fluid particles move in a zig-zag way." [25]

2.3 Types of Fluid

The fluids are classified into the following types:

Definition 2.3.1. (**Ideal Fluid**)

"A fluid, which is incompressible and has no viscosity, is known as an ideal fluid. Ideal fluid is only an imaginary fluid as all the fluids, which exist, have some viscosity." [25]

Definition 2.3.2. (**Real Fluid**)

"A fluid, which possesses viscosity, is known as a real fluid. In actual practice, all the fluids are real fluids." Examples are water, diesel and honey. [25]

Definition 2.3.3. (**Newtonian Fluid**)

"A real fluid, in which the shear stress is directly proportional to the rate of shear strain (or velocity gradient), is known as a Newtonian fluid."
Examples are water, oil and alcohol. [25]

Definition 2.3.4. (**Non-Newtonian Fluid**)

"A real fluid in which the shear stress is not directly proportional to the rate of shear strain (or velocity gradient), is known as a non-Newtonian fluid."
Some examples of non-Newtonian fluids are paint, shampoo, and mayonnaise etc. [25]

Definition 2.3.5. (**Ideal Plastic Fluid**)

"A fluid, in which shear stress is more than the yield value and shear stress is proportion to the rate of shear strain (or velocity gradient), is known as ideal plastic fluid."
Examples are blood and saliva. [25]

2.4 Modes of Heat Transfer and Mass Transfer

Heat transfer is the phenomenon of transferring energy and entropy from one place to another. The formal definition of heat transfer and its different types are given below.

Definition 2.4.1. (**Heat Transfer**)
"Heat transfer is a branch of engineering that deals with the transfer of thermal energy from one point to another within a medium or from one medium to another due to the occurrence of a temperature difference. Heat transfer may take place in one or more of its three basic forms: conduction, convection, and radiation." [31]

Definition 2.4.2. (**Conduction**)
"The transfer of heat within a medium due to a diffusion process is called conduction. The Fourier heat conduction law states that the heat flow is proportional to the temperature gradient."
Examples are during the ironing process, heat is transferred from the iron to the fabric. Chocolate candy in a hand will eventually melt as heat is conducted from a hand to the chocolate. [31]

Definition 2.4.3. (**Convection**)
"Convection heat transfer is usually defined as energy transport effected by the motion of a fluid. The convection heat transfer between two dissimilar media is governed by Newton's law of cooling. It states that the heat flow is proportional to the difference of the temperatures of the two media. The proportionality coefficient is called the convection heat transfer coefficient."
Examples are heating water on the stove and air Conditioner. [31]

Definition 2.4.4. (**Thermal Radiation**)
"Thermal radiation is defined as radiant (electromagnetic) energy emitted by a medium and is solely to the temperature of the medium."
Examples are microwaves from an oven, X rays from an X-ray tube and ultraviolet light from the sun. [31]

Definition 2.4.5. (**Mass transfer**)

"Mass transfer is the flow of molecules from one body to another when these bodies are in contact or within a system consisting of two components when the distribution of materials is not uniform. When a copper plate is placed on a steel plate, some molecules from either side will diffuse into the other side. When salt is placed in a glass and water poured over it, after sufficient time the salt molecules will diffuse into the water body. A more common example is drying of clothes or the evaporation of water spilled on the floor when water molecules diffuse into the air surrounding it. Usually mass transfer takes place from a location where the particular component is proportionately high to a location where the component is proportionately low. Mass transfer may also take place due to potentials other than concentration difference.” [29]

2.5 Dimensionless Numbers

The following dimensionless numbers will appear in discussion given in the next chapters.

Definition 2.5.1. (**Eckert Number**)

“It expresses the ratio of kinetic energy to a thermal energy change. Mathematically, it can be written as

$$E_c = \frac{w_\infty^2}{C_p \delta T}$$

where w_∞ is fluid flow velocity far from body, C_p is the specific heat capacity of fluid and δT denote the temperature difference” [32]

Definition 2.5.2. (**Prandtl Number**)

“ The Prandtl number is the ratio of momentum to heat diffusivities. Mathematically, it can be defined as

$$Pr = \frac{\nu}{\alpha} = \frac{\frac{\mu}{\rho}}{\frac{k}{C_p \rho}} = \frac{\mu C_p}{k}$$

where μ represents the dynamic viscosity, C_p denotes the specific heat and k stands for thermal conductivity.” [33]

Definition 2.5.3. (**Skin Friction Coefficient**)

“The skin friction coefficient can be defined as

$$C_f = \frac{2\tau_w}{\rho w_\infty^2}$$

where τ_w denotes the wall shear stress, ρ is the density and the velocity of free fluid flow is denoted by w_∞." [32]

Definition 2.5.4. (**Nusselt Number**)

"It is a dimensionless number, first introduced by a German engineer Ernst Kraft Wilhelm Nusselt and Mathematically,

$$Nu = \frac{\alpha L}{k}$$

where α represents the heat transfer coefficient, L denotes the characteristic length and k is the thermal conductivity. It expresses the ratio of the total heat transfer in a system to the heat transfer by conduction." [32]

Definition 2.5.5. (**Biot Number**)

"This number expresses the ratio of the heat flow transferred by convection on a body surface to the heat flow transferred by conduction in a body. Mathematically

$$B_i = \alpha(2\pi f \lambda c Q)^{\frac{-1}{2}}$$

Where α is Heat transfer coeffient, f is frequency, c is specific heat capacity, Q is density and λ is thermal conductivity." [32]

Definition 2.5.6. (**Reynolds Number**)

"It is defined as the ratio of inertial forces ρU^2 to viscous forces $\mu U/L$. Mathematically,

$$Re = \frac{\rho U L}{\mu},$$

Here ρ denotes the density of the fluid, U the characteristic flow velocity, μ is the fluid viscosity, and L is a characteristic dimension of the flow region." [31]

Definition 2.5.7. (**Sherwood Number**)

"The Sherwood number was first introduced by an American chemical engineer, Thomas Kilgore Sherwood and is defined as,

$$Sh = \frac{BL}{D},$$

where B is the mass transfer coefficient, L denotes the characteristic length and D stands for molecular diffusivity. It expresses the ratio of the heat transfer to the molecular diffusion. It characterizes the mass transfer intensity at the interface of phases." [32]

2.6 Conservation Laws

Conservation laws such as conservation of mass, energy and momentum are of great importance for researchers. These laws apply to closed systems and extend to regions in space called controlled volumes. Here we briefly discuss the conservation laws.

Definition 2.6.1. (**Continuity Equation**)
"The principle of conservation of mass can be stated as the time rate of change of mass in a fixed volume is equal to the net rate of flow of mass across the surface. The mathematical statement of the principle results in the following equation, known as the continuity (of mass) equation

$$\frac{\partial \rho}{\partial t} + \nabla.(\rho \mathbf{v}) = 0,$$

where t is time , ρ is density of fluid and $\mathbf{v}$ is the fluid velocity., and ∇ is the nabla or del operator. By introducing the material derivative $\frac{D}{Dt}$.

$$\frac{D}{Dt} = \frac{\partial}{\partial t} + \mathbf{v}.\nabla,$$

the above continuity equation can be expressed in the alternate, non-conservation form

$$\frac{\partial \rho}{\partial t} + \mathbf{v}.\nabla \rho + \rho \nabla.\mathbf{v} = \frac{D\rho}{Dt} + \rho \nabla.\mathbf{v} = 0$$

For steady-state conditions, the continuity equation becomes

$$\nabla.(\rho \mathbf{v}),$$

when the density changes following a fluid particle are negligible, the continuum is termed incompressible and we have $\frac{D\rho}{Dt} = 0$.
The continuity equation then becomes

$$\nabla.\mathbf{v} = 0$$

which is often referred to as the incompressibility condition or incompressibility constraint." [31]

Definition 2.6.2. (**Momentum Equation**)

"The momentum equation states that the time rate of change of linear momentum of a given set of particles is equal to the vector sum of all the external forces acting on the particles of the set, provided Newton's third law of action and reaction governs the internal forces. Newton's second law can be written as:

$$\frac{\partial(\rho\mathbf{v})}{\partial t} + \nabla.[(\rho\mathbf{v}) \otimes \mathbf{v}] = \nabla.\mathbf{T} + \rho\mathbf{g},$$

where $\otimes$ is the tensor (or dyadic) product of two vectors, $\mathbf{g}$ is the body force vector, measured per unit mass and normally taken to be the gravity vector, $\mathbf{T}$ is the Cauchy stress tensor ($\frac{N}{m^2}$), ρ is density of fluid and $\mathbf{v}$ is the fluid velocity and ∇ is the nabla or del operator.

The form of momentum equation shown above is the conservation form that is most often utilised for compressible flows. This equation may be simplifed to a form more commonly used with incompressible flows. Expanding the first two derivatives and collecting terms

$$\rho\left(\frac{\partial\mathbf{v}}{\partial t} + \mathbf{v}\nabla.\mathbf{v}\right) + \mathbf{v}\left(\frac{\partial\rho}{\partial t} + \nabla.\rho\mathbf{v}\right) = \nabla.\mathbf{T} + \rho\mathbf{g},$$

The second term in the parentheses is continuity equation and neglecting this term allows to reduce to the non-conservation form

$$\rho\frac{D\mathbf{v}}{Dt} = \nabla.\mathbf{T} + \rho\mathbf{g}.\text{"} \ [31]$$

Definition 2.6.3. (**Energy Equation**)

"The law of conservation of energy(or the first law of thermodynamics) states that the time rate of change of the total energy is equal to the sum of the rate of work done by applied forces and change of heat content per unit time.

$$\frac{\partial \rho e}{\partial t} + \nabla . \rho \mathbf{v} \ e = -\nabla . \mathbf{q} + Q + \phi,$$

where ϕ is the dissipation function, e is the internal energy $\mathbf{q}$ is the heat flux vector and Q is internel heat generation." [31]

2.7 Shooting Method

Shooting technique is utilized to solve the boundary value problem arise from the main problem. Take the following nonlinear boundary value problem into consideration to further explain the shooting method.

$$\left.\begin{aligned} & f'''(\eta) = (-1/2) f(\eta) f''(\eta) \\ & f(0) = 0, f'(0) = 0 \qquad f'(\eta) = 1. \end{aligned}\right\} \tag{2.1}$$

Introduce the following notations, to reduce the order of above boundary value problem.

$$f = Y_1 \qquad f' = Y_1' = Y_2 \qquad f'' = Y_2' = Y_3 \qquad f''' = Y_3'. \tag{2.2}$$

As a result, (2.1) is converted into the following system of first order ODEs.

$$Y_1' = Y_2, \qquad Y_1(0) = 0, \tag{2.3}$$

$$Y_2' = Y_3, \qquad Y_2(0) = 0, \tag{2.4}$$

$$Y_3' = (-1/2) Y_1 Y_3 \qquad Y_3(0) = w, \tag{2.5}$$

where w is a guess for the missing initial condition.

The RK-4 approach will be used to numerically solve the above IVP. Choose the missing condition w in such a way that.

$$Y_2(\eta, w) = 1. \tag{2.6}$$

For convenience, now onward $Y_2(\eta, w)$ will be denoted by $Y_2(w)$.
Let us further denote $Y_2(w) - 1$ by $H(w)$, so that

$$H(w) = 0. \tag{2.7}$$

The above equation can be solved by using Newton's method with the following iterative formula.

$$w^{n+1} = w^n - \frac{H(w^n)}{\frac{\partial H(w^n)}{\partial w}}, \qquad n = 0, 1, 2, 3...$$

or

$$w^{n+1} = w^n - \frac{Y_2(w^n) - 1}{\frac{\partial Y_2(w^n)}{\partial w}}. \tag{2.8}$$

To find $\frac{\partial Y_2(w^n)}{\partial w}$, introduce the following notations.

$$\frac{\partial Y_1}{\partial w} = Y_4, \quad \frac{\partial Y_2}{\partial w} = Y_5, \quad \frac{\partial Y_3}{\partial w} = Y_6 \tag{2.9}$$

As a result of these new notations the Newton's iterative scheme, will then get the form.

$$w^{n+1} = w^n - \frac{Y_2(w^n) - J}{Y_5(w^n)}. \tag{2.10}$$

Now differentiating the system of two first order ODEs (2.3)-(2.5) with respect to w, we get three new ODEs, as follows.

$$Y_4' = Y_5, \qquad Y_4(0) = 0. \tag{2.11}$$

$$Y_5' = Y_6, \qquad Y_5(0) = 0. \tag{2.12}$$

$$Y_6' = (-1/2)\Big(Y_1 Y_6 + Y_3 Y_4\Big), \qquad Y_6(0) = 1. \tag{2.13}$$

Writing all the six ODEs following initial value problem is obtained.

$$\begin{aligned}
&Y_1' = Y_2, && Y_1(0) = 0,\\
&Y_2' = Y_3, && Y_2(0) = 0,\\
&Y_3' = (-1/2)Y_1Y_3, && Y_3(0) = w,\\
&Y_4' = Y_5, && Y_4(0) = 0,\\
&Y_5' = Y_6, && Y_5(0) = 0,\\
&Y_6' = (-1/2)\Big(Y_1Y_6 + Y_3Y_4\Big), && Y_6(0) = 1.
\end{aligned}$$

The above IVP will be solved numerically by Runge-Kutta method of order four. The stopping criteria for the Newton's technique is set as,

$$| Y_2(w) - 1 |< \epsilon,$$

where $\epsilon > 0$ is an arbitrarily small positive number.

Chapter 3

The Enhanced Thermal Performance of Prandtl–Eyring Hybrid Nanofluid

3.1 Introduction

This chapter discusses the in-depth study of the work of Jamshed et al. [23]. In this article, heat transport through P-E hybrid nanofluids and entropy formation are investigated. Using a slippery heated surface, the flow and thermal transport characteristics of P-EHNF nanofluid are examined. Additionally, the impacts of porous medium, C-C heat flow, and thermal radiative flux will be examined in this investigation. In this work, engine oil (EO) is used as a base fluid to study single-walled carbon nanotubes (SWCNT) and multi-walled carbon nanotubes (MWCNT). Significant findings for various variables are shown by measurements of flow, temperature, drag force, Nusselt number, and entropy. Graphs are presented to depict the physical significance of various dimensionless values. We observed the trend of the velocity, temperature and entropy distributions by changing the values of the various factors.

3.2 Mathematical Modeling

The stretching velocity of movable horizontal plate is given as

$$U_w(x,t) = bx,$$

where b is a ratio of expanding plate. The surface heat is $\mathcal{T}_w(x,t) = \mathcal{T}_\infty + \mathbf{b}x$, where $\mathbf{b}$, $\mathcal{T}_w$ and $\mathcal{T}_\infty$ denote the degree of temperature change, surface heat, and surroundings, respectively. The plate is designed to be slippery, while the temperature of the surface is changing.

Primarily SWCNT nano solid particles synthesise the nanofluid in the EO-based liquid at an interaction volume fraction ϕ_{ST}, and it is fixed at 0.18 during the analysis. MWCNT nano molecules are extended in combination to obtain a hybrid nanofluid at the concentration size ϕ_{MT}.

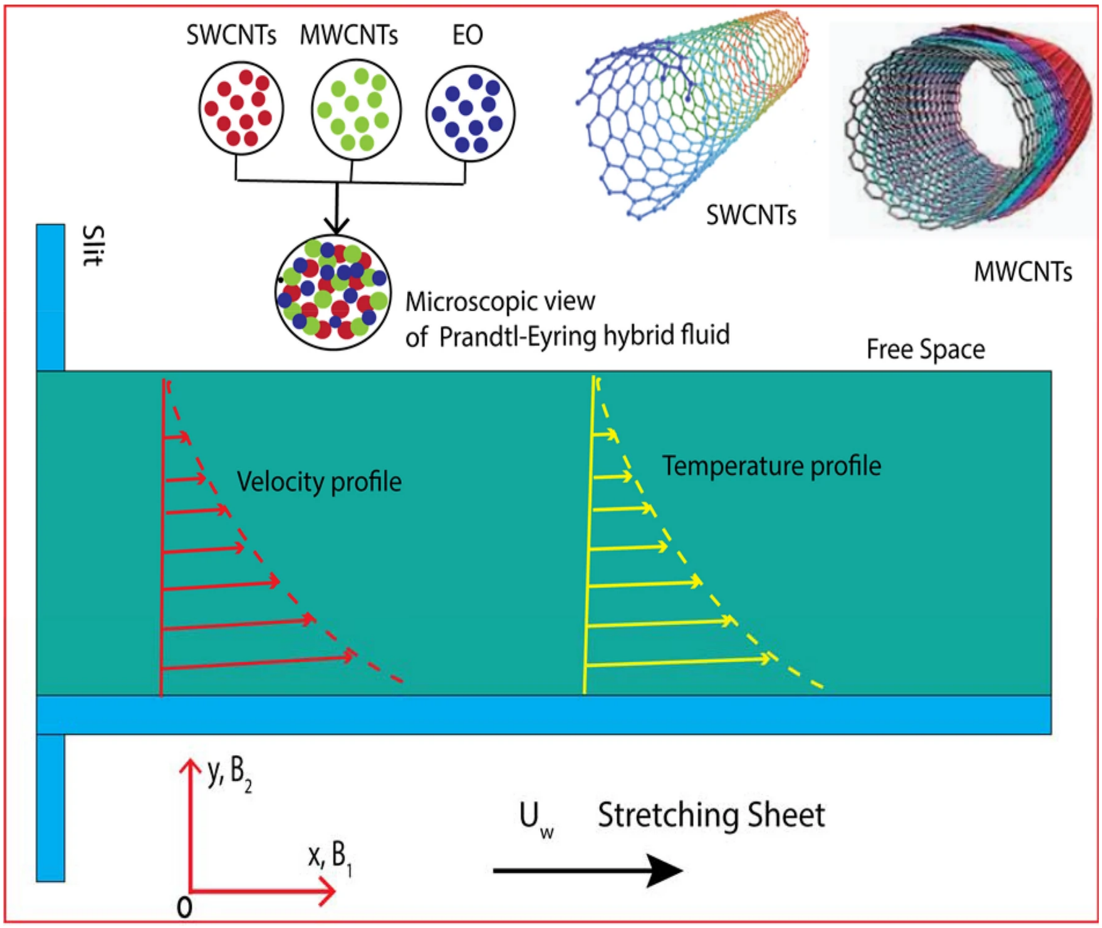

FIGURE 3.1: Geometry of flow model.

3.2.1 Prandtl–Eyring Fluid Stress Tensor

Prandtl–Eyring fluid stress tensor is given in the following mathematical shape by Mekheimer and Ramadan [34].

$$\tau = \frac{A_d \sin^{-1}\left(\frac{1}{C}\left[\left(\frac{\partial B_1}{\partial y}\right) + \left(\frac{\partial B_2}{\partial x}\right)^2\right]^{\frac{1}{2}}\right)}{\left[\left(\frac{\partial B_1}{\partial y}\right) + \left(\frac{\partial B_2}{\partial x}\right)^2\right]^{\frac{1}{2}}}\left(\frac{\partial B_1}{\partial y}\right),$$

where A_d and C are the material constants of the Prandtl fluid model and the curving velocity shows the mechanisms $\overleftarrow{B} = [B_1(\text{x,y,0}),\ B_2(\text{x,y,0}),\ 0]$.

3.2.2 Suppositions and Terms of System

The flow system is governed by the constraints and the following guiding principles:

i. 2-D laminar time-dependent flow

ii. Single phase (Tiwari-Das) scheme

iii. CCHFM

iv. Thermal radiative flow

v. Nano solid particles shape-factor

vi. slippery boundary constraints

3.2.3 Governing Equations

The flow formulas of the viscous Prandtl–Eyring hybrid nanofuid, in combination with a porous material, Cattaneo–Christov heat flux and thermal radiative flow utilising the approximate boundary-layer are

$$\frac{\partial B_1}{\partial x} + \frac{\partial B_2}{\partial y} = 0, \tag{3.1}$$

$$B_1\frac{\partial B_1}{\partial x} + B_2\frac{\partial B_2}{\partial y} = \frac{A_d}{C\rho_{hnf}}\left(\frac{\partial^2 B_1}{\partial y^2}\right) - \frac{A_d}{2C^3\rho_{hnf}}\frac{\partial^2 B_1}{\partial y^2}\left(\frac{\partial B_1}{\partial y}\right)^2 - \frac{\mu_{hnf}}{\rho_{hnf}k}B_1, \tag{3.2}$$

$$\begin{aligned} B_1\frac{\partial \mathcal{T}}{\partial x} + B_2\frac{\partial \mathcal{T}}{\partial y} = {} & \frac{1}{(\rho C_p)_{hnf}}\left(k_{hnf}\left(\frac{\partial^2 \mathcal{T}}{\partial y^2}\right) + \mu_{hnf}\left(\frac{\partial B_1}{\partial y}\right)^2 - \frac{\partial q_r}{\partial y}\right) \\ & - \lambda_0\left(B_1\frac{\partial B_1}{\partial x}\frac{\partial \mathcal{T}}{\partial x} + B_2\frac{\partial B_2}{\partial y}\frac{\partial \mathcal{T}}{\partial y} + B_1\frac{\partial B_2}{\partial x}\frac{\partial \mathcal{T}}{\partial y} + B_2\frac{\partial B_1}{\partial y}\frac{\partial \mathcal{T}}{\partial x}\right. \\ & \left. + B_1^2\frac{\partial^2 \mathcal{T}}{\partial x^2} + B_2^2\frac{\partial^2 \mathcal{T}}{\partial y^2} + 2B_1B_2\frac{\partial^2 \mathcal{T}}{\partial x\partial y}\right) \end{aligned} \tag{3.3}$$

Here Eq. (3.1) is continuity equation. The components of velocity in the x and y direction are denoted by B_1 and B_2 respectively and $\mathcal{T}$ is temparature of fluid. The associated BCs are taken as. [35]

$$B_1(x,0) = U_w + N_\varsigma\left(\frac{\partial B_1}{\partial y}\right), \quad B_2(x,0) = V_\varsigma, \quad -k_\varsigma\left(\frac{\partial \mathcal{T}}{\partial y}\right) = h_\varsigma(\mathcal{T}w - \mathcal{T}) \tag{3.4}$$

$$B_1 \to 0, \quad \mathcal{T} \to \mathcal{T}_\infty, \quad \text{as} \quad y \to \infty. \tag{3.5}$$

Following are the vital parameters appearing in (3.1)-(3.5):

Surface permeability V_ς,

Heat transfer coefficient h_ς,

Porosity (k),

Rigid heat conductivity k_ς,

Radiative heat flux constant is q_r.

3.2.4 Rosseland Approximation

P-EHNF is non-Newtonian and thicker fluid. The Rosseland approximation is applied to optically thick media and gives the net radiation heat flux by expression.

$$q_r = -\frac{4\sigma^*}{3k^*}\frac{\partial \mathcal{T}^4}{\partial y},$$

where σ^* is the Stefan-Boltzman constant and k^* is the absorption coefficient. If the temperature difference is very small, then the temperature $\mathcal{T}^4$ can be expanded about T_∞ using Taylor series, as follows.

$$\mathcal{T}^4 = \mathcal{T}_\infty^4 + 4\mathcal{T}_\infty^3(\mathcal{T} - \mathcal{T}_\infty) + 6\mathcal{T}_\infty^2(\mathcal{T} - \mathcal{T}_\infty)^2 + ...$$

neglecting the higher degree terms,

$$\begin{aligned}
\mathcal{T}^4 &= \mathcal{T}_\infty^4 + 4\mathcal{T}_\infty^3(\mathcal{T} - \mathcal{T}_\infty), \\
&= \mathcal{T}_\infty^4 + 4\mathcal{T}_\infty^3\mathcal{T} - 4\mathcal{T}_\infty^4, \\
&= -3\mathcal{T}_\infty^4 + 4\mathcal{T}_\infty^3\mathcal{T}, \\
&= 4\mathcal{T}_\infty^3\mathcal{T} - 3\mathcal{T}_\infty^4.
\end{aligned}$$

3.2.5 Thermophysical Properties

The thermophysical properties of nanofluid and hybrid nanofluid are shown in the following tables which are taken from [23]:

TABLE 3.1: Thermo-physical properties of Nanofluid

Feature	Nanofluid
Density	$\rho_{nf} = (1-\phi)\rho_f - \phi\rho_s$,
Dynamical viscidness	$\mu_{nf} = \frac{\mu_f}{(1-\phi)^{2.5}}$,
Heat capacity	$(\rho C_p)_{nf} = (1-\phi)(\rho C_p)_f + \phi(\rho C_p)_s$,
Thermal conductivity	$\frac{\kappa_{nf}}{\kappa_f} = \frac{(\kappa_\varsigma+(m-1)\kappa_f)-(m-1)\phi(\kappa_f-\kappa_\varsigma)}{(\kappa_\varsigma+(m-1)\kappa_f)+\phi(\kappa_f-\kappa_\varsigma)}$.

ϕ is the nano solid-particle size coeffcient. μ_f , ρ_f , $(C_p)_f$ and κ_f are dynamical viscosity, intensity, functioning thermal capacity, and thermal conductivity of the standard fluid, respectively. The additional characteristics ρ_s, $(C_p)_s$ and κ_s are the concentration, effective heat capacitance, and heat conductance of the nano molecules, correspondingly.

Table 3.2: Thermo-physical properties of Hybrid nanofluid

Feature	Hybrid nanofluid
Viscosity (μ)	$\mu_{hnf} = \mu_f(1-\phi_{ST})^{-2.5}(1-\phi_{MT})^{-2.5}$
Density (ρ)	$\rho_{hnf} = [(1-\phi_{MT})(1-\phi_{ST})\rho_f + \phi_{ST}\rho_{p_1}] + \phi_{MT}\rho_{p_2}$
Heat Capacity (ρC_p)	$(\rho C_p)_{hnf} = (1-\phi_{MT})[(1-\phi_{ST})(\rho C_p)_f + \phi_{ST}(\rho C_p)_{p_1}] + \phi_{MT}(\rho C_p)_{p_2}$
Thermal conductivity (κ)	$\frac{\kappa_{hnf}}{\kappa_{nf}} = \left[\frac{\kappa_{p_2}+(m-1)\kappa_{nf}-(m-1)\phi_{MT}(\kappa_{nf}-\kappa_{p_2})}{\kappa_{p_2}+(m-1)\kappa_{nf}+\phi_{MT}(\kappa_{nf}-\kappa_{p_2})}\right]$, $\frac{\kappa_{nf}}{\kappa_f} = \left[\frac{\kappa_{p_1}+(m-1)\kappa_f-(m-1)\phi_{ST}(\kappa_{1f}-\kappa_{p_1})}{\kappa_{p_1}+(m-1)\kappa_f+\phi_{ST}(\kappa_f-\kappa_{p_1})}\right]$

μ_{hnf} , ρ_{hnf} , $(\rho Cp)_{hnf}$ and κ_{hnf} are mixture nanofuid functional viscosity, concentration, exact thermal capacitance, and thermal conductance.

Following notations are used for simplification purpose:

$$\phi_a = (1-\phi_{ST})^{2.5}(1-\phi_{MT})^{2.5}, \tag{3.6}$$

$$\phi_b = (1-\phi_{MT})\Big((1-\phi_{ST}) + \phi_{ST}\frac{\rho_{p_1}}{\rho_f}\Big) + \phi_{MT}\frac{\rho_{p_2}}{\rho_f}, \tag{3.7}$$

$$\phi_c = (1-\phi_{MT})[(1-\phi_{ST}) + \phi_{ST}\frac{(\rho C_p)_{p_1}}{(\rho C_p)_f}] + \phi_{MT}\frac{(\rho C_p)_{p_2}}{(\rho C_p)_f}, \tag{3.8}$$

$$\begin{aligned}\phi_d = &\left[\frac{\kappa_{p_2}+(m-1)\kappa_{nf}-(m-1)\phi_{MT}(\kappa_{nf}-\kappa_{p_2})}{\kappa_{p_2}+(m-1)\kappa_{nf}+\phi_{MT}(\kappa_{nf}-\kappa_{p_2})}\right]\\ &\times\left[\frac{\kappa_{p_1}+(m-1)\kappa_f-(m-1)\phi_{ST}(\kappa_f-\kappa_{p_1})}{\kappa_{p_1}+(m-1)\kappa_f+\phi_{ST}(\kappa_f-\kappa_{p_1})}\right].\end{aligned} \tag{3.9}$$

3.2.6 Dimensionless Formulation of the Flow Model

For the conversion of the mathematical model (3.1)-(3.3) into the system of ODEs, the following similarity transformation are used which are taken from [23].

$$\left.\begin{aligned} &\Omega(x,y) = \sqrt{\frac{b}{\nu_f}}y, \qquad \theta(\Omega) = \frac{\mathcal{T}-\mathcal{T}_\infty}{\mathcal{T}_w-\mathcal{T}_\infty},\\ &\psi = \sqrt{\nu_f b}xf(\Omega),\end{aligned}\right\} \tag{3.10}$$

where ψ denotes the stream function.

The detailed procedure for the conversion of (3.1)-(3.3) into the dimensionless form is mentioned below.

$$\begin{aligned}
B_1 &= \frac{\partial \psi}{\partial y} \\
&= \frac{\partial}{\partial y}\left(\sqrt{\nu_f b} x f(\Omega))\right) \\
&= \sqrt{\nu_f b} f'(\Omega)\frac{\partial \Omega}{\partial y} \\
&= bxf'(\Omega). \qquad (3.11) \\
B_2 &= -\frac{\partial \psi}{\partial x} \\
&= -\frac{\partial}{\partial x}\left(\sqrt{\nu_f b} x f(\Omega))\right) \\
&= -\Big(f(\Omega)\sqrt{\nu_f b}(1) + \sqrt{\nu_f b} x f'(0)\Big) \\
&= -f(\Omega)\sqrt{\nu_f b} \qquad (3.12) \\
\frac{\partial B_1}{\partial x} &= \frac{\partial}{\partial x}\left(bxf'(\Omega)\right) \\
&= f'(\Omega)b + bxf''(0) \\
&= f'(\Omega)b. \qquad (3.13) \\
\frac{\partial B_2}{\partial y} &= \frac{\partial}{\partial y}\Big[-f(\Omega)\sqrt{\nu_f b}\Big] \\
&= -(\sqrt{\nu_f b} f'(\Omega)\frac{\partial \Omega}{\partial x}) \\
&= -(\sqrt{\nu_f b} f'(\Omega)\sqrt{(b)/(\nu_f)}) \\
&= -bf'(\Omega). \qquad (3.14) \\
\frac{\partial B_1}{\partial y} &= bxf''(\Omega)\sqrt{\frac{b}{\nu_f}}. \qquad (3.15) \\
\frac{\partial^2 B_1}{\partial y^2} &= \frac{\partial}{\partial y}\left(bxf''(\Omega)\sqrt{b/\nu_f}\right) \\
&= bxf'''(\Omega)\sqrt{b/\nu_f}\frac{\partial \Omega}{\partial y} \\
&= bxf'''(\Omega)\sqrt{b/\nu_f}\sqrt{b/\nu_f} \\
&= \frac{b^2}{\nu_f} x f'''(\Omega). \qquad (3.16) \\
\left(\frac{\partial B_1}{\partial y}\right)^2 &= x^2\frac{b^3}{\nu_f}(f''(\Omega))^2. \qquad (3.17) \\
\frac{\partial B_2}{\partial x} &= 0 \qquad (3.18)
\end{aligned}$$

Equation (3.1) is quickly satisfied by using (3.13) and (3.14), as follows

$$\frac{\partial B_1}{\partial x} + \frac{\partial B_2}{\partial y} = f'(\Omega)b - f'(\Omega)b = 0. \tag{3.19}$$

Now, the dimensionless form of the momentum equation can be obtained by using the derivatives calculated earlier.

$$B_1\frac{\partial B_1}{\partial x} + B_2\frac{\partial B_1}{\partial y} = \frac{A_d}{C\rho_{hnf}}\left(\frac{\partial^2 B_1}{\partial y^2}\right) - \frac{A_d}{2C^3\rho_{hnf}}\frac{\partial^2 B_1}{\partial y^2}\left(\frac{\partial B_1}{\partial y}\right)^2 - \frac{\mu_{hnf}}{\rho_{hnf}k}B_1$$

$$\Rightarrow\left(bxf'(\Omega)\right)\left(f'(\Omega)b\right) + \left(-f(\Omega)\sqrt{\nu_f b}\right)\left(bxf''(\Omega)\sqrt{\frac{b}{\nu_f}}\right) = \frac{A_1^*\mu_f C}{C\rho_{hnf}}\left(\frac{b^2}{\nu_f}xf'''(\Omega)\right)$$

$$-\frac{A_1^*\mu_f C}{2C^3\rho_{hnf}}\left(\frac{b^2}{\nu_f}xf'''(\Omega)\right)\left(bxf''(\Omega)\sqrt{\frac{b}{\nu_f}}\right)^2 - \frac{\mu_{hnf}}{\rho_{hnf}k}bxf'(\Omega)$$

$$\Rightarrow\left(bxf'(\Omega)\right)\left(f'(\Omega)b\right) + \left(-f(\Omega)\sqrt{\nu_f b}\right)\left(bxf''(\Omega)\sqrt{\frac{b}{\nu_f}}\right) = \frac{A_1^*\mu_f}{\rho_{hnf}}\left(\frac{b^2}{\nu_f}xf'''(\Omega)\right)$$

$$-\frac{A_1^*\mu_f}{2C^2\rho_{hnf}}\left(\frac{b^2}{\nu_f}xf'''(\Omega)\right)\left(x^2\big(f''(\Omega)\big)^2\frac{b^3}{\nu_f}\right) - \frac{\mu_{hnf}}{\rho_{hnf}k}(bxf'(\Omega)$$

$$\Rightarrow\left(b^2x\big(f'(\Omega)\big)^2\right) - \left(f(\Omega)f''(\Omega)xb^2\right) = \frac{A_1^*\mu_f}{\rho_{hnf}}\left(\frac{b^2}{\nu_f}xf'''(\Omega)\right)$$

$$-\frac{A_1^*\mu_f}{2C^2\rho_{hnf}}\left(\frac{b^5}{\nu_f^2}x^3f'''(\Omega)\big(f''(\Omega)\big)^2\right) - \frac{\mu_{hnf}}{\rho_{hnf}k}(bxf'(\Omega))$$

Since,

$\rho_{hnf} = \big(1-\phi_{MT}\big)\big[(1-\phi_{ST})\rho_f + \phi_{ST}\rho_{p_1}\big] + \phi_{MT}\rho_{p_2}$

$\mu_{hnf} = \mu_f\big(1-\phi_{ST}\big)^{-2.5}\big(1-\phi_{MT}\big)^{-2.5}$

$K_\varsigma = \frac{\nu_f}{bk}$

$\nu_f = \frac{\mu_f}{\rho_f}$

$$\therefore\quad \left(b^2x\big(f'(\Omega)\big)^2\right) - \left(f(\Omega)f''(\Omega)xb^2\right) =$$

$$\frac{A_1^*\mu_f}{\big(1-\phi_{MT}\big)\big[(1-\phi_{ST})\rho_f + \phi_{ST}\rho_{p_1}\big] + \phi_{MT}\rho_{p_2}}\left(\frac{b^2}{\frac{\mu_f}{\rho_f}}xf'''(\Omega)\right)$$

$$-\frac{A_1^*\mu_f}{2C^2\big(1-\phi_{MT}\big)\big[(1-\phi_{ST})\rho_f + \phi_{ST}\rho_{p_1}\big] + \phi_{MT}\rho_{p_2}}\left(\frac{b^5}{\frac{\mu_f}{\rho_f}\nu_f}x^3f'''(\Omega)\big(f''(\Omega)\big)^2\right)$$

$$-\frac{\mu_f\big(1-\phi_{ST}\big)^{-2.5}\big(1-\phi_{MT}\big)^{-2.5}}{\big(1-\phi_{MT}\big)\big[(1-\phi_{ST})\rho_f + \phi_{ST}\rho_{p_1}\big] + \phi_{MT}\rho_{p_2}}\frac{1}{\nu_f}\big(b^2xK_\varsigma f'(\Omega)\big)$$

$$
\begin{aligned}
\Rightarrow \quad & \big(f'(\Omega)\big)^2 - f(\Omega)f''(\Omega) = \\
& \frac{A_1^*}{(1-\phi_{MT})\left[(1-\phi_{ST})+\phi_{ST}\frac{\rho_{p1}}{\rho_f}\right]+\phi_{MT}\frac{\rho_{p2}}{\rho_f}} f'''(\Omega) \\
& - \frac{A_1^*}{(1-\phi_{MT})\left[(1-\phi_{ST})+\phi_{ST}\frac{\rho_{p1}}{\rho_f}\right]+\phi_{MT}\frac{\rho_{p2}}{\rho_f}} \left(\frac{b^3x^2}{2C^2\nu_f} f'''(\Omega)\big(f''(\Omega)\big)^2\right) \\
& - \frac{(1-\phi_{ST})^{-2.5}(1-\phi_{MT})^{-2.5}}{(1-\phi_{MT})\left[(1-\phi_{ST})+\phi_{ST}\frac{\rho_{p1}}{\rho_f}\right]+\phi_{MT}\frac{\rho_{p2}}{\rho_f}} \big(K_\varsigma f'(\Omega)\big)
\end{aligned}
$$

using (3.6) and (3.7)

$$
\Rightarrow \big(f'(\Omega)\big)^2 - f(\Omega)f''(\Omega) = \frac{A_1^*}{\phi_b} f'''(\Omega) - \frac{A_1^*A_2^*}{\phi_b} f'''(\Omega)\big(f''(\Omega)\big)^2 - \frac{1}{\phi_a\phi_b} K_\varsigma f'(\Omega)
$$

$$
A_1^* f'''(\Omega)\big(1 - A_2^* f''(\Omega)^2\big) + \phi_b\big(f(\Omega)f''(\Omega) - f'(\Omega)^2\big) - \frac{1}{\phi_a} K_\varsigma f'(\Omega) = 0. \quad (3.20)
$$

The following dimensionless parameters are used in equation (3.20),

$$
A_1^* = \frac{A_d}{\mu_f C}, \qquad A_2^* = \frac{b^3x^2}{2C^2\nu_f}, \qquad K_\varsigma = \frac{\nu_f}{bk}.
$$

Now, for the conversion of energy equation (3.3), the following derivatives are required.

$$
\begin{aligned}
\theta(\Omega) &= \frac{\mathcal{T} - \mathcal{T}_\infty}{\mathcal{T}_w - \mathcal{T}_\infty}. \\
\Rightarrow \qquad \mathcal{T} &= \theta(\Omega)(\mathcal{T}_w - \mathcal{T}_\infty) + \mathcal{T}_\infty \\
&= \theta(\Omega)bx + \mathcal{T}_\infty \\
\frac{\partial \mathcal{T}}{\partial x} &= b\theta(\Omega) && (3.21) \\
\frac{\partial^2 \mathcal{T}}{\partial x} &= 0. && (3.22) \\
\frac{\partial \mathcal{T}}{\partial y} &= \frac{\partial}{\partial y}\Big(\theta(\Omega)bx + \mathcal{T}_\infty\Big) \\
&= bx\theta'(\Omega)\left(\sqrt{\frac{b}{\nu_f}}\right). && (3.23) \\
\frac{\partial^2 \mathcal{T}}{\partial y^2} &= \frac{b^2}{\nu_f} x\theta''(\Omega). && (3.24) \\
\frac{\partial}{\partial x}\left(\frac{\partial \mathcal{T}}{\partial y}\right) &= \frac{\partial}{\partial x}\left(bx\theta'(\Omega)\sqrt{\frac{b}{\nu_f}}\right)
\end{aligned}
$$

$$\frac{\partial^2 \mathcal{T}}{\partial x \partial y} = b\sqrt{\frac{b}{\nu_f}}\theta'(\Omega) \tag{3.25}$$

$$\begin{aligned} q_r &= -\frac{4\sigma^*}{3k^*}\frac{\partial \mathcal{T}^4}{\partial y} \\ &= -\frac{4\sigma^*}{3k^*}\frac{\partial}{\partial y}(4\mathcal{T}_\infty^3\mathcal{T} - 3\mathcal{T}_\infty^4) \\ &= -\frac{4\sigma^*}{3k^*}\frac{\partial}{\partial y}(4\mathcal{T}_\infty^3\mathcal{T}) \\ &= -\frac{16\sigma^*}{3k^*}\mathcal{T}_\infty^3\frac{\partial \mathcal{T}}{\partial y}. \\ \Rightarrow \quad \frac{\partial q_r}{\partial y} &= -\frac{16\sigma^*}{3k^*}\mathcal{T}_\infty^3\frac{\partial^2 \mathcal{T}}{\partial y^2} \\ &= -\frac{16\sigma^*}{3k^*}\mathcal{T}_\infty^3\left(\frac{b^2}{\nu_f}x\theta''(\Omega)\right). \end{aligned} \tag{3.26}$$

The governing equation for the conservation of energy takes the following form:

$$\begin{aligned} &B_1\frac{\partial \mathcal{T}}{\partial x} + B_2\frac{\partial \mathcal{T}}{\partial y} = \frac{1}{(\rho C_p)_{hnf}}\left(k_{hnf}\Big(\frac{\partial^2 \mathcal{T}}{\partial y^2}\Big) + \mu_{hnf}\Big(\frac{\partial B_1}{\partial y}\Big)^2 - \frac{\partial q_r}{\partial y}\right) \\ &- \lambda_0\left(B_1\frac{\partial B_1}{\partial x}\frac{\partial \mathcal{T}}{\partial x} + B_2\frac{\partial B_2}{\partial y}\frac{\partial \mathcal{T}}{\partial y} + B_1\frac{\partial B_2}{\partial x}\frac{\partial \mathcal{T}}{\partial y} + B_2\frac{\partial B_1}{\partial y}\frac{\partial \mathcal{T}}{\partial x} + B_1^2\frac{\partial^2 \mathcal{T}}{\partial x^2}\right. \\ &\left. + B_2^2\frac{\partial^2 \mathcal{T}}{\partial y^2} + 2B_1B_2\frac{\partial^2 \mathcal{T}}{\partial x \partial y}\right) \\ \Rightarrow \quad &\Big(bxf'(\Omega)\Big)\Big(b\theta(\Omega)\Big) + \Big(-f(\Omega)\sqrt{\nu_f b}\Big)\Big(bx\theta'(\Omega)\Big(\sqrt{\frac{b}{\nu_f}}\Big)\Big) = \\ &\frac{1}{(\rho C_p)_{hnf}}\left(k_{hnf}\big(\frac{b^2x}{\nu_f}\theta''(\Omega)\big) + \mu_{hnf}\big(\frac{b^3x^2}{\nu_f}(f''(\Omega))^2\big) + \frac{16\sigma^*}{3k^*}\mathcal{T}_\infty^3\Big(\frac{b^2}{\nu_f}x\theta''(\Omega)\Big)\right) \\ &- \lambda_0\left((bxf'(\Omega))\big(f'(\Omega)b\big)\big(b\theta(\Omega)\big) + \big(-\sqrt{\nu_f b}f(\Omega)\big)\big(-bf'(\Omega)\big)\big(bx\sqrt{\frac{b}{\nu_f}}\theta'(\Omega)\big)\right. \\ &+ 0 + \big(-\sqrt{\nu_f b}f(\Omega)\big)\big(bx\sqrt{\frac{b}{\nu_f}}f''(\Omega)\big)\big(b\theta(\Omega)\big) + 0 + \big(f(\Omega)\big)^2\big(b\nu_f\big)\big(\frac{b^2}{\nu_f}x\theta''(\Omega)\big) \\ &\left. + \big(2bxf'(\Omega)\big)\big(-\sqrt{\nu_f b}f(\Omega)\big)\big(b\sqrt{\frac{b}{\nu_f}}\theta(\Omega)\big)\right) \\ \Rightarrow \quad &\Big(b^2xf'(\Omega)\theta(\Omega)\Big) - \Big(b^2xf(\Omega)\theta'(\Omega)\Big) = \\ &\frac{1}{(\rho C_p)_{hnf}}\left(k_{hnf}\big(\frac{b^2x}{\nu_f}\theta''(\Omega)\big) + \mu_{hnf}\big(\frac{b^3x^2}{\nu_f}(f''(\Omega))^2\big) + \frac{16\sigma^*}{3k^*}\mathcal{T}_\infty^3\Big(\frac{b^2}{\nu_f}x\theta''(\Omega)\Big)\right) \end{aligned}$$

$$\Bigg(-\lambda_0 \quad \big(b^3x(f'(\Omega))^2\theta(\Omega)\big) + \big(b^3xf(\Omega)f'(\Omega)\theta'(\Omega)\big) - \big(b^3xf(\Omega)f''(\Omega)\theta(\Omega)\big)$$

$$+\big(b^3x(f(\Omega))^2\theta''(\Omega)\big) - \big(2b^3xf(\Omega)f'(\Omega)\theta'(\Omega)\big)\Bigg)$$

From Table 3.2,

$$\kappa_{hnf} = \Big[\frac{\kappa_{p_2} + (m-1)\kappa_{nf} - (m-1)\phi_{MT}(\kappa_{nf} - \kappa_{p_2})}{\kappa_{p_2} + (m-1)\kappa_{nf} + \phi_{MT}(\kappa_{nf} - \kappa_{p_2})}\Big] \times \Big[\frac{\kappa_{p_1} + (m-1)\kappa_{f} - (m-1)\phi_{ST}(\kappa_{f} - \kappa_{p_1})}{\kappa_{p_1} + (m-1)\kappa_{f} + \phi_{ST}(\kappa_{f} - \kappa_{p_1})}\Big]\kappa_f$$

$$\Rightarrow \quad \kappa_{hnf} = \phi_d\kappa_f.$$

$$(\rho C_p)_{hnf} = \Big[(1-\phi_{MT})[(1-\phi_{ST})(\rho C_p)_f + \phi_{ST}(\rho C_p)_{p1}] + \phi_2(\rho C_p)_{p2}\Big] \times \frac{(\rho C_p)_{hnf}}{(\rho C_p)_{hnf}} = \phi_c(\rho C_p)_f.$$

$$\mu_{hnf} = \mu_f(1-\phi_{ST})^{-2.5}(1-\phi_{MT})^{-2.5}.$$

$$\mu_{hnf} = \frac{\mu_f}{\phi_a}.$$

$$So, \quad \Big(b^2xf'(\Omega)\theta(\Omega)\Big) - \Big(b^2xf(\Omega)\theta'(\Omega)\Big) =$$

$$\frac{1}{\phi_c(\rho C_p)_f}\Bigg(\phi_d k_f\big(\frac{b^2x}{\nu_f}\theta''(\Omega)\big) + \frac{\mu_f}{\phi_a}\big(\frac{b^3x^2}{\nu_f}(f''(\Omega))^2\big) + \frac{16\sigma^*}{3k^*}\mathcal{T}_\infty^3\Big(\frac{b^2}{\nu_f}x\theta''(\Omega)\Big)\Bigg)$$

$$-\lambda_0\Bigg(\big(b^3x(f'(\Omega))^2\theta(\Omega)\big) + \big(b^3xf(\Omega)f'(\Omega)\theta'(\Omega)\big) - \big(b^3xf(\Omega)f''(\Omega)\theta(\Omega)\big)$$

$$+\big(b^3x(f(\Omega))^2\theta''(\Omega)\big) - \big(2b^3xf(\Omega)f'(\Omega)\theta'(\Omega)\big)\Bigg).$$

$$\Rightarrow \quad \frac{\phi_d}{\phi_c}\frac{1}{P\varsigma}\big(b^2x\theta''(\Omega)\big) + \frac{1}{\phi_a\phi_c(C_p)_f}\big(b^3x^2(f'')^2\big) + N_\varsigma\frac{1}{\phi_c}\big(b^2x\theta''(\Omega)\big)$$

$$-\lambda_0\Bigg(\big(b^3x(f'(\Omega))^2\theta(\Omega)\big) + \big(b^3xf(\Omega)f'(\Omega)\theta'(\Omega)\big) - \big(b^3xf(\Omega)f''(\Omega)\theta(\Omega)\big)$$

$$+\big(b^3x(f(\Omega))^2\theta''(\Omega)\big) - \big(2b^3xf(\Omega)f'(\Omega)\theta'(\Omega)\big)\Bigg) + b^2xf(\Omega)\theta'(\Omega)$$

$$-b^2xf'(\Omega)\theta(\Omega) = 0$$

$$\Rightarrow \quad \frac{\phi_d}{\phi_c}\frac{1}{P\varsigma}\big(b\theta''(\Omega)\big) + \frac{E_\varsigma}{\phi_a\phi_c}\big(b(f''(\Omega)^2)\big) + N_\varsigma\frac{1}{\phi_c}b\theta''(\Omega) - \lambda_0\Bigg(b^2(f')^2\theta(\Omega)$$

$$+b^2f(\Omega)f'(\Omega)\theta'(\Omega) - b^2f(\Omega)f''(\Omega)\theta(\Omega) + b^2(f(\Omega))^2\theta''(\Omega)$$

$$-2b^2f(\Omega)f'(\Omega)\theta'(\Omega)\Bigg)bf(\Omega)\theta'(\Omega) - bf'(\Omega)\theta(\Omega) = 0.$$

$$\begin{aligned}
\Rightarrow\quad & \frac{\phi_d}{\phi_c}\frac{1}{P\varsigma}\big(\theta''(\Omega)\big)\big(1+\frac{1}{\phi_d}P\varsigma N_\varsigma\big)+\frac{E_\varsigma}{\phi_a\phi_c}\big((f''(\Omega)^2)\big)-\epsilon_\varsigma\bigg((f')^2\theta(\Omega)\\
& +f(\Omega)f'(\Omega)\theta'(\Omega)-f(\Omega)f''(\Omega)\theta(\Omega)+(f(\Omega))^2\theta''(\Omega)\\
& -f(\Omega)f'(\Omega)\theta'(\Omega)\bigg)f(\Omega)\theta'(\Omega)-f'(\Omega)\theta(\Omega)=0.\\
\Rightarrow\quad & \big(1+\frac{1}{\phi_d}P\varsigma N_\varsigma\big)\theta''+\frac{\phi_c}{\phi_d}P\varsigma\bigg(f\theta'-f'\theta+\frac{E_\varsigma}{\phi_a\phi_c}(f'')^2\\
& -\epsilon_\varsigma\big((f')^2\theta-ff'\theta'-ff''\theta+f^2\theta''\big)\bigg)=0.
\end{aligned} \tag{3.27}$$

The dimensionless parameters used in equation (3.27) are:

$$\begin{aligned}
&\epsilon_\varsigma=\lambda_0(b), \qquad \alpha_f=\tfrac{\kappa_f}{(\rho C_p)_f}, \qquad P_\varsigma=\tfrac{\nu_f}{\alpha_f},\\
&E_\varsigma=\tfrac{U_w^3}{(C_p)_f(\mathcal{T}_w-\mathcal{T}_\infty)}, \qquad N_\varsigma=\tfrac{16\sigma^*}{3\kappa^*}\tfrac{\mathcal{T}_\infty^3}{\nu_f(\rho C_p)_f}.
\end{aligned}$$

The related BCs are converted into the dimensionless form by the following procedure. Firstly when y=0 which implies Ω=0

$$\begin{aligned}
& B_1(x,0)=U_w+N_\varsigma\big(\frac{\partial B_1}{\partial y}\big),\\
\Rightarrow\quad & f'(\Omega)bx=bx+N_\varsigma\bigg(bxf''(\Omega)\sqrt{\frac{b}{\nu_f}}\bigg),\\
\Rightarrow\quad & f'(\Omega)bx=bx\bigg(1+N_\varsigma\sqrt{\frac{b}{\nu_f}}f''(\Omega)\bigg),\\
\Rightarrow\quad & f'(0)=1+A_\varsigma f''(0).\\
& B_2(x,0)=V_\varsigma,\\
\Rightarrow\quad & -f(\Omega)\sqrt{\nu_f b}=V_\varsigma,\\
\Rightarrow\quad & -f(\Omega)=\frac{V_\varsigma}{\sqrt{\nu_f b}},\\
\Rightarrow\quad & -f(0)=\frac{V_\varsigma}{\sqrt{\nu_f b}}\\
\Rightarrow\quad & \qquad f(0)=S,\\
& -\kappa_s\Big[\frac{\partial\mathcal{T}}{\partial y}\Big]=h_\varsigma(\mathcal{T}_w-\mathcal{T}),\\
\Rightarrow\quad & -\kappa_s\bigg(\theta'\sqrt{\frac{b}{\nu_f}}(\mathcal{T}_w-\mathcal{T}_\infty)\bigg)=h_\varsigma\Big(\mathcal{T}_\infty-\mathcal{T}\Big),
\end{aligned}$$

$$\Rightarrow \quad \theta' = \frac{h_\varsigma\big(\mathcal{T}_w - \mathcal{T}\ \big)}{-\kappa_s\sqrt{\frac{b}{\nu_f}}\big(\mathcal{T}_w - \mathcal{T}_\infty\big)},$$

$$\Rightarrow \quad \theta'(\Omega) = -H_\varsigma\left(\frac{\mathcal{T}_w - \big((\mathcal{T}_w - \mathcal{T}_\infty)\theta(\Omega) + \mathcal{T}_\infty\big)}{\mathcal{T}_w - \mathcal{T}_\infty}\right),$$

$$\Rightarrow \quad \theta'(\Omega) = -H_\varsigma\left(\frac{(\mathcal{T}_w - \mathcal{T}_\infty) - \big((\mathcal{T}_w - \mathcal{T}_\infty)\theta(\Omega)\big)}{\mathcal{T}_w - \mathcal{T}_\infty}\right),$$

$$\Rightarrow \quad \theta'(0) = -H_\varsigma(1 - \theta(0)).$$

Now choose $\mathrm{y}{\to}\infty \implies \Omega{\to}\infty$

$$B_1 \to 0,$$

$$\Rightarrow \quad f'(\Omega) \to 0,$$

$$\mathcal{T} \to \mathcal{T}_\infty,$$

$$\Rightarrow \quad \theta(\Omega) \to 0$$

The final dimensionless form of the governing equations along with the converted boundary conditions are

$$A_1^* f'''(\Omega)\big(1 - A_2^* f''(\Omega)^2\big) + \phi_b\big(f(\Omega)f''(\Omega) - f'(\Omega)^2\big) - \frac{1}{\phi_a}K_\varsigma f'(\Omega) = 0, \tag{3.28}$$

$$\big(1 + \frac{1}{\phi_d}P\varsigma N_\varsigma\big)\theta'' + \frac{\phi_c}{\phi_d}P\varsigma\Bigg(f\theta' - f'\theta + \frac{E_\varsigma}{\phi_a\phi_c}(f'')^2 - \epsilon_\varsigma\big((f')^2\theta - ff'\theta' - ff''\theta + f^2\theta''\big)\Bigg) = 0 \tag{3.29}$$

$$\left.\begin{aligned} &f(0) = S, \quad f'(0) = 1 + A_\varsigma f''(0), \quad f'(\Omega) \to 0, \quad \text{as } \ \Omega \to \infty, \\ &\theta'(0) = -H_\varsigma(1 - \theta(0)), \quad \theta(\Omega) \to 0, \quad \text{as } \ \Omega \to \infty. \end{aligned}\right\} \tag{3.30}$$

3.2.7 Some Dimensionless Quantities

The skin friction coefficient, is given as follows,

$$C_f = \frac{\tau_w}{\frac{1}{2}\rho_f U_w^2}\ , \tag{3.31}$$

where

$$\tau_w = \left(\frac{A_d}{C} \frac{\partial B_1}{\partial y} + \frac{A_d}{6C^3} \Big(\frac{\partial B_1}{\partial y} \Big)^3 \right)_{y=0}. \tag{3.32}$$

Therefore

$$\begin{aligned}
C_f &= \frac{\left(\frac{A_d}{C} bxf''(\Omega)\sqrt{\frac{b}{\nu_f}} + \frac{A_d}{6C^3} b^3x^3 \big(f''(\Omega)\big)^3 \big(\sqrt{\frac{b}{\nu_f}}\big)^3 \right)_{y=0}}{\frac{1}{2}\rho_f (bx)^2} \\
&= \frac{\left(\frac{A_d}{C} bxf''(\Omega)\sqrt{\frac{b}{\nu_f}} + \frac{A_d}{6C^3} b^3x^3 \big(f''(\Omega)\big)^3 \big(\sqrt{\frac{b}{\nu_f}}\big)^3 \right)_{y=0}}{\frac{1}{2}\frac{\mu_f}{\nu_f}(bx)(bx)} \\
&= \frac{\left(\frac{A_d}{C} bxf''(\Omega)\sqrt{\frac{b}{\nu_f}} + \frac{A_d}{6C^3} b^3x^3 \big(f''(\Omega)\big)^3 \big(\sqrt{\frac{b}{\nu_f}}\big)^3 \right)_{y=0}}{\frac{1}{2}Re_x \mu_f b} \\
&= \frac{\left(\frac{A_d}{\mu_f C} xf''(\Omega)\sqrt{\frac{b}{\nu_f}} + \frac{A_d}{\mu_f C} \frac{b^2x^3}{6C^2} \big(f''(\Omega)\big)^3 \big(\sqrt{\frac{b}{\nu_f}}\big)^3 \right)}{\frac{1}{2}Re_x} \\
&= \frac{\left(A_1^* f''(\Omega) x\sqrt{\frac{b}{\nu_f}} + A_1^* \frac{b^2x^3}{6C^2} \big(f''(\Omega)\big)^3 \big(\sqrt{\frac{b}{\nu_f}}\big)^3 \right)}{\frac{1}{2}Re_x} \\
\frac{1}{2}C_f Re_x &= x\sqrt{\frac{b}{\nu_f}} \left(A_1^* f''(\Omega) + A_1^* \frac{b^2x^2}{6C^2} \big(f''(\Omega)\big)^3 \big(\sqrt{\frac{b}{\nu_f}}\big)^2 \right) \\
\frac{1}{2}C_f Re_x &= \sqrt{Re_x} \left(A_1^* f''(\Omega) + \frac{1}{3} A_1^* A_2^* \big(f''(\Omega)\big)^3 \right) \\
\frac{1}{2}C_f (Re_x)^{\frac{1}{2}} &= \left(A_1^* f''(\Omega) + \frac{1}{3} A_1^* A_2^* \big(f''(\Omega)\big)^3 \right) \\
\Rightarrow \quad C_f (Re_x)^{\frac{1}{2}} &= \left(2A_1^* f''(\Omega) + \frac{2}{3} A_1^* A_2^* \big(f''(\Omega)\big)^3 \right).
\end{aligned} \tag{3.33}$$

Here $Re_x = \frac{U_w x}{\nu_f}$ denotes the local Reynolds number.

Nusselt number is defined as follows.

$$Nu_x = \frac{xq_w}{\kappa_f (\mathcal{T}_w - \mathcal{T}_\infty)}. \tag{3.34}$$

The dimensionless form of Nu_x is produced by the following steps:

$$q_w = -\kappa_{hnf}\Big(1+\frac{16\sigma^*\mathcal{T}_\infty^3}{3k^*\nu_f(\rho C_p)_f}\Big)\Big(\frac{\partial\mathcal{T}}{\partial y}\Big)_{y=0}. \tag{3.35}$$

$$\begin{aligned} Nu_x &= -\frac{x\kappa_{hnf}\Big(1+\frac{16\sigma^*\mathcal{T}_\infty^3}{3k^*\nu_f(\rho C_p)_f}\Big)\Big(\frac{\partial\mathcal{T}}{\partial y}\Big)_{y=0}}{\kappa_f(\mathcal{T}_w-\mathcal{T}_\infty)}\\ &= -\frac{\kappa_{hnf}\Big(1+\frac{16\sigma^*\mathcal{T}_\infty^3}{3k^*\nu_f(\rho C_p)_f}\Big)x\theta'(0)\sqrt{\frac{b}{\nu_f}}}{\kappa_f}\\ &= -\frac{\kappa_{hnf}\Big(1+\frac{16\sigma^*\mathcal{T}_\infty^3}{3k^*\nu_f(\rho C_p)_f}\Big)\sqrt{x}\sqrt{x}\theta'(0)\sqrt{\frac{b}{\nu_f}}}{\kappa_f}\\ &= -\frac{\kappa_{hnf}\Big(1+\frac{16\sigma^*\mathcal{T}_\infty^3}{3k^*\nu_f(\rho C_p)_f}\Big)\theta'(0)\sqrt{\frac{bxx}{\nu_f}}}{\kappa_f}\\ &= -\frac{\kappa_{hnf}\Big(1+\frac{16\sigma^*\mathcal{T}_\infty^3}{3k^*\nu_f(\rho C_p)_f}\Big)\theta'(0)\sqrt{\frac{U_wx}{\nu_f}}}{\kappa_f} \end{aligned}$$

$$\Rightarrow \quad Nu_xRe_x^{-\frac{1}{2}} = -\frac{\kappa_{hnf}}{\kappa_f}(1+Ns)\theta'(0). \tag{3.36}$$

The entropy generation rate N_G is defined as:

$$N_G = \frac{\mathcal{T}_\infty^2 b^2 E_G}{\kappa_f(\mathcal{T}_w-\mathcal{T}_\infty)^2}. \tag{3.37}$$

The dimensionless form of N_G can be produced through the following steps:

$$E_G = \frac{\kappa_{hnf}}{\mathcal{T}_\infty^2}\Bigg(\Big(\frac{\partial\mathcal{T}}{\partial y}\Big)^2+\frac{16}{3}\frac{\sigma^*\mathcal{T}_\infty^3}{k^*\nu_f(\rho C_p)_f}\Big(\frac{\partial\mathcal{T}}{\partial y}\Big)^2\Bigg)+\frac{\mu_{hnf}}{\mathcal{T}_\infty}\Big(\frac{\partial B_1}{\partial y}\Big)^2+\frac{\mu_{hnf}B_1^2}{k\mathcal{T}_\infty}. \tag{3.38}$$

$$\begin{aligned} \therefore \quad N_G &= \frac{\mathcal{T}_\infty^2 b^2}{\kappa_f(\mathcal{T}_w-\mathcal{T}_\infty)^2}\Bigg(\frac{k_{hnf}}{\mathcal{T}_\infty^2}\Big(\big(bx\theta'\sqrt{\frac{b}{\nu_f}}\big)^2+\frac{16}{3}\frac{\sigma^*\mathcal{T}_\infty^3}{k^*\nu_f(\rho C_p)_f}\big(bx\theta'\sqrt{\frac{b}{\nu_f}}\big)^2\Big)\\ &\quad+\frac{\mu_{hnf}}{\mathcal{T}_\infty}\big(bxf''\sqrt{\frac{b}{\nu_f}}\big)^2+\frac{\mu_{hnf}}{k\mathcal{T}_\infty}(bxf')^2\Bigg)\\ N_G &= \frac{b^2}{\kappa_f(\mathcal{T}_w-\mathcal{T}_\infty)^2}\Bigg(k_{hnf}\Big(\big(b^2x^2(\theta')^2\frac{b}{\nu_f}\big)+N_\varsigma\big(b^2x^2(\theta')^2\frac{b}{\nu_f}\big)\Big)\\ &\quad+\mathcal{T}_\infty\mu_{hnf}\big(b^2x^2(f'')^2\frac{b}{\nu_f}\big)+\frac{\mathcal{T}_\infty\mu_{hnf}}{k}b^2x^2(f')^2\Bigg) \end{aligned}$$

$$
\begin{aligned}
N_G = & \frac{1}{\kappa_f(\mathcal{T}_w - \mathcal{T}_\infty)^2} \quad k_{hnf} \left(\frac{b^5 x^2 (\theta\prime)^2}{\nu_f}\right) [1 + N_\varsigma] \\
& + \mathcal{T}_\infty \mu_{hnf} \left(\frac{b^5 x^2 (f'')^2}{\nu_f}\right) + \frac{\mathcal{T}_\infty \mu_{hnf}}{k} b^4 x^2 (f')^2 \Bigg) \\
= & \frac{R_e}{\kappa_f(\mathcal{T}_w - \mathcal{T}_\infty)^2} \Bigg(k_{hnf}(b^2 x^2 (\theta')^2 (1 + N_\varsigma) + \mathcal{T}_\infty \mu_{hnf}(b^2 x^2 (f'')^2) \\
& + \frac{\mathcal{T}_\infty \mu_{hnf}}{k} \nu_f b x^2 (f')^2 \Bigg) \\
= & R_e \left(\phi_d (1 + N_\varsigma)(\theta')^2 + \frac{\mathcal{T}_\infty \mu_f b^2 x^2 (f'')^2}{\phi_a \kappa_f (\mathcal{T}_w - \mathcal{T}_\infty)^2} + \frac{\mathcal{T}_\infty \mu_f \nu_f b x^2 (f')^2}{\phi_a \kappa_f k (\mathcal{T}_w - \mathcal{T}_\infty)^2} \right) \\
= & R_e \left(\phi_d (1 + N_\varsigma)(\theta')^2 + \frac{\mu_f b^2 x^2}{\phi_a \kappa_f (\mathcal{T}_w - \mathcal{T}_\infty)} \left(\frac{\mathcal{T}_\infty}{\mathcal{T}_w - \mathcal{T}_\infty} (f'')^2 + \frac{\mathcal{T}_\infty \nu_f (f')^2}{k b (\mathcal{T}_w - \mathcal{T}_\infty)} \right) \right) \\
= & R_e \left(\phi_d (1 + Ns) \theta'^2 + \frac{1}{\phi_a} \frac{Bs}{\eta} \left(f''^2 + \frac{\nu_f}{kb} (f')^2 \right) \right) \\
N_G = & R_e \left(\phi_d (1 + Ns) \theta'^2 + \frac{1}{\phi_a} \frac{Bs}{\eta} \left(f''^2 + K_\varsigma (f')^2 \right) \right). \qquad (3.39)
\end{aligned}
$$

where $R_e = \frac{U_w b^2}{\nu_f x}$, $B_\varsigma = \frac{\mu_f U_w^2}{\kappa_f(\mathcal{T}_w - \mathcal{T}_\infty)}$, and $\eta = \frac{(\mathcal{T}_w - \mathcal{T}_\infty)}{\mathcal{T}_\infty}$ denote the Reynolds number, Brinkmann number and dimensionless temperature gradient respectively.

3.3 Numerical Method for Solution

Since equation (3.28) is independent of θ. Hence it can be solved independently by using the shooting technique.

$$
f''' = \frac{K_\varsigma f'}{\phi_a A_1^* \left(1 - A_2^* f''^2\right)} - \frac{\phi_b \left(f f'' - f'^2\right)}{A_1^* \left(1 - A_2^* f''^2\right)}. \qquad (3.40)
$$

The following notations are used for this purpose:

$$
\begin{aligned}
f &= J_1, \\
f' &= J_1' = J_2, \\
f'' &= J_1'' = J_2' = J_3.
\end{aligned}
$$

The momentum equation is then turned into the system of first-order ODEs represented follows.

$$
\begin{aligned}
J_1' &= J_2, && J_1(0) = S.\\
J_2' &= J_3, && J_2(0) = 1 + A_\varsigma J_3(0).\\
J_3' &= \frac{K_\varsigma J_2}{\phi_a A_1^*\big(1 - A_2^* J_3^2\big)} - \frac{\phi_b\big(J_1 J_3 - J_2^2\big)}{A_1^*\big(1 - A_2^* J_3^2\big)}, && J_3(0) = q.
\end{aligned}
$$

The Runge-Kutta technique of order four will be used to solve the above IVP.

The domain of the problem is to be bounded. i.e. $[0,\ \Omega_\infty]$, where Ω_∞ is a +ve real number. In this flow prolem Ω_∞ is taken as 6.The missing condition q is to be selected such that.

$$J_2(\Omega_\infty, q) = 0.$$

To determine q, Newton's technique will be utilised. The iterative technique for this method is as follows:

$$q_{n+1} = q_n - \frac{J_2(\Omega_\infty, q_n)}{\left(\frac{\partial}{\partial q} J_2(\Omega_\infty, q)\right)_{q=q_n}}.$$

To incorporate the above iterative scheme we further need the following derivatives.

$$
\begin{aligned}
\frac{\partial J_1}{\partial q} &= J_4,\\
\frac{\partial J_2}{\partial q} &= J_5,\\
\frac{\partial J_3}{\partial q} &= J_6.
\end{aligned}
$$

As a consequence of such new notations, Newton's iterative technique took the following form:

$$q_{n+1} = q_n - \frac{J_2(\Omega_\infty, q_n)}{J_5(\Omega_\infty, q_n)}, \qquad n = 0, 1, 2, 3, ...$$

Differentiating the above system of three first order ODEs with regard to q yields the following system of ODEs.

$$
\begin{aligned}
&J_4' = J_5, && J_4(0) = 0.\\
&J_5' = J_6, && J_5(0) = A_\varsigma.\\
&J_6' = \frac{2A_1^*A_2^*J_3J_6}{\big(A_1^* - A_1^*A_2^*J_3^2\big)^2}\bigg(\big(\frac{K_\varsigma J_2}{\phi_a}\big) - \phi_b\big(J_1J_3 - J_2^2\big)\bigg) \\
&\quad + \big(\frac{K_\varsigma J_5}{\phi_a}\big) - \phi_b\big(J_1J_6 + J_3J_4 - 2J_2J_5\big)\bigg(\frac{1}{A_1^* - A_1^*A_2^*J_3^2}\bigg), && J_6(0) = 1.
\end{aligned}
$$

Following stopping criteria is used for Newton's Method.

$$
\mid J_2(\Omega_\infty, q) \mid < \epsilon,
$$

where $\epsilon > 0$ is a suitable small value, which are taken to be 10^{-5}.

To solve (3.29) numerically, shooting method is used. This equation contains two dependent variable θ and f. Solution of f is incorporated numerically to solve (3.29).

More precisely the shooting approach is used to approximate the ordinary differential equation (3.29), assuming f as a known function.

$$
\begin{aligned}
\theta'' = &\frac{1}{1 + \frac{P_\varsigma N_\varsigma}{\phi_d} - \epsilon_\varsigma(f^2)\frac{\phi_c}{\phi_d}P_\varsigma}\bigg(- P_\varsigma\frac{\phi_c}{\phi_d} \times \Big(f\theta' - f'\theta + \frac{E_\varsigma}{\phi_a\phi_c}f''^2 \\
&- \epsilon_\varsigma\big(f'^2\theta - ff'\theta' - ff''\theta\big)\Big)\bigg).
\end{aligned} \tag{3.41}
$$

Following notations are used.

$$
\begin{aligned}
\theta &= L_1,\\
\theta' &= L_1' = L_2.
\end{aligned}
$$

The energy equation (3.41) is then transformed into the system of first-order ODEs shown below.

$$
L_1' = L_2, \qquad\qquad L_1(0) = r.
$$

$$L_2' = \frac{1}{1 + \frac{P\varsigma N_\varsigma}{\phi_d} - \epsilon_\varsigma (J_1^2)\frac{\phi_c}{\phi_d} P\varsigma} \Bigg(- P\varsigma \frac{\phi_c}{\phi_d} \times \Big(J_1 L_2 - J_2 L_1 + \frac{E_\varsigma}{\phi_a \phi_c} J_3^2$$

$$- \epsilon_\varsigma \big(J_2^2 L_1 - J_1 J_2 L_2 - J_1 J_3 L_1 \big) \Big) \Bigg), \qquad L_2(0) = -H_\varsigma (1 - L_1(0)).$$

The above IVP will be solved using the Runge-Kutta technique of order four. The missing condition r is to selected in such a way that.

$$L_1(\Omega_\infty, r) = 0.$$

The above equation can be solved by using Newton's method for the value with the following iterative formula.

$$r_{n+1} = r_n - \frac{L_1(\Omega_\infty, r_n)}{(\frac{\partial}{\partial r} L_1(\Omega_\infty, r))_{r=r_n}}. \qquad n = 0, 1, 2, 3, ...$$

Introduce the notations shown below:

$$\frac{\partial L_1}{\partial r} = L_3, \qquad \frac{\partial L_2}{\partial r} = L_4.$$

As a result of these new notations, the Newton's iterative scheme gets the form:

$$r_{n+1} = r_n - \frac{L_1(\Omega_\infty, r_n)}{L_3(\Omega_\infty, r_n)}.$$

Now differentiating the system of two first order ODEs with respect to r, we get another system of ODEs, as follows.

$$L_3' = L_4, \qquad L_3(0) = 1.$$

$$L_4' = \frac{1}{1 + \frac{P\varsigma N_\varsigma}{\phi_d} - \epsilon_\varsigma (J_1^2)\frac{\phi_c}{\phi_d} P\varsigma}$$

$$\Bigg(- P\varsigma \frac{\phi_c}{\phi_d} \times \Big(J_1 L_4 - J_2 L_3 - \epsilon_\varsigma \big(J_2^2 L_3 - J_1 J_2 L_4 - J_1 J_3 L_3 \big) \Big) \Bigg), L_4(0) = H_\varsigma.$$

The stopping criteria for the Newton's method is set as:

$$\mid L_1(\Omega_\infty, r) \mid < 10^{-5}.$$

3.4 Representation of Graphs and Tables

A thorough discussion on the graphs and tables is conducted which contains the impact of dimensionless parameters on the skin friction coefficient $(Re_x)^{\frac{1}{2}}C_f$ and local Nusselt number $(Re_x)^{\frac{-1}{2}}Nu_x$. Tables 3.3 and 3.4 explains the impact of parameter A_1^*, A_2^*, porosity parameter K_ς, nanoparticle volume fractions ϕ_{ST}, ϕ_{MT}, velocity slip A_ς, injection parameter S, thermal radiation parameter N_ς, relaxation time parameter ϵ_ς and Biot number H_ς on $(Re_x)^{\frac{1}{2}}C_f$.

For the rising values of ϕ_{ST} and ϕ_{MT}, the skin fraction coefficient $(Re_x)^{\frac{1}{2}}C_f$ decreases. In Tables 3.5 and 3.6, the effect of significant parameters on local Nusselt number $(Re_x)^{\frac{-1}{2}}Nu_x$ has been discussed. The rising pattern is found in $(Re_x)^{\frac{-1}{2}}Nu_x$ due to increasing values of A_1^*.

3.4.1 Influence of Prandtl-Eyring Parameter A_1^*

Figures 3.2, 3.3 and 3.4 show the impact of the Prandtl-Eyring parameter A_1^* on the velocity $f'(\Omega)$, energy $\theta(\Omega)$ and entropy generation N_G of PEHNF. Velocity fluctuation $f'(\Omega)$ for increasing value of A_1^* is shown in Figure 3.2. As the value of A_1^* is increased the velocity profile is increased for both fluid. The physical cause of this phenomenon is that, the increased value of A_1^* reduce the viscosity which inturns reduce resistance while increasing fluid velocity. MWCNT-SWCNT hybrid nanofluid, accelerates more quickly than SWCNT nanofluid. It is explained by the fact that the hybrid nanofluid has a much greater density impact than the nanofluid.

The energy $\theta(\Omega)$ for the Prandtl–Eyring parameter A_1^* is shown in Figure 3.3. Due to the increased value of A_1^*, the MWCNT-SWCNT hybrid nanofluid has a higher temperature profile, whereas the SWCNT nanofluid has a lower temperature profile. Another observation is that the hybrid nanofluid has significantly less thermal conductivity than pure nanofluid. Prandtl-Eyring hybrid nanofluid entropy fluctuation N_G based on its parameterA_1^* is depicted in Figure 3.4. As the value of A_1^* increases, the amount of entropy generation decreased. MWCNT-SWCNT fluid have a higher entropy profile than SWCNT hybrid nanofluid. This phenomena occurs due to the reason that less temperature slows down the motion of hybrid nanofluid which causes decrease in entropy generation.

3.4.2 Influence of Prandtl-Eyring Parameter A_2^*

The impact of Prandtl-Eyring Parameter A_2^* on the Prandtl-Eyring hybrid nanofluid velocity, temperature, and entropy generation profile is shown in Figure 3.5 to Figure 3.7.

Figure 3.5 displays the impact of increasing A_2^* on velocity profile of fluid. Resistance is produced by hybrid nanofluid particles because they vary inversely with momentum diffusivity. As a result, the velocity of the flow is reduced.

Figure 3.6 indicates the temperature change with respect to Prandtl-Eyring parameter A_2^*. As the value of A_2^* increases temperature profile decreases.

Figure 3.7 exhibits the entropy change as a function of the Prandtl-Eyring parameter A_2^*. The entropy profile increases as the value of A_2^* is increased, which clearly demonstrating a relationship between entropy and A_2^*. It indicates that A_2^* enhance the system's obstacle by increasing the entropy of the system.

3.4.3 Impact of Porous Media Variable K_ς.

Figures 3.8, 3.9, and 3.10 show that surface porousness has an impact on flow rate, heat domain, and entropy generation.

In Figure 3.8 raising the value of K_ς, porousity of the surface is enhanced, which allows more fluid to pass through. In comparison to SWCNT/EO nanofluid, the hybrid nanofluid moves slowly across the porous medium. This slow speed may be caused by the extra particles delaying the flow of the hybrid nanofluid through the porous surface.

Figure 3.9 illustrates that by increasing the porous medium variable (K_ς) , the temperature dispersion is improved throughout the domain of fluid. Due to the porous medium the flow is slowed down and surface needs more time to absorb the heat.

Figure 3.10 shows the impact of K_ς on entropy generation, by enhancing the values of K_ς the entropy profile also increases.

3.4.4 Impact of Velocity Slip Variable A_ς.

The effects of enhanced slip conditions on flow nature, thermal characteristics, and entropy formation are reviewed through Figures 3.11 , 3.12, and 3.13.

These figures illustrate the impact of A_ς on $f'(\Omega)$, $\theta(\Omega)$ and N_G. The flow conditions in the hybrid Prandtl-Eyring fluid are primarily focused on the viscous behavior as shown in Figure 3.11. This occurrence in fluids makes slip conditions extremely important. The viscous properties and higher number of flow slip parameter in a hybrid Prandtl-Eyring nanofluid lead to complicated fluidity conditions, which causes the fluidity of the single nanofluid to drop quickly.

The MWCNT-SWCNT/EO nanofluid maintains a higher temperature state than SWCNT/EO hybrid nanofluid, as shown in Figure 3.12. The decrease in velocity will have a similar impact on the increase in boundary layer viscosity. The nanofluid has lower viscosity than the hybrid nanofluid. Hence MWCNT-SWCNT/EO is expected to have a higher temperature than SWCNT-EO.

In Figure 3.13 higher slip parameter shows a descending trend in entropy formation because the slipped flow acts against the domain's entropy formation.

3.4.5 Influence of Thermal Radiative Parameter N_ς and Relaxation Time Parameter ϵ_ς.

Figures 3.14 and 3.15 describes the thermal diffusion and entropy generation while raising the value of thermal radiative parameter N_ς.

In Figure 3.14 temperature is raised by increasing the values of N_ς. Physical reason of temperature increase is that thermal radiation are transformed into electromagnetic energy, as a result, radiation is emitted from a greater distance, away from the surface, ultimately superheating the boundary layer flow. Therefore, the thermal radiative variable plays a significant role in determining the temperature profile of the system.

Impact of N_ς on entropy generation is illustrated in Figure 3.15. MWCNT-SWCNT hybrid nanofluid have higher entropy profile than SWCNT nanofluid. This occurrence can be clarified by the system's irreversible heat transfer mechanism.

Figures 3.16 and 3.17 displays the impact of ϵ_ς on the temperature and entropy. In Figure 3.16, rising the values of ϵ_ς, the temperature profile decreases.
Figure 3.17 shows the engine oil based entropy profile, when value of ϵ_ς increases entropy profile also increases.

3.4.6 Effect of the Solid Particle Shape m.

Nanoparticles have enhanced thermal conductivity and heat transfer rates under various physical conditions. In porous medium it is very difficult to handle these nano particles. The forms assumed here are ranged from spherical (m=3) to lamina (m=16.176).
Figure 3.18 shows the impact of shape factor m on the temperature. By rising the values of m, the temperature profile decreases. The MWCNT-SWCNT with base fluid EO has a more notable impact than SWCNT with base fluid EO. In comparison to nanofluid, hybrid nanofluid has a wider thermal layer of boundary and better thermal distribution.

In the MWCNT-SWCNT with base fluid EO, the lamina (m=16.176) shaped particles remain in front of the other particles. The physical explanation for this phenomenon is that lamina-shaped particles exhibit the most notable viscosity, whereas spheres exhibit the least viscosity.

Figure 3.19 describes the influence of shape factor m on the entropy. Increasing values of m increased entropy generation.

In comparison to SWCNT-EO mono nanofluid, MWCNT-SWCNT/EO NHF have a more significant impact and higher entropy rate.

3.4.7 Impact of Entropy for Reynolds Number (R_e) and Brinkman Number (B_ς).

Figure 3.20 shows the influence of Reynolds number Re, on N_G. Entropy profile N_G is increased by increasing the value of R_e.

All Reynolds number supports nanoparticles to move in porous media due to inertia on viscous forces in the system. Due to the combined effeciency of the particles entropy rate of MWCNT-SWCNT/EO is higher than SWCNT/EO nanofluid.

Figure 3.21 shows the impact of Brinkmann amount B_ς, on N_G. By increasing values of B_ς, the entropy profile N_G) is increased.

The Brinkman number (B_ς) are used to depicts the heat generated by viscous properties as viscous properties increase the generated heat. Ability of such viscous properties enhanced heat that promotes entropy generation in system.

TABLE 3.3: Results of $(Re_x)^{\frac{1}{2}}C_f$ for various parameters, P_ς= 6450

A_1^*	A_2^*	K_ς	ϕ_{ST}	ϕ_{MT}	A_ς	S	N_ς	ϵ_ς	H_ς	$(Re_x)^{\frac{1}{2}}C_f$ SWCNT
1.0	0.4	0.1	0.18	0.09	0.3	0.4	0.3	0.2	0.3	-2.4151
1.1										-2.5093
1.2										-2.6016
	0.2									-2.1406
	0.4									-2.4151
	0.6									-2.8523

A_1^*	A_2^*	K_ς	ϕ_{ST}	ϕ_{MT}	A_ς	S	N_ς	ϵ_ς	H_ς	$(Re_x)^{\frac{1}{2}}C_f$ SWCNT
		0.1								-2.4151
		0.15								-2.4803
		0.18								-2.5189
			0.09							-2.2102
			0.15							-2.3461
			0.18							-2.4151
				0.0						-
				0.06						-
				0.09						-
					0.27					-2.5682
					0.30					-2.4151
					0.33					-2.4151
						0.2				-2.2847
						0.4				-2.3148
						0.6				-2.4151
							0.2			-2.7454
							0.3			-2.4151
							0.4			-2.4151
								0.1		-2.4151
								0.2		-2.4151
								0.3		-2.4151
									0.1	-2.4151
									0.3	-2.4151
									0.5	-2.4151

TABLE 3.4: Results of $(Re_x)^{\frac{1}{2}}C_f$ for various parameters, P_ς= 6450

A_1^*	A_2^*	K_ς	ϕ_{ST}	ϕ_{MT}	A_ς	S	N_ς	ϵ_ς	H_ς	$(Re_x)^{\frac{1}{2}}C_f$ MWCNT
1.0										-2.4906
1.1										-2.5861
1.2										-2.6798
	0.2									-2.1937
	0.4									-2.4906
	0.6									-2.9851
		0.1								-2.4906
		0.15								-2.5718
		0.18								-2.6199
			0.09							-2.2953
			0.15							-2.4243
			0.18							-2.4906
				0.0						-2.4151
				0.06						-2.4642
				0.09						-2.4906
					0.27					-2.6553
					0.30					-2.4906
					0.33					-2.3514
						0.2				-2.1987
						0.4				-2.4906
						0.6				-2.8376
							0.2			-2.4906
							0.3			-2.4906
							0.4			-2.4906
								0.1		-2.4906
								0.2		-2.4906
								0.3		-2.4906
									0.1	-2.4906
									0.3	-2.4906
									0.5	-2.4906

TABLE 3.5: Results of $N_u(Re_x)^{\frac{-1}{2}}$ for various parameters, P_ς= 6450

A_1^*	A_2^*	K_ς	ϕ_{ST}	ϕ_{MT}	A_ς	S	N_ς	ϵ_ς	H_ς	$N_u(Re_x)^{\frac{-1}{2}}$ SWCNT
1.0										0.1796
1.1										0.1815
1.2										0.1833
	0.2									0.1799
	0.4									0.1796
	0.6									0.1799
		0.1								0.1796
		0.15								0.1786
		0.18								0.1781
			0.09							0.2444
			0.15							0.1994
			0.18							0.1796
				0.0						-
				0.06						-
				0.09						-
					0.27					0.1779
					0.30					0.1796
					0.33					0.1811
						0.2				0.1566
						0.4				0.1796
						0.6				0.1872
							0.2			0.1899
							0.3			0.1688
							0.4			0.1796
								0.1		0.1751
								0.2		0.1796
								0.3		0.1836
									0.1	0.0637
									0.3	0.1796
									0.5	0.2823

TABLE 3.6: Results of $N_u(Re_x)^{\frac{-1}{2}}$ for various parameters, P_ς= 6450

A_1^*	A_2^*	K_ς	ϕ_{ST}	ϕ_{MT}	A_s	S	N_ς	ϵ_ς	H_ς	$N_u(Re_x)^{\frac{-1}{2}}$ MWCNT
1.0										0.1650
1.1										0.1674
1.2										0.1696
	0.2									0.1654
	0.4									0.1650
	0.6									0.1658
		0.1								0.1650
		0.15								0.1636
		0.18								0.1629
			0.09							0.2311
			0.15							0.1852
			0.18							0.1650
				0.0						0.1796
				0.06						0.1702
				0.09						0.1650
					0.27					0.1627
					0.30					0.1650
					0.33					0.1670
						0.2				0.1567
						0.4				0.1650
						0.6				0.1734
							0.2			0.1749
							0.3			0.1545
							0.4			0.1650
								0.1		0.1601
								0.2		0.1650
								0.3		0.1695
									0.1	0.0586
									0.3	0.1650
									0.5	0.2591

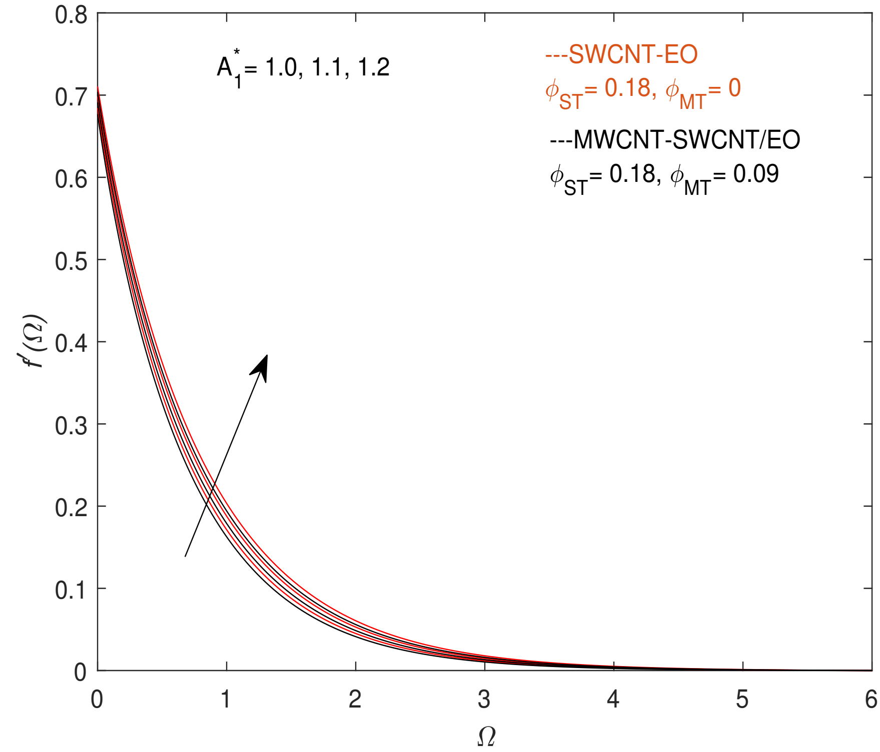

FIGURE 3.2: Impact of velocity against A_1^*

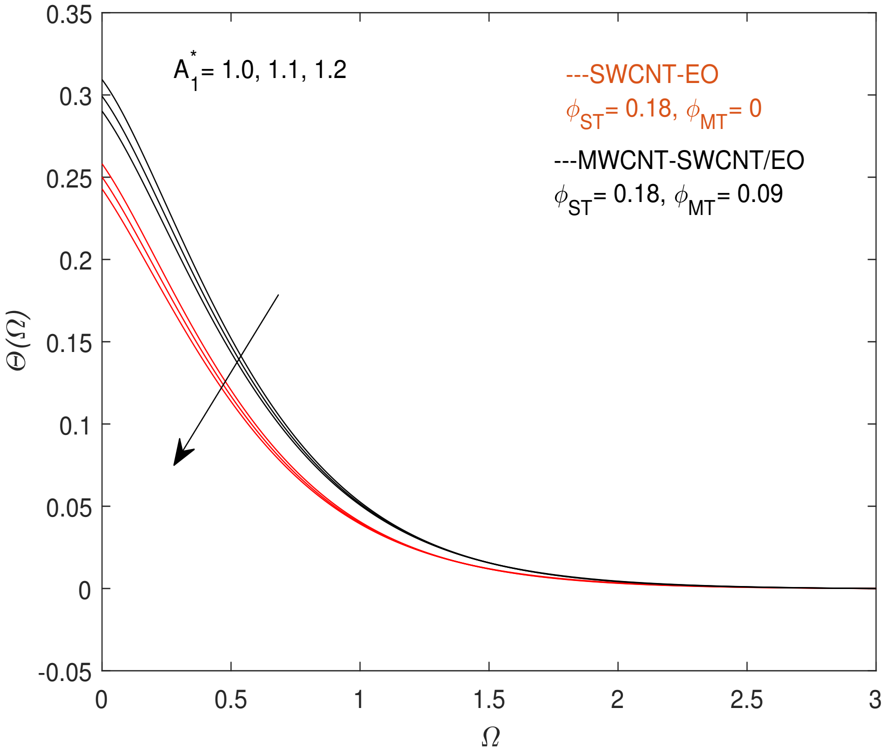

FIGURE 3.3: Impact of temperature against A_1^*

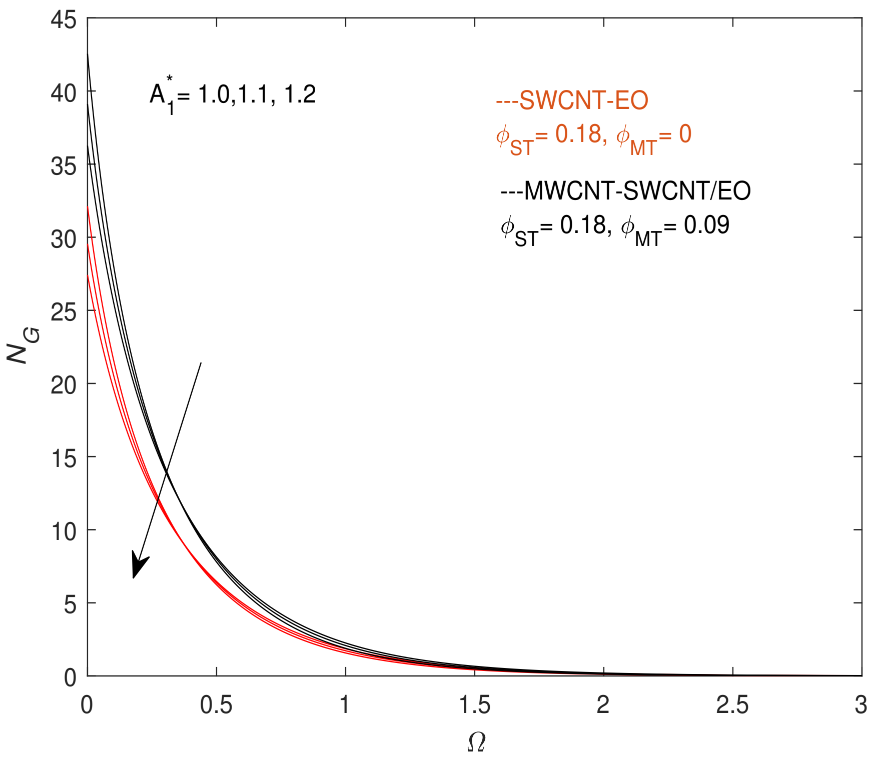

FIGURE 3.4: Impact of entropy against A_1^*

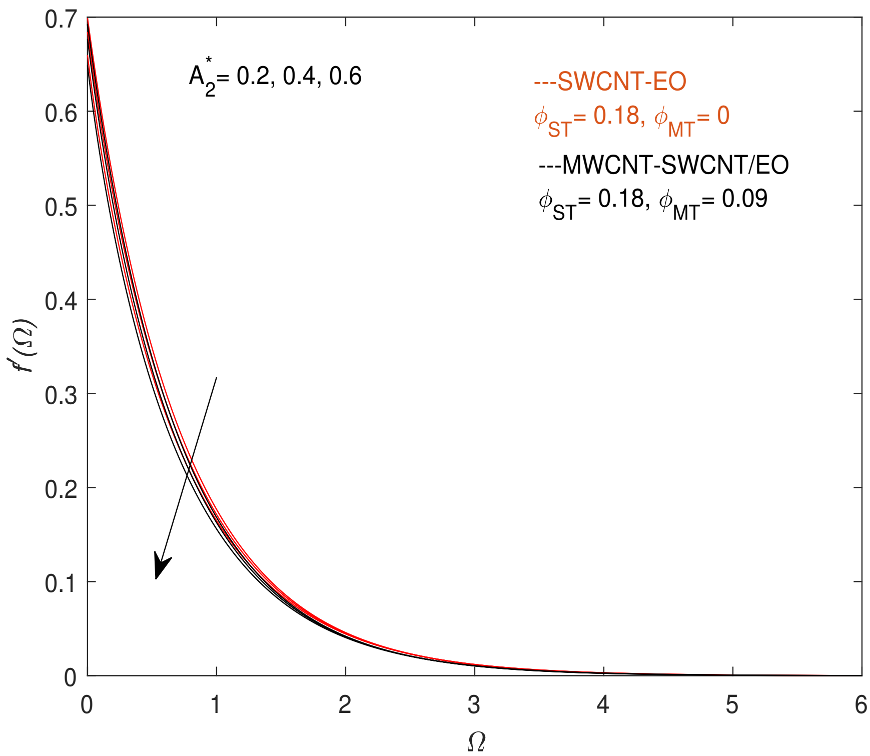

FIGURE 3.5: Impact of velocity against A_2^*

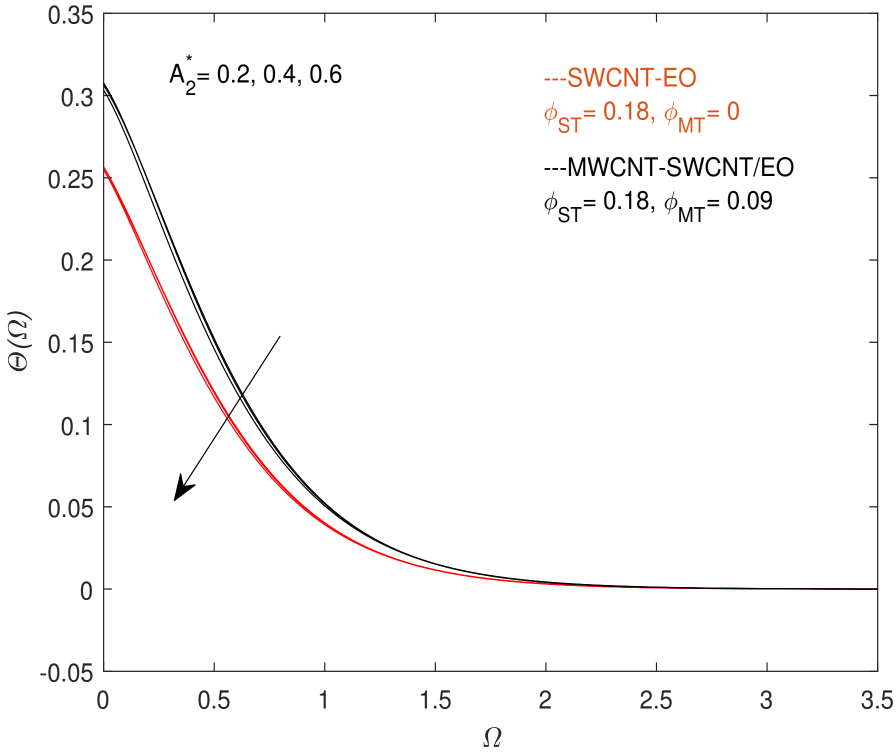

FIGURE 3.6: Impact of temperature against A_2^*

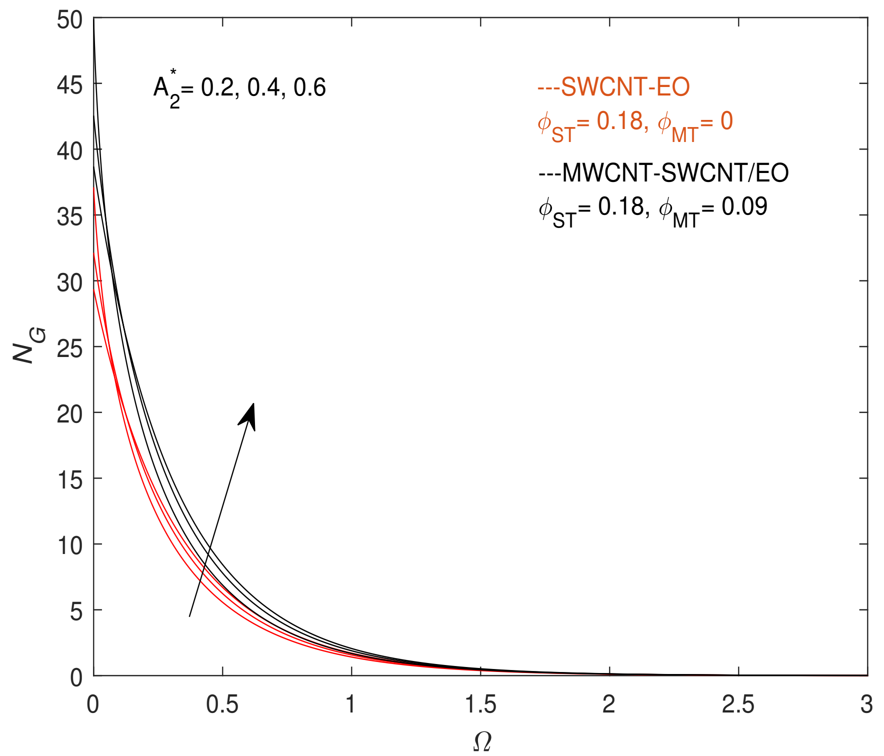

FIGURE 3.7: Impact of entropy against A_2^*

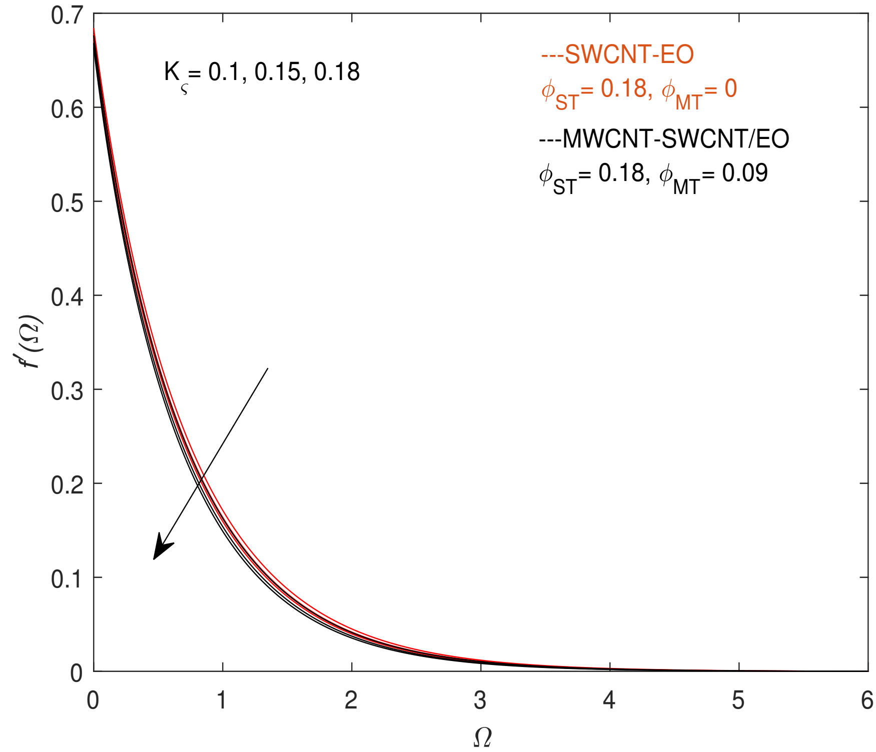

FIGURE 3.8: Impact of velocity against K_ς

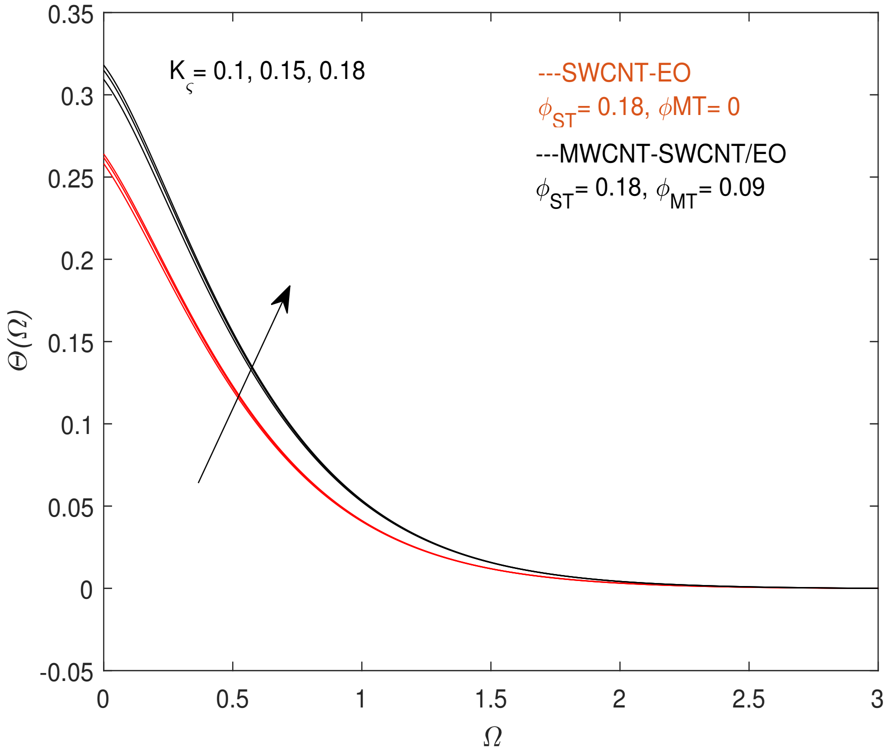

FIGURE 3.9: Impact of temperature against K_ς

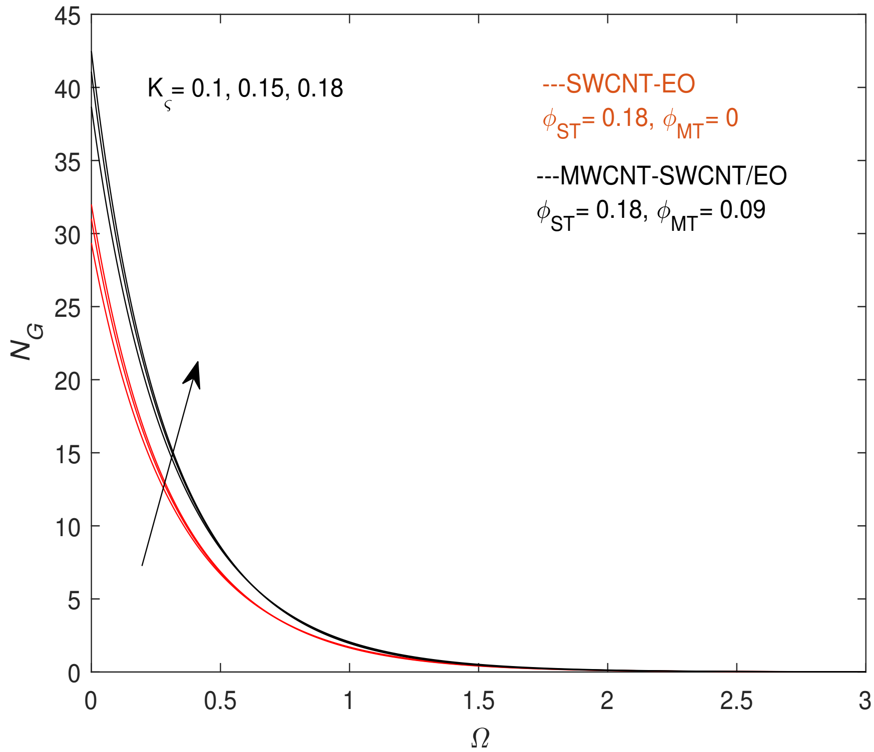

FIGURE 3.10: Impact of entropy against K_ς

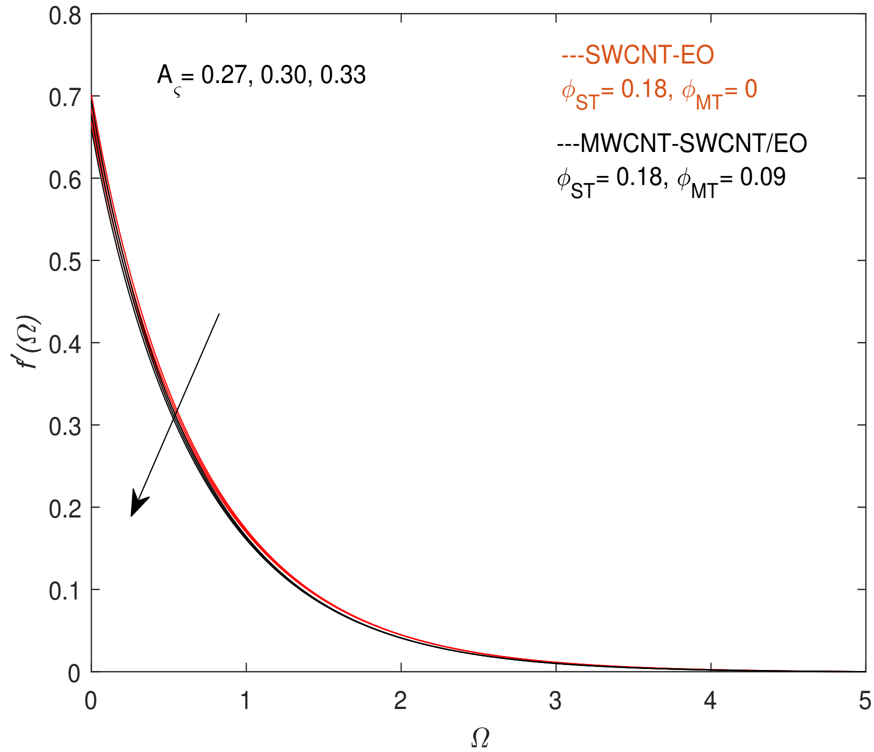

FIGURE 3.11: Impact of velocity against A_ς

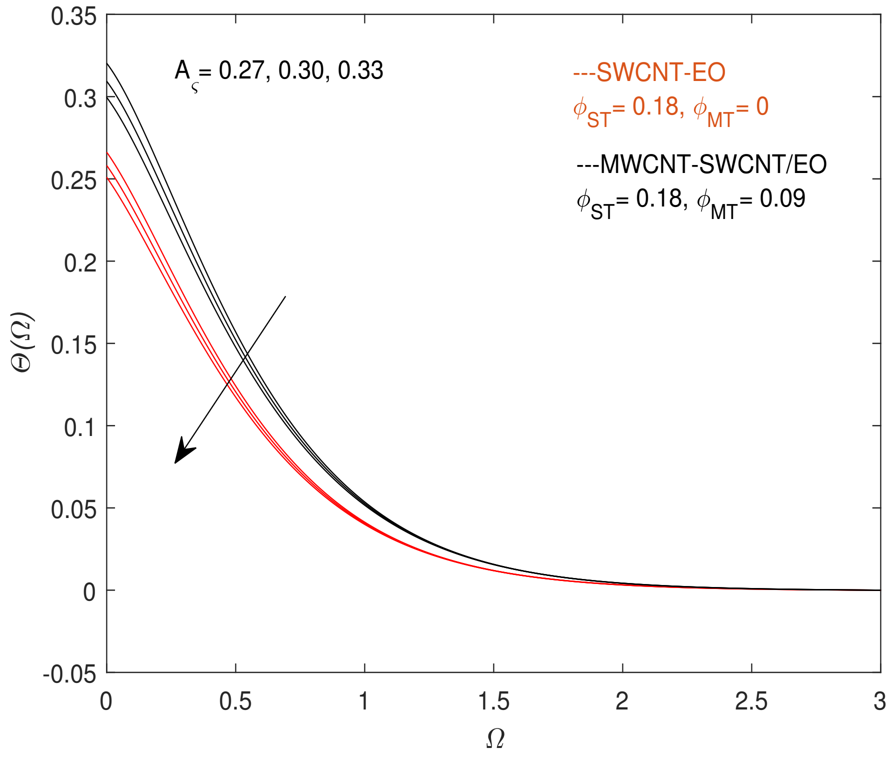

FIGURE 3.12: Impact of temperature against A_ς

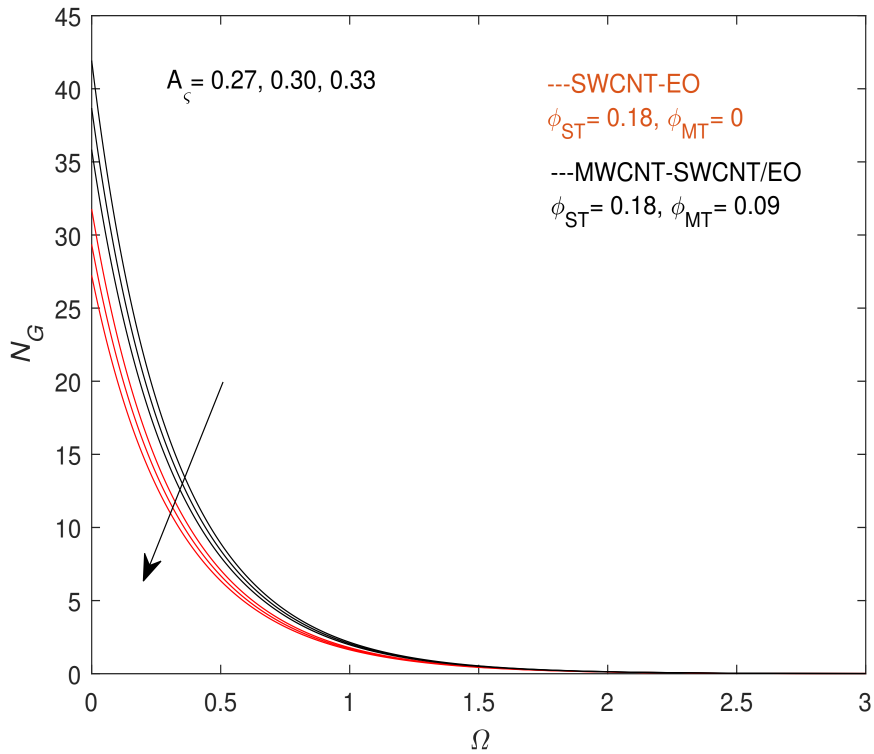

FIGURE 3.13: Impact of entropy against A_ς

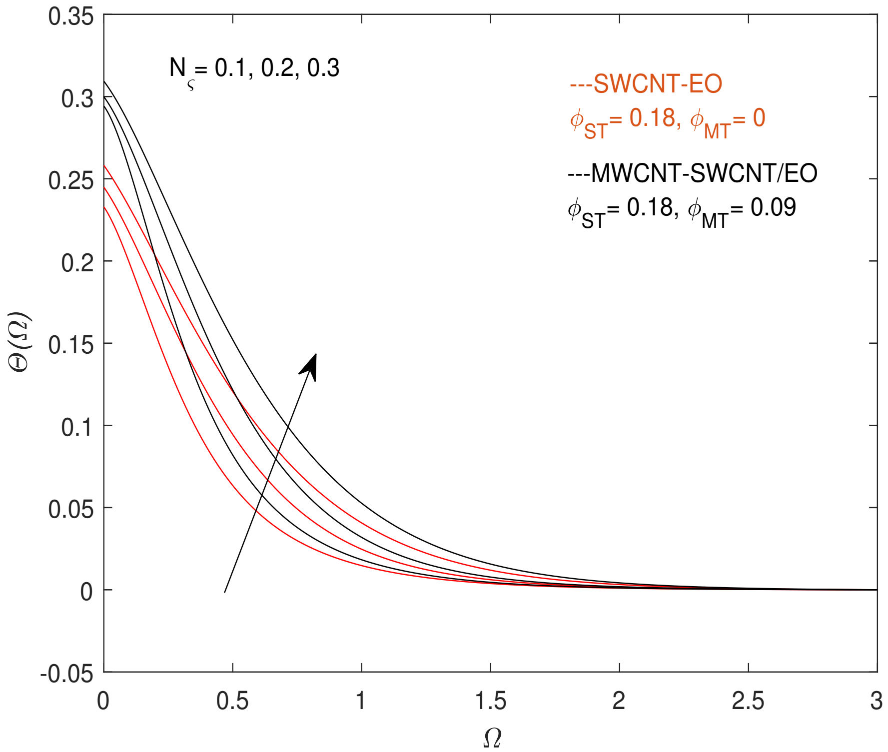

FIGURE 3.14: Impact of temperature against N_ς

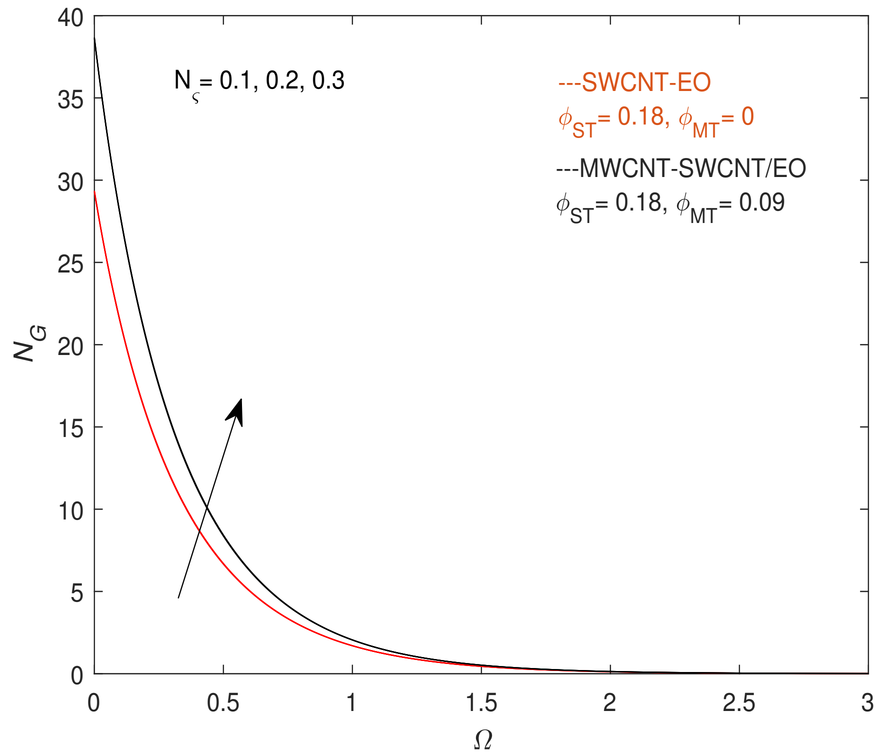

FIGURE 3.15: Impact of entropy against N_ς

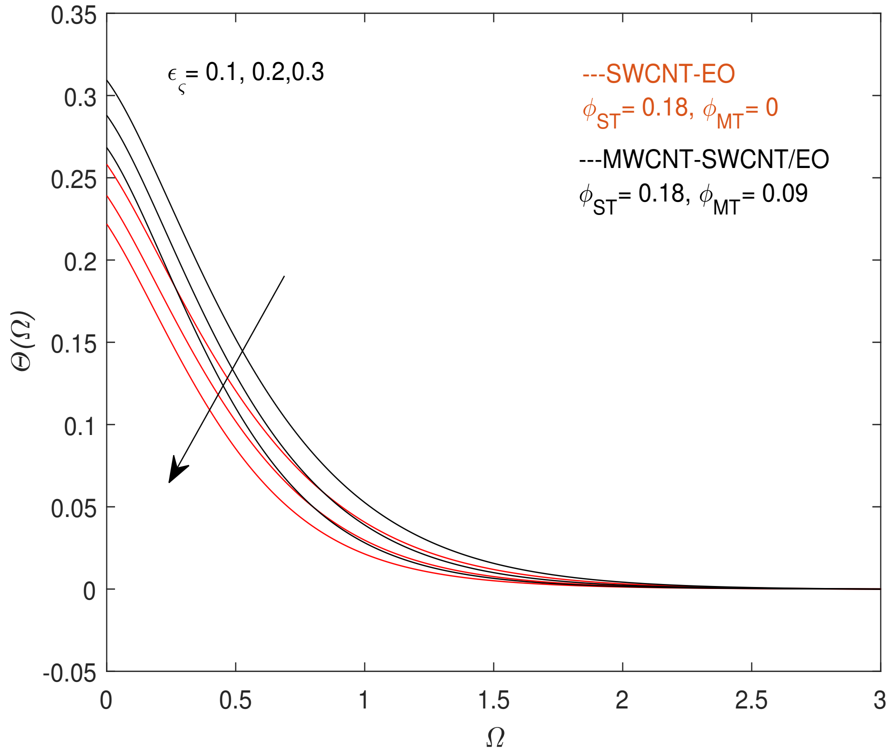

FIGURE 3.16: Impact of temperature against ϵ_ς

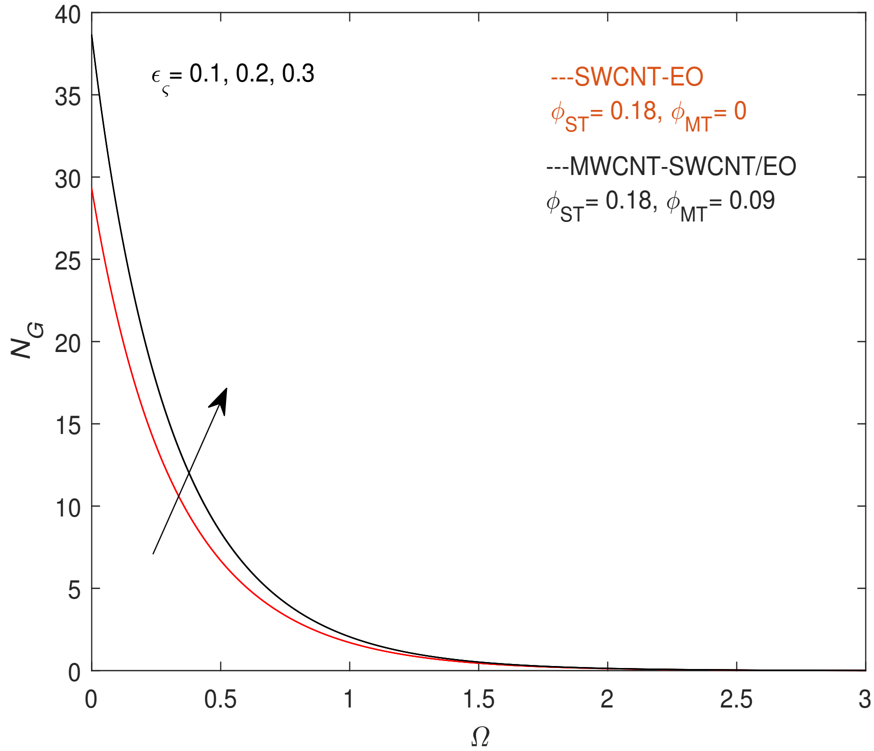

FIGURE 3.17: Impact of entropy against ϵ_ς

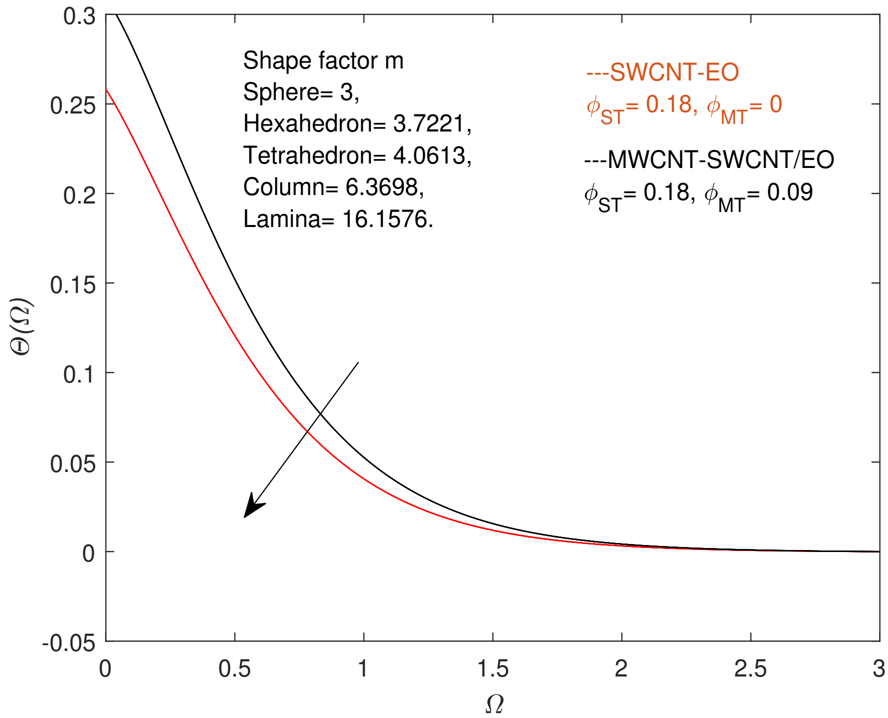

FIGURE 3.18: Impact of temperature against m

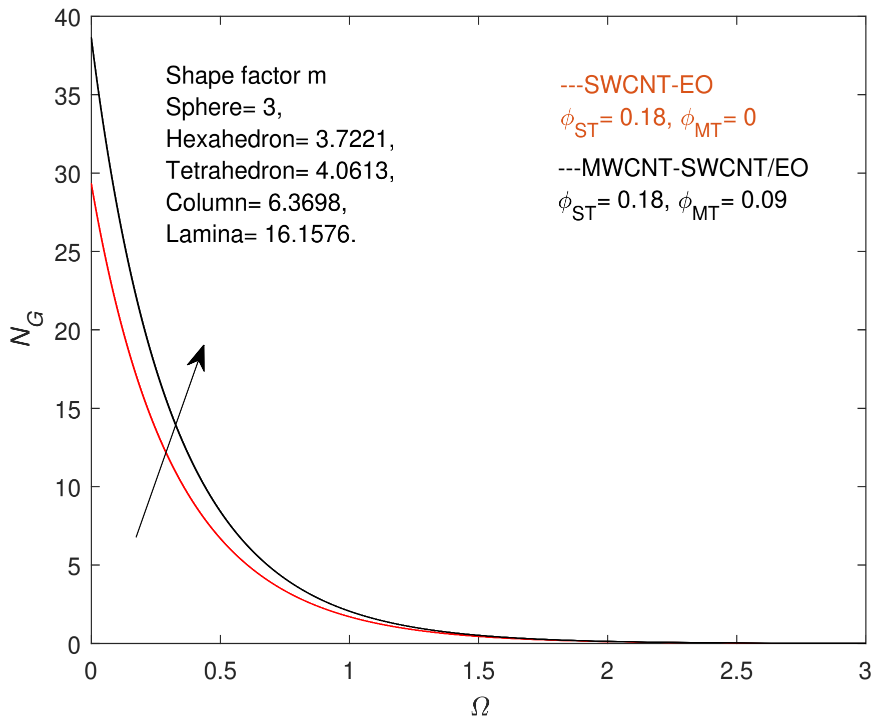

FIGURE 3.19: Impact of entropy against m

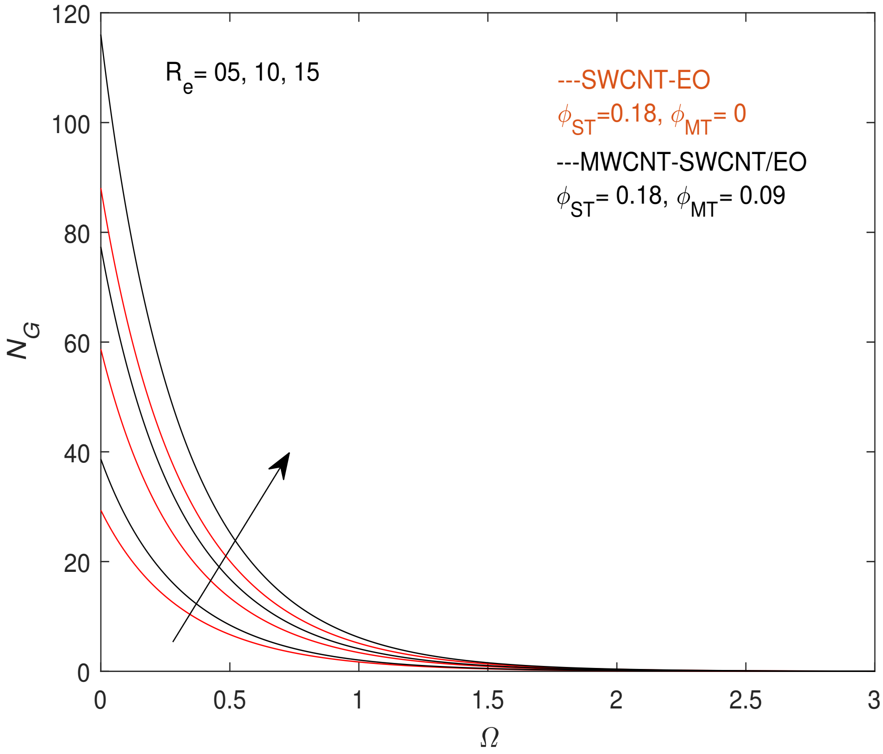

FIGURE 3.20: Impact of entropy against R_e

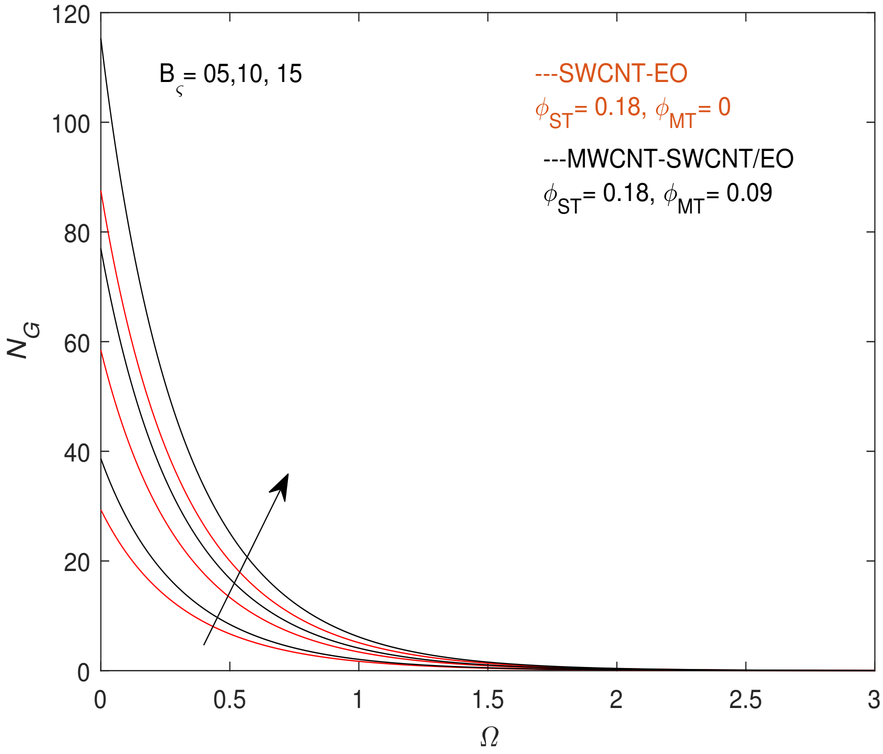

FIGURE 3.21: Impact of entropy against B_ς

Chapter 4

Heat and Mass Transfer for Prandtl-Eyring Hybrid Nanofluid

4.1 Introduction

Bio-convection is natural phenominon that occurs by random movement in single-cell or colony like microorganisms. The model discussed in chapter 3 is extended by discussing the motion of microorganisms. Furthermore concentration equation is also added in this model to discuss the mass transfer. In this chapter, we will conduct a numerical study of the flow, heat transfer, heat and mass transfer of the Prandtl-Eyring hybrid nanofluid.

4.2 Mathematical Modeling

The Prandtl-Eyring hybrid nanofluid is used to extend the problem considered in Chapter 3. The geometry of problem is given in Figure (3.1). The flow is discussed using continuity, momentum, energy, concentration, and motile microorganism equation.

4.2.1 Governing Equations

The set of equations describing the flow are as follows.

$$\frac{\partial B_1}{\partial x}+\frac{\partial B_2}{\partial y}=0, \tag{4.1}$$

$$B_1\frac{\partial B_1}{\partial x}+B_2\frac{\partial B_2}{\partial y}=\frac{A_d}{C\rho_{hnf}}\left(\frac{\partial^2 B_1}{\partial y^2}\right)-\frac{A_d}{2C^3\rho_{hnf}}\frac{\partial^2 B_1}{\partial y^2}\left(\frac{\partial B_1}{\partial y}\right)^2-\frac{\mu_{hnf}}{\rho_{hnf}k}B_1 \tag{4.2}$$

$$\begin{aligned}B_1\frac{\partial \mathcal{T}}{\partial x}+B_2\frac{\partial \mathcal{T}}{\partial y}=&\frac{1}{(\rho C_p)_{hnf}}\left(k_{hnf}\Big(\frac{\partial^2 \mathcal{T}}{\partial y^2}\Big)+\mu_{hnf}\Big(\frac{\partial B_1}{\partial y}\Big)^2-\frac{\partial q_r}{\partial y}\right)\\&-\lambda_0\left(B_1\frac{\partial B_1}{\partial x}\frac{\partial \mathcal{T}}{\partial x}+B_2\frac{\partial B_2}{\partial y}\frac{\partial \mathcal{T}}{\partial y}+B_1\frac{\partial B_2}{\partial x}\frac{\partial \mathcal{T}}{\partial y}+B_2\frac{\partial B_1}{\partial y}\frac{\partial \mathcal{T}}{\partial x}\right.\\&\left.+B_1^2\frac{\partial^2 \mathcal{T}}{\partial x^2}+B_2^2\frac{\partial^2 \mathcal{T}}{\partial y^2}+2B_1B_2\frac{\partial^2 \mathcal{T}}{\partial x\partial y}\right),\end{aligned} \tag{4.3}$$

$$B_1\frac{\partial C}{\partial x}+B_2\frac{\partial C}{\partial y}=\frac{\partial^2 C}{\partial y^2}D_B+\left(\frac{\partial^2 \mathcal{T}}{\partial y^2}\right)\frac{D_T}{\mathcal{T}_\infty}+k_r\big(C_\infty-C\big), \tag{4.4}$$

$$B_2\frac{\partial N}{\partial y}+B_1\frac{\partial N}{\partial x}=D_m\frac{\partial^2 N}{\partial y^2}+\frac{b_w}{(C_\infty-C_w)}\frac{\partial}{\partial y}\big(N\frac{\partial C}{\partial y}\big). \tag{4.5}$$

The associated BCs are taken as from [35, 36].

$$\begin{aligned}&B_1(x,0)=U_w+N_\varsigma\Big(\frac{\partial B_1}{\partial y}\Big),\quad B_2(x,0)=V_\varsigma,\quad -k_\varsigma\Big(\frac{\partial \mathcal{T}}{\partial y}\Big)=h_\varsigma(\mathcal{T}w-\mathcal{T}),\\&C_w=C,\qquad N_w=N.\end{aligned} \tag{4.6}$$

$$B_1\to 0,\quad \mathcal{T}\to\mathcal{T}_\infty,\quad C_\infty=C,\qquad N_\infty=N\quad as\quad y\to\infty. \tag{4.7}$$

C_∞ is ambient concentration and N_∞ is ambient motile microorganism.

For the conversion of the mathematical model (4.1)-(4.5) into the system of ODEs, the following similarity transformation are used which are taken from [22, 23].

$$\left.\begin{aligned}&\Omega(x,y)=\sqrt{\frac{b}{\nu_f}}y,\qquad \theta(\Omega)=\frac{\mathcal{T}-\mathcal{T}_\infty}{\mathcal{T}_w-\mathcal{T}_\infty},\\&\psi=\sqrt{\nu_f b}xf(\Omega),\qquad \Phi(\Omega)=\frac{C_\infty-C}{C_\infty-C_w},\\&\chi(\Omega)=\frac{N-N_\infty}{N_w-N_\infty}\end{aligned}\right\} \tag{4.8}$$

The identical satisfaction of (4.1) is already discussed and (4.2),(4.3) are also discussed in chapter 3.

The governing equation of conservation of concentration(4.4) is

$$
\begin{aligned}
& B_1 \frac{\partial C}{\partial x} + B_2 \frac{\partial C}{\partial y} = \frac{\partial^2 C}{\partial y^2} D_B + \left(\frac{\partial^2 \mathcal{T}}{\partial y^2} \right) \frac{D_T}{\mathcal{T}_\infty} + k_r \big(C_\infty - C \big). \\
& \Phi(\Omega) = \frac{C_\infty - C}{C_\infty - C_w} \\
& C = C_\infty - \Phi(\Omega) \big(C_\infty - C_w \big) && (4.9) \\
& B_1 = bx f'(\Omega) && (4.10) \\
& B_2 = -\sqrt{\nu_f b} f(\Omega) && (4.11) \\
& \frac{\partial C}{\partial x} = \frac{\partial}{\partial x} \Big(C_\infty - \Phi(\Omega) \big(C_\infty - C_w \big) \Big) \\
& \frac{\partial C}{\partial x} = 0 && (4.12) \\
& \frac{\partial C}{\partial y} = \frac{\partial}{\partial y} \Big(C_\infty - \Phi(\Omega) \big(C_\infty - C_w \big) \Big) \\
& \frac{\partial C}{\partial y} = \left(-\big(C_\infty - C_w \big) \Phi'(\Omega) \sqrt{\frac{b}{\nu_f}} \right) && (4.13) \\
& \frac{\partial^2 C}{\partial y^2} = \left(-\big(C_\infty - C_w \big) \Phi''(\Omega) \frac{b}{\nu_f} \right) && (4.14) \\
& \frac{\partial^2 \mathcal{T}}{\partial y^2} = \frac{b^2}{\nu_f} x \theta''(\Omega) && (4.15)
\end{aligned}
$$

Now, the dimensionless form of the concentration equation can be obtained by using (4.9)-(4.15)

$$
\begin{aligned}
& \sqrt{\nu_f b} f(\Omega) \left(\big(C_\infty - C_w \big) \phi'(\Omega) \sqrt{\frac{b}{\nu_f}} \right) = \left(-\big(C_\infty - C_w \big) \Phi''(\Omega) \frac{b}{\nu_f} \right) D_B \\
& + \frac{b^2}{\nu_f} x \theta''(\Omega) \frac{D_T}{\infty} + k_r \big(C_\infty - C \big) \\
\Rightarrow \quad & b \big(C_\infty - C_w \big) f(\Omega) \theta'(\Omega) = \left(-\big(C_\infty - C_w \big) \Phi''(\Omega) \frac{b}{\nu_f} \right) D_B \\
& \qquad + \frac{b^2}{\nu_f} x \theta''(\Omega) \frac{D_T}{\infty} + k_r \big(C_\infty - C \big) \\
\Rightarrow \quad & \left(-\big(C_\infty - C_w \big) \Phi''(\Omega) \frac{b}{\nu_f} \right) D_B + \frac{b^2}{\nu_f} x \theta''(\Omega) \frac{D_T}{\infty} \\
& + k_r \big(C_\infty - C \big) - b \big(C_\infty - C_w \big) f(\Omega) \theta'(\Omega) = 0
\end{aligned}
$$

$$
\begin{aligned}
\Rightarrow \quad & \theta''(\Omega) + \left(\frac{b^2 x\theta''(\Omega)}{\nu_f}\right)\frac{D_T}{\mathcal{T}\infty}\left(\frac{\nu_f}{-(C_\infty - C_w)bD_B}\right) + k_r\big(C_\infty - C\big) \\
& \left(\frac{\nu_f}{-(C_\infty - C_w)bD_B}\right) - b\big(C_\infty - C_w\big)f(\Omega)\theta'(\Omega)\left(\frac{\nu_f}{-(C_\infty - C_w)bD_B}\right) = 0 \\
\Rightarrow \quad & \Phi''(\Omega) + \frac{N_t}{N_b}\theta''(\Omega) + \mathcal{L}_e f(\Omega)\Phi'(\Omega) + k_r\big(C_\infty - C\big)\left(\frac{\nu_f}{-(C_\infty - C_w)bD_B}\right) = 0 \\
\Rightarrow \quad & \Phi''(\Omega) + \frac{N_t}{N_b}\theta''(\Omega) + \mathcal{L}_e f(\Omega)\Phi'(\Omega) - \frac{k_r}{b}\Phi(\Omega)\mathcal{L}_e = 0 \\
& \Phi''(\Omega) + \mathcal{L}_e f(\Omega)\Phi'(\Omega) + \frac{N_t}{N_b}\theta''(\Omega) - \gamma\Phi(\Omega) = 0 \qquad (4.16)
\end{aligned}
$$

The following dimensionless parameters are used in equation (4.16),

$$
\mathcal{L}_e = \tfrac{\nu_f}{D_B}, \qquad N_t = \tfrac{\left(\mathcal{T}_w - \mathcal{T}\infty\right)\tau D_T}{\nu_f \mathcal{T}\infty}, \qquad N_b = \tfrac{\tau D_B\left(C_w - C - \infty\right)}{\nu_f},
$$
$$
\Phi(\Omega) = \tfrac{C_\infty - C}{C_\infty - C_w}, \qquad \gamma = \tfrac{k_r}{b}\mathcal{L}_e.
$$

Now, for the conversion of motile microorganism equation (4.5) the following derivates are required.

$$
\begin{aligned}
& \chi(\Omega) = \frac{N - N_\infty}{N_w - N_\infty} \\
& N = \chi(\Omega)\big(N_w - N_\infty\big) + N_\infty \qquad (4.17) \\
& \frac{\partial N}{\partial x} = 0 \qquad (4.18) \\
& \frac{\partial N}{\partial y} = \sqrt{\frac{b}{\nu_f}}\big(N_w - N_\infty\big)\chi'(\Omega) \qquad (4.19) \\
& \frac{\partial^2 N}{\partial y^2} = \big(N_w - N_\infty\big)\chi''(\Omega)\frac{b}{\nu_f} \qquad (4.20) \\
& N\frac{\partial C}{\partial y} = \big(\chi(\Omega)\big(N_w - N_\infty\big) + N_\infty\big)\Big(\Big(-\big(C_\infty - C_w\big)\Phi'(\Omega)\sqrt{\frac{b}{\nu_f}}\Big) \\
& N\frac{\partial C}{\partial y} = -\big(C_\infty - C_w\big)\big(N_w - N_\infty\big)\sqrt{\frac{b}{\nu_f}}\big(\chi(\Omega)\Phi'(\Omega)\big) \\
& \qquad\qquad - N_\infty\big(C_\infty - C_w\big)\sqrt{\frac{b}{\nu_f}}\big(\Phi'(\Omega)\big) \qquad (4.21) \\
& \frac{\partial}{\partial y}\left(N\frac{\partial C}{\partial y}\right) = -\big(C_\infty - C_w\big)\big(N_w - N_\infty\big)\left(\Phi'(\Omega)\chi'(\Omega)\frac{b}{\nu_f} + \chi(\Omega)\Phi''(\Omega)\frac{b}{\nu_f}\right) \\
& \qquad\qquad - N_\infty\big(C_\infty - C_w\big)\frac{b}{\nu_f}\Phi''(\Omega)
\end{aligned}
$$

$$\frac{\partial}{\partial y}\left(N\frac{\partial C}{\partial y}\right) = -\big(C_\infty - C_w\big)\big(N_w - N_\infty\big)\frac{b}{\nu_f}\Big(\Phi'(\Omega)\chi'(\Omega) + \chi(\Omega)\Phi''(\Omega)\Big)$$
$$- N_\infty\big(C_\infty - C_w\big)\frac{b}{\nu_f}\Phi''(\Omega) \tag{4.22}$$

Using (4.17)-(4.22) in governing equation for motile microorganism equation are

$$\Rightarrow \quad -\sqrt{\nu_f b}f(\Omega)\left(\big(N_w - N_\infty\big)\chi'(\Omega)\sqrt{\frac{b}{\nu_f}}\right) = D_m\left(\big(N_w - N_\infty\big)\chi''(\Omega)\frac{b}{\nu_f}\right)$$
$$+ \frac{bw_c}{\big(C_\infty - C_w\big)}\Bigg(-\big(C_\infty - C_w\big)\big(N_w - N_\infty\big)\frac{b}{\nu_f}\Big(\Phi'(\Omega)\chi'(\Omega) + \chi(\Omega)\Phi''(\Omega)\Big)$$
$$- N_\infty\big(C_\infty - C_w\big)\frac{b}{\nu_f}\Phi''(\Omega)\Bigg)$$
$$\Rightarrow \quad -bf(\Omega)\big(N_w - N_\infty\big)\chi'(\Omega) = D_m\left(\big(N_w - N_\infty\big)\chi''(\Omega)\frac{b}{\nu_f}\right)$$
$$+ \frac{bw_c}{\big(C_\infty - C_w\big)}\Bigg(-\big(C_\infty - C_w\big)\big(N_w - N_\infty\big)\frac{b}{\nu_f}\Big(\Phi'(\Omega)\chi'(\Omega) + \chi(\Omega)\Phi''(\Omega)\Big)$$
$$- N_\infty\big(C_\infty - C_w\big)\frac{b}{\nu_f}\Phi''(\Omega)\Bigg)$$
$$\Rightarrow \quad \chi''(\Omega) + \frac{bw_c}{\big(C_\infty - C_w\big)}\left(\frac{\nu_f}{b\big(N_w - N_\infty D_m\big)}\right)$$
$$\Bigg(-\big(C_\infty - C_w\big)\big(N_w - N_\infty\big)\frac{b}{\nu_f}\Big(\Phi'(\Omega)\chi'(\Omega) + \chi(\Omega)\Phi''(\Omega)\Big)$$
$$- N_\infty\big(C_\infty - C_w\big)\frac{b}{\nu_f}\phi''(\Omega)\Bigg) + b\big(N_w - N_\infty\big)\left(\frac{\nu_f}{b\big(N_w - N_\infty\big)D_m}\right)$$
$$\big(f(\Omega)\chi'(\Omega)\big) = 0$$
$$\Rightarrow \quad \chi''(\Omega) + \mathcal{L}_b f(\Omega)\chi'(\Omega) + \left(-\frac{w_c b}{D_m}\big(\Phi'(\Omega)\chi'(\Omega) + \chi(\Omega)\Phi''(\Omega)\big)\right)$$
$$-\left(\frac{w_c b}{D_m}\frac{N_\infty}{N_w - N_\infty}\Phi''(\Omega)\right) = 0$$
$$\Rightarrow \quad \chi''(\Omega) + \mathcal{L}_b f(\Omega)\chi'(\Omega) - \frac{w_c b}{D_m}\Bigg(\Phi'(\Omega)\chi'(\Omega) + \chi(\Omega)\Phi''(\Omega)$$
$$+ \frac{N_\infty}{N_w - N_\infty}\Phi''(\Omega)\Bigg) = 0$$
$$\Rightarrow \quad \chi''(\Omega) + \mathcal{L}_b f(\Omega)\chi'(\Omega) - P_e\Big(\Phi'(\Omega)\chi'(\Omega) + \big(\omega + \chi(\Omega)\big)\Phi''(\Omega)\Big) = 0$$
$$\Rightarrow \quad \chi''(\Omega) + \mathcal{L}_b f(\Omega)\chi'(\Omega) - \Big(\Phi'(\Omega)\chi'(\Omega) + \big(\omega + \chi(\Omega)\big)\Phi''(\Omega)\Big)P_e = 0 \tag{4.23}$$

The dimensionless parameters used in (4.23) are:

$$P_e = \frac{bw_c}{D_m}, \qquad \omega = \frac{N_\infty}{N_w - N\infty}, \qquad \mathcal{L}_b = \frac{\nu_f}{D_m}$$

The related BCs are converted into the dimensionless form by the following procedure. Firstly when y=0 which implies Ω=0

$$
\begin{aligned}
& B_1(x,0) = U_w + N_\varsigma\big(\frac{\partial B_1}{\partial y}\big),\\
\Rightarrow \quad & f'(\Omega)bx = bx + N_\varsigma\left(bxf''(\Omega)\sqrt{\frac{b}{\nu_f}}\right),\\
\Rightarrow \quad & f'(\Omega)bx = bx\left(1 + N_\varsigma\sqrt{\frac{b}{\nu_f}}f''(\Omega)\right),\\
\Rightarrow \quad & f'(0) = 1 + A_\varsigma f''(0).\\
& B_2(x,0) = V_\varsigma,\\
\Rightarrow \quad & -f(\Omega)\sqrt{\nu_f b} = V_\varsigma\\
\Rightarrow \quad & -f(\Omega) = \frac{V_\varsigma}{\sqrt{\nu_f b}},\\
\Rightarrow \quad & -f(0) = \frac{V_\varsigma}{\sqrt{\nu_f b}},\\
\Rightarrow \quad & \qquad f(0) = S,\\
& -\kappa_s\left[\frac{\partial \mathcal{T}}{\partial y}\right] = h_\varsigma(\mathcal{T}_w - \mathcal{T}),\\
\Rightarrow \quad & -\kappa_s\left(\theta'\sqrt{\frac{b}{\nu_f}}(\mathcal{T}_w - \mathcal{T}_\infty)\right) = h_\varsigma\Big(\mathcal{T}_\infty - \mathcal{T}\Big),\\
\Rightarrow \quad & \theta' = \frac{h_\varsigma\big(\mathcal{T}_w - \mathcal{T}\big)}{-\kappa_s\sqrt{\frac{b}{\nu_f}}\big(\mathcal{T}_w - \mathcal{T}_\infty\big)},\\
\Rightarrow \quad & \theta'(\Omega) = -H_\varsigma\left(\frac{\mathcal{T}_w - \big((\mathcal{T}_w - \mathcal{T}_\infty)\theta(\Omega) + \mathcal{T}_\infty\big)}{\mathcal{T}_w - \mathcal{T}_\infty}\right),\\
\Rightarrow \quad & \theta'(0) = -H_\varsigma(1 - \theta(0)).\\
& C_w = C,\\
\Rightarrow \quad & \Phi(\Omega) = \frac{C_\infty - C}{C_\infty - C_w},\\
\Rightarrow \quad & \Phi(\Omega) = \frac{C_\infty - C_w}{C_\infty - C_w},
\end{aligned}
$$

$$
\begin{aligned}
\Rightarrow \quad & \Phi(\Omega) = 1, \\
\Rightarrow \quad & \Phi(0) = 1. \\
& N_w = N, \\
\Rightarrow \quad & \chi(\Omega) = \frac{N - N_\infty}{N_w - N_\infty}, \\
\Rightarrow \quad & \chi(\Omega) = \frac{N_w - N_\infty}{N_w - N_\infty}, \\
\Rightarrow \quad & \chi(\Omega) = 1, \\
\Rightarrow \quad & \chi(0) = 1
\end{aligned}
$$

Now choose y $\rightarrow \infty \implies \Omega \rightarrow \infty$

$$
\begin{aligned}
& B_1 \rightarrow 0, \\
\Rightarrow \quad & f'(\Omega) \rightarrow 0, \\
& \mathcal{T} \rightarrow \mathcal{T}_\infty, \\
\Rightarrow \quad & \theta(\Omega) \rightarrow 0, \\
& C \rightarrow C_\infty, \\
\Rightarrow \quad & \Phi(\Omega) \rightarrow 0, \\
& N \rightarrow N_\infty, \\
\Rightarrow \quad & \chi(\Omega) \rightarrow 0,
\end{aligned}
$$

The final dimensionless form of the governing equations along with the converted boundary conditions are:

$$
\left.
\begin{aligned}
& A_1^* f'''(\Omega)\big(1 - A_2^* f''(\Omega)^2\big) + \phi_b\big(f(\Omega)f''(\Omega) - f'(\Omega)^2\big) - \frac{1}{\phi_a}K_\varsigma f'(\Omega) = 0, \\
& \big(1 + \frac{1}{\phi_d}P\varsigma N_\varsigma\big)\theta'' + \frac{\phi_c}{\phi_d}P\varsigma\bigg(f\theta' - f'\theta + \frac{E_\varsigma}{\phi_a\phi_c}(f'')^2 - \epsilon_\varsigma\big((f')^2\theta - ff'\theta' \\
& - ff''\theta + f^2\theta''\big)\bigg) = 0 \\
& \Phi''(\Omega) + \mathcal{L}_e f(\Omega)\Phi'(\Omega) + \frac{N_t}{N_b}\theta''(\Omega) - \gamma\Phi(\Omega) = 0 \\
& \chi''(\Omega) + \mathcal{L}_b f(\Omega)\chi'(\Omega) - \big(\Phi'(\Omega)\chi'(\Omega) + \big(\omega + \chi(\Omega)\big)\Phi''(\Omega)\big)P_e = 0
\end{aligned}
\right\} \tag{4.24}
$$

$$\left.\begin{aligned}
&f(0) = S, \quad f'(0) = 1 + A_\varsigma f''(0), \quad f'(\Omega) \to 0, \quad as \ \ \Omega \to \infty,\\
&\theta'(0) = -H_\varsigma(1-\theta(0)), \quad \theta(\Omega) \to 0, \quad as \ \ \Omega \to \infty.\\
&\Phi(0) = 1, \qquad\qquad\qquad \Phi(\Omega) \to 0, \quad as \ \ \Omega \to \infty.\\
&\chi(0) = 1, \qquad\qquad\qquad \chi(\Omega) \to 0, \quad as \ \ \Omega \to \infty.
\end{aligned}\right\} \tag{4.25}$$

4.3 Numerical Method for Solution

Equations (3.29), (4.16) and (4.23) are solved simultaneously by incorporating the solution of (3.28) numerically.

Now the ordinary differential equations (3.29),(4.16) and (4.23) are solved using shooting method.

Consider the following equations.

$$\begin{aligned}
\theta'' = \frac{1}{1 + \frac{P_\varsigma N_\varsigma}{\phi_d} - \epsilon_\varsigma (f^2)\frac{\phi_c}{\phi_d} P_\varsigma}\Bigg(&- P_\varsigma \frac{\phi_c}{\phi_d} \times \Big(f\theta' - f'\theta + \frac{E_\varsigma}{\phi_a \phi_c} f''^2 \\
&- \epsilon_\varsigma \big(f'^2\theta - ff'\theta' - ff''\theta \big)\Big)\Bigg).
\end{aligned} \tag{4.26}$$

$$\Phi'' = \gamma\Phi(\Omega) - \mathcal{L}_e f(\Omega)\Phi'(\Omega) - \frac{N_t}{N_b}\theta''. \tag{4.27}$$

$$\chi'' = P_e\Big(\chi'\Phi' + \big(\omega + \chi\big)\Phi''(\Omega) - \mathcal{L}_b f \chi'(\Omega)\Big). \tag{4.28}$$

Following notions are used for the solution.

$$\begin{aligned}
&\theta = L_1,\\
&\theta' = L_1' = L_2.\\
&\Phi = L_3.\\
&\Phi' = L_3' = L_4.\\
&\chi = L_5.\\
&\chi' = L_5' = L_6.
\end{aligned}$$

Above equations are then transformed into the system of first-order ODEs shown below.

$$
\begin{aligned}
&L_1' = L_2, && L_1(0) = r.\\
&L_2' = \frac{1}{1+\frac{P\varsigma N_\varsigma}{\phi_d} - \epsilon_\varsigma (J_1^2)\frac{\phi_c}{\phi_d}P\varsigma}\Bigg(- P\varsigma\frac{\phi_c}{\phi_d} \times \Big(J_1L_2 - J_2L_1 + \frac{E_\varsigma}{\phi_a\phi_c}J_3^2\\
&- \epsilon_\varsigma\big(J_2^2L_1 - J_1J_2L_2 - J_1J_3L_1\big)\Big)\Bigg), && L_2(0) = -H_\varsigma(1 - L_1(0)).\\
&L_3' = L_4, && L_3(0) = 1.\\
&L_4' = \gamma L_3 - \mathcal{L}_eJ_1L_4 - \frac{N_t}{N_b}\Bigg(\frac{1}{1+\frac{P\varsigma N_\varsigma}{\phi_d} - \epsilon_\varsigma (J_1^2)\frac{\phi_c}{\phi_d}P\varsigma}\Bigg(- P\varsigma\frac{\phi_c}{\phi_d} \times \Big(J_1L_2 - J_2L_1\\
&\quad + \frac{E_\varsigma}{\phi_a\phi_c}J_3^2 - \epsilon_\varsigma\big(J_2^2L_1 - J_1J_2L_2 - J_1J_3L_1\big)\Big)\Bigg)\Bigg), && L_4(0) = m.\\
&L_5' = L_6, && L_5(0) = 1.\\
&L_6' = P_e\Bigg[L_6L_4 + \big(\omega + L_5\big)\Bigg(\gamma L_3 - \mathcal{L}_eJ_1L_4 - \frac{N_t}{N_b}\Bigg(\frac{1}{1+\frac{P\varsigma N_\varsigma}{\phi_d} - \epsilon_\varsigma (J_1^2)\frac{\phi_c}{\phi_d}P\varsigma}\\
&\quad\Bigg(- P\varsigma\frac{\phi_c}{\phi_d} \times \Big(J_1L_2 - J_2L_1 + \frac{E_\varsigma}{\phi_a\phi_c}J_3^2 - \epsilon_\varsigma\big(J_2^2L_1 - J_1J_2L_2 - J_1J_3L_1\big)\Big)\Bigg)\Bigg)\Bigg)\\
&- \mathcal{L}_bJ_1L_6\Bigg], && L_6(0) = u.
\end{aligned}
$$

The above IVP will be solved by Runge-Kutta method of oder four. The missing condition r,m and u are to selected in such a way that.

$$
\begin{aligned}
L_1(\Omega_\infty, r) &= 0,\\
L_3(\Omega_\infty, m) &= 0,\\
L_5(\Omega_\infty, u) &= 0.
\end{aligned}
$$

The above equations are solved for r,m and u by Newton's Method using following itterative scheme.

$$\begin{bmatrix} r \\ m \\ u \end{bmatrix}_{(n+1)} = \begin{bmatrix} r \\ m \\ u \end{bmatrix}_{(n)} - \begin{bmatrix} \frac{\partial L_1}{\partial r} & \frac{\partial L_1}{\partial m} & \frac{\partial L_1}{\partial u} \\ \frac{\partial L_3}{\partial r} & \frac{\partial L_3}{\partial m} & \frac{\partial L_3}{\partial u} \\ \frac{\partial L_5}{\partial r} & \frac{\partial L_5}{\partial m} & \frac{\partial L_5}{\partial u} \end{bmatrix}_{(n)}^{-1} \begin{bmatrix} L_1 \\ L_3 \\ L_5 \end{bmatrix}_{(n)}$$

To successfully iterate the above formula we need the following:

$$\frac{\partial L_1}{\partial r} = L_7, \quad \frac{\partial L_2}{\partial r} = L_8, \quad \frac{\partial L_3}{\partial r} = L_9, \quad \frac{\partial L_4}{\partial r} = L_{10}, \frac{\partial L_5}{\partial r} = L_{11}, \frac{\partial L_6}{\partial r} = L_{12}.$$
$$\frac{\partial L_1}{\partial m} = L_{13}, \quad \frac{\partial L_2}{\partial m} = L_{14}, \quad \frac{\partial L_3}{\partial m} = L_{15}, \quad \frac{\partial L_4}{\partial m} = L_{16}, \frac{\partial L_5}{\partial m} = L_{17}, \frac{\partial L_6}{\partial m} = L_{18}.$$
$$\frac{\partial L_1}{\partial m} = L_{19}, \quad \frac{\partial L_2}{\partial m} = L_{20}, \quad \frac{\partial L_3}{\partial m} = L_{21}, \quad \frac{\partial L_4}{\partial m} = L_{22}, \frac{\partial L_5}{\partial m} = L_{23}, \frac{\partial L_6}{\partial m} = L_{24}.$$

As a result of these new notations, the Newton's iterative scheme gets the form:

$$\begin{bmatrix} r \\ m \\ u \end{bmatrix}_{(n+1)} = \begin{bmatrix} r \\ m \\ u \end{bmatrix}_{(n)} - \begin{bmatrix} L_7 & L_{13} & L_{19} \\ L_9 & L_{15} & L_{21} \\ L_{11} & L_{17} & L_{23} \end{bmatrix}_{(n)}^{-1} \begin{bmatrix} L_1 \\ L_3 \\ L_5 \end{bmatrix}_{(n)}$$

Now differentiating the system of first order ODEs with respect to r, m, and u we get the following system of ODEs.

$$L_7' = L_8, \qquad L_7(0) = 1.$$
$$L_8' = \frac{1}{1 + \frac{P\varsigma N_\varsigma}{\phi_d} - \epsilon_\varsigma (J_1^2) \frac{\phi_c}{\phi_d} P\varsigma} \left(- P\varsigma \frac{\phi_c}{\phi_d} \times \left(J_1 L_8 - J_2 L_7 - \epsilon_\varsigma \left(J_2^2 L_7 - J_1 J_2 L_8 - J_1 J_3 L_7 \right) \right) \right), \quad L_8(0) = H_\varsigma.$$
$$L_9' = L_{10}, \qquad L_9(0) = 0.$$
$$L_{10}' = \gamma L_9 - \mathcal{L}_e J_1 L_{10} - \frac{N_t}{N_b} \left(\frac{1}{1 + \frac{P\varsigma N_\varsigma}{\phi_d} - \epsilon_\varsigma (J_1^2) \frac{\phi_c}{\phi_d} P\varsigma} \left(- P\varsigma \frac{\phi_c}{\phi_d} \times \left(J_1 L_8 - J_2 L_7 - \epsilon_\varsigma \left(J_2^2 L_7 - J_1 J_2 L_8 - J_1 J_3 L_7 \right) \right) \right) \right), \qquad L_{10}(0) = 0.$$
$$L_{11}' = L_{12}, \qquad L_{11}(0) = 0.$$

$$L'_{12} = \Bigg[P_e \;\; L_6L_{10} + L_4L_{12} + L_{11}\Bigg(\gamma L_9 - \mathcal{L}_e J_1 L_{10} - \frac{N_t}{N_b}\Bigg(\frac{1}{1+\frac{P\varsigma N_\varsigma}{\phi_d} - \epsilon_\varsigma(J_1^2)\frac{\phi_c}{\phi_d}P\varsigma}$$
$$\Bigg(-P\varsigma\frac{\phi_c}{\phi_d} \times \Big(J_1L_8 - J_2L_7 - \epsilon_\varsigma\big(J_2^2L_7 - J_1J_2L_8 - J_1J_3L_7\big)\Big)\Bigg)\Bigg)\Bigg)\Bigg]$$
$$-\mathcal{L}_b J_1 L_{12}, \qquad L_{12}(0) = 0.$$

$$L'_{13} = L_{14}, \qquad L_{13}(0) = 0.$$

$$L'_{14} = \frac{1}{1+\frac{P\varsigma N_\varsigma}{\phi_d} - \epsilon_\varsigma(J_1^2)\frac{\phi_c}{\phi_d}P\varsigma}\Bigg(-P\varsigma\frac{\phi_c}{\phi_d} \times \Big(J_1L_{14} - J_2L_{13}$$
$$-\epsilon_\varsigma\big(J_2^2L_{13} - J_1J_2L_{14} - J_1J_3L_{13}\big)\Big)\Bigg), \qquad L_{14}(0) = 0.$$

$$L'_{15} = L_{16}, \qquad L_{15}(0) = 0.$$

$$L'_{16} = \gamma L_{15} - \mathcal{L}_e J_1 L_{16} - \frac{N_t}{N_b}\Bigg(\frac{1}{1+\frac{P\varsigma N_\varsigma}{\phi_d} - \epsilon_\varsigma(J_1^2)\frac{\phi_c}{\phi_d}P\varsigma}\Bigg(-P\varsigma\frac{\phi_c}{\phi_d} \times \Big(J_1L_{14}$$
$$-J_2L_{13} - \epsilon_\varsigma\big(J_2^2L_{13} - J_1J_2L_{14} - J_1J_3L_{13}\big)\Big)\Bigg)\Bigg), \qquad L_{16}(0) = 1.$$

$$L'_{17} = L_{18}, \qquad L_{17}(0) = 0.$$

$$L'_{18} = P_e\Bigg[L_6L_{16} + L_4L_{18} + L_{17}\Bigg(\gamma L_{15} - \mathcal{L}_e J_1 L_{16} - \frac{N_t}{N_b}\Bigg(\frac{1}{1+\frac{P\varsigma N_\varsigma}{\phi_d} - \epsilon_\varsigma(J_1^2)\frac{\phi_c}{\phi_d}P\varsigma}$$
$$\Bigg(-P\varsigma\frac{\phi_c}{\phi_d} \times \Big(J_1L_{14} - J_2L_{13} - \epsilon_\varsigma\big(J_2^2L_{13} - J_1J_2L_{14} - J_1J_3L_{13}\big)\Big)\Bigg)\Bigg)\Bigg)\Bigg]$$
$$-\mathcal{L}_b J_1 L_{18}, \qquad L_{18}(0) = 0.$$

$$L'_{19} = L_{20}, \qquad L_{19}(0) = 0.$$

$$L'_{20} = \frac{1}{1+\frac{P\varsigma N_\varsigma}{\phi_d} - \epsilon_\varsigma(J_1^2)\frac{\phi_c}{\phi_d}P\varsigma}\Bigg(-P\varsigma\frac{\phi_c}{\phi_d} \times \Big(J_1L_{20} - J_2L_{19}$$
$$-\epsilon_\varsigma\big(J_2^2L_{19} - J_1J_2L_{20} - J_1J_3L_{19}\big)\Big)\Bigg), \qquad L_{20}(0) = 0.$$

$$L'_{21} = L_{22}, \qquad L_{21}(0) = 0.$$

$$L'_{22} = \gamma L_{21} - \mathcal{L}_e J_1 L_{22} - \frac{N_t}{N_b}\Bigg(\frac{1}{1+\frac{P\varsigma N_\varsigma}{\phi_d} - \epsilon_\varsigma(J_1^2)\frac{\phi_c}{\phi_d}P\varsigma}\Bigg(-P\varsigma\frac{\phi_c}{\phi_d} \times \Big(J_1L_{20} - J_2L_{19}$$
$$-\epsilon_\varsigma\big(J_2^2L_{19} - J_1J_2L_{20} - J_1J_3L_{19}\big)\Big)\Bigg)\Bigg), \qquad L_{22}(0) = 0.$$

$$L'_{23} = L_{24}, \qquad L_{23}(0) = 0.$$

$$
\begin{aligned}
L'_{24} = & \Bigg[P_e \ \ L_6 L_{22} + L_4 L_{24} + L_{23}\Bigg(\gamma L_{21} - \mathcal{L}_e J_1 L_{22} - \frac{N_t}{N_b}\Bigg(\frac{1}{1 + \frac{P_\varsigma N_\varsigma}{\phi_d} - \epsilon_\varsigma (J_1^2)\frac{\phi_c}{\phi_d} P_\varsigma} \\
& \Bigg(- P_\varsigma \frac{\phi_c}{\phi_d} \times \Big(J_1 L_{20} - J_2 L_{19} - \epsilon_\varsigma \big(J_2^2 L_{19} - J_1 J_2 L_{20} - J_1 J_3 L_{19}\big)\Big)\Bigg)\Bigg)\Bigg)\Bigg] \\
& - \mathcal{L}_b J_1 L_{24}, \qquad\qquad\qquad\qquad\qquad\qquad L_{24}(0) = 1.
\end{aligned}
$$

The stopping criteria for the Newton's method is set as:

$$
\mid L_1(\Omega_\infty, r_n, m_n, u_n) \mid, \mid L_3(\Omega_\infty, r_n, m_n, u_n) \mid, \mid L_5(\Omega_\infty, r_n, m_n, u_n) \mid < 10^{-5}.
$$

4.4 Results and Discussion

Figure 4.1 shows the influence of chemical reaction parameter γ on $\Phi(\Omega)$. As the values of γ increases the concentration profile decreases. It is also observed that MWCNT-SWCNT/EO hybrid nanofluid has higher concentration profile as compare to SWCNT/EO nanofluid. Figure 4.2 shows the impact of bioconvection Lewis number $\mathcal{L}_b$ on motile microbes profile $\chi(\Omega)$. It is noted that as the values of $\mathcal{L}_b$ are increases, the motile microorganism profile decreases. Figure 4.3 depicts the effect of Brownian motion parameter N_b against the $\Phi(\Omega)$. MWCNT-SWCNT/EO hybrid nanofluid have higher concentration profile whereas, SWCNT-EO have lower concentration profile.

Figure 4.4 shows the impact of bioconvection constant ω on $\chi(\Omega)$. Here values of ω are taken 0.2, 0.4, 0.6, 0.8, as the values of ω rises the motile profile decreases. MWCNT-SWCNT/EO hybrid nanofluid have higher motile profile than SWCNRT/EO nanofluid. Figure 4.5 illustrates the influence of the parameter of thermophoresis N_t on $\Phi(\Omega)$. MWCNT-SWCNT/EO hybrid nanofluid maintains a higher concentration profile than SWCNT/EO nanofluid. Figure 4.6 shows the effect of peclet number P_e against $\chi(\Omega)$. By increasing the peclet number motile profile decreases. Figure 4.7 depicts the impact of Lewis number $\mathcal{L}_e$ against $\Phi(\Omega)$. The MWCNT-SWCNT with base fluid engine oil has a more notable impact than SWCNT-EO. By rising the values of $\mathcal{L}_e$ concentration profile decreases.

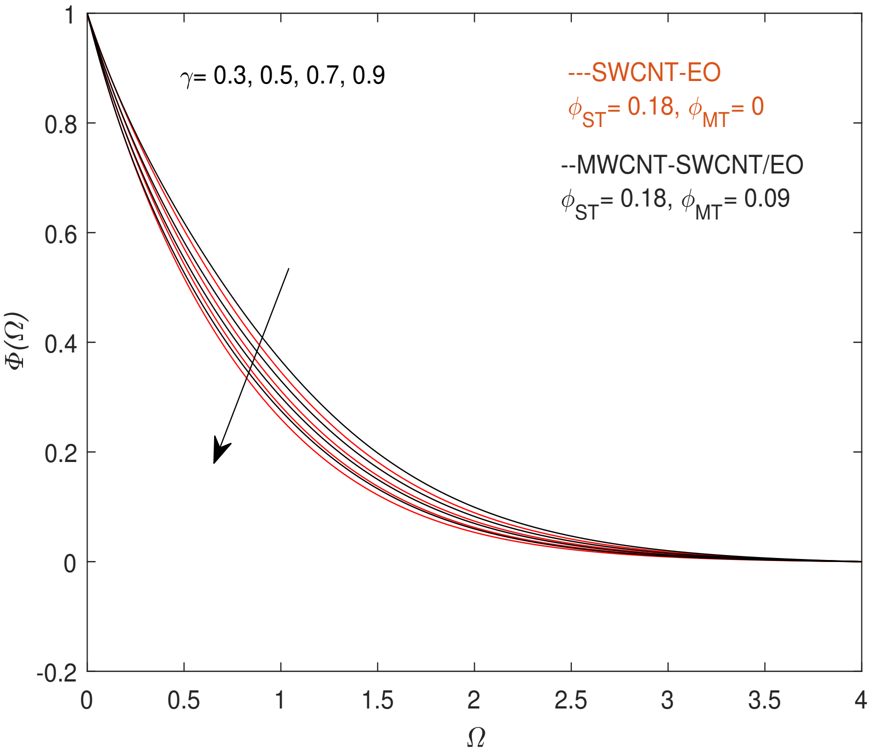

FIGURE 4.1: Impact of concentration against γ

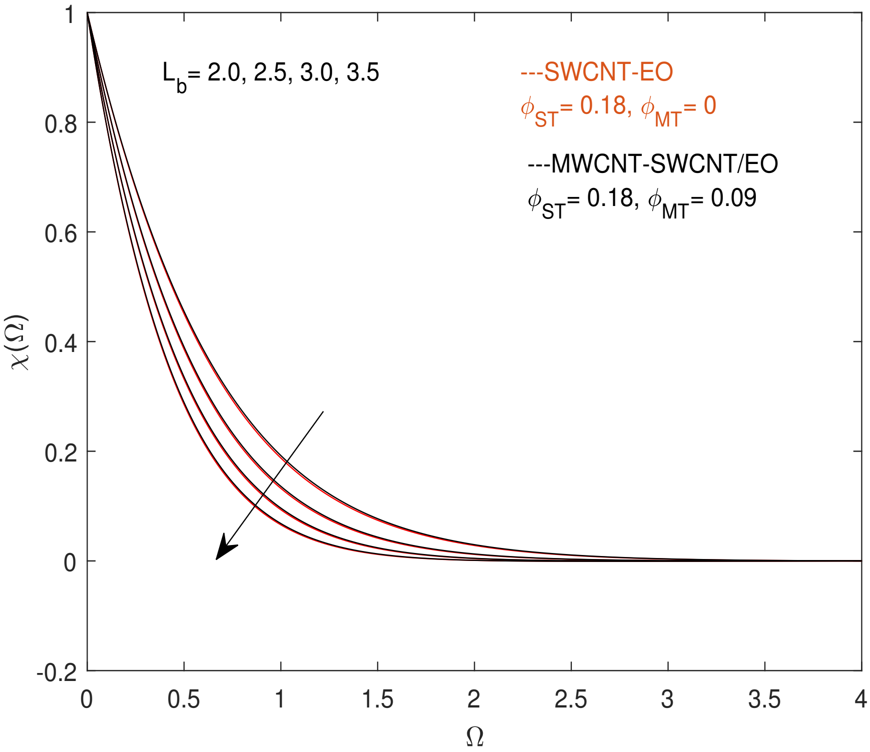

FIGURE 4.2: Impact of Motile against $\mathcal{L}_b$

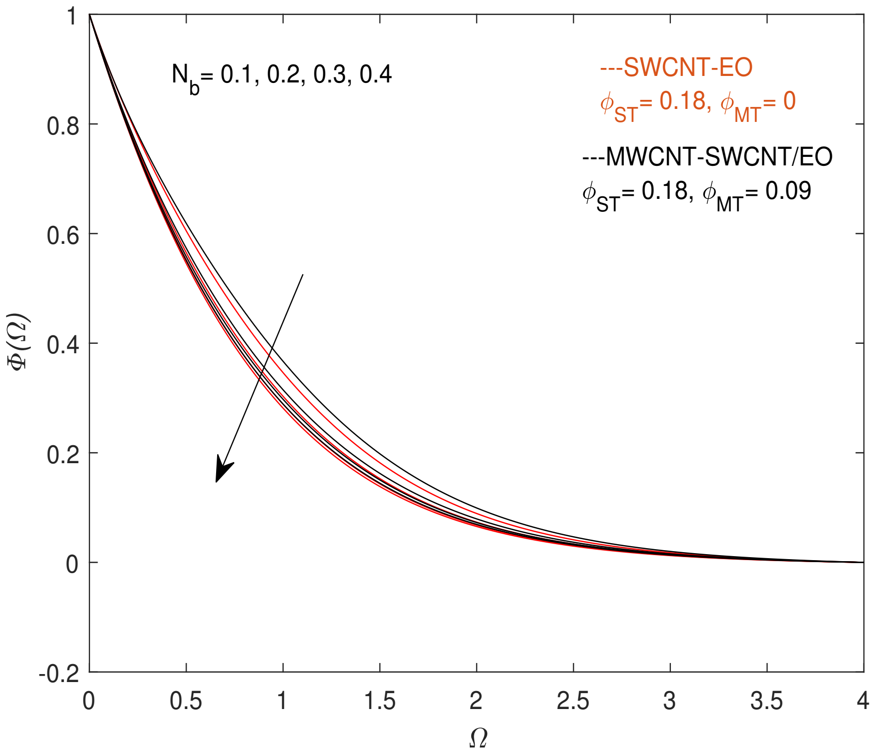

FIGURE 4.3: Impact of concentration against N_b

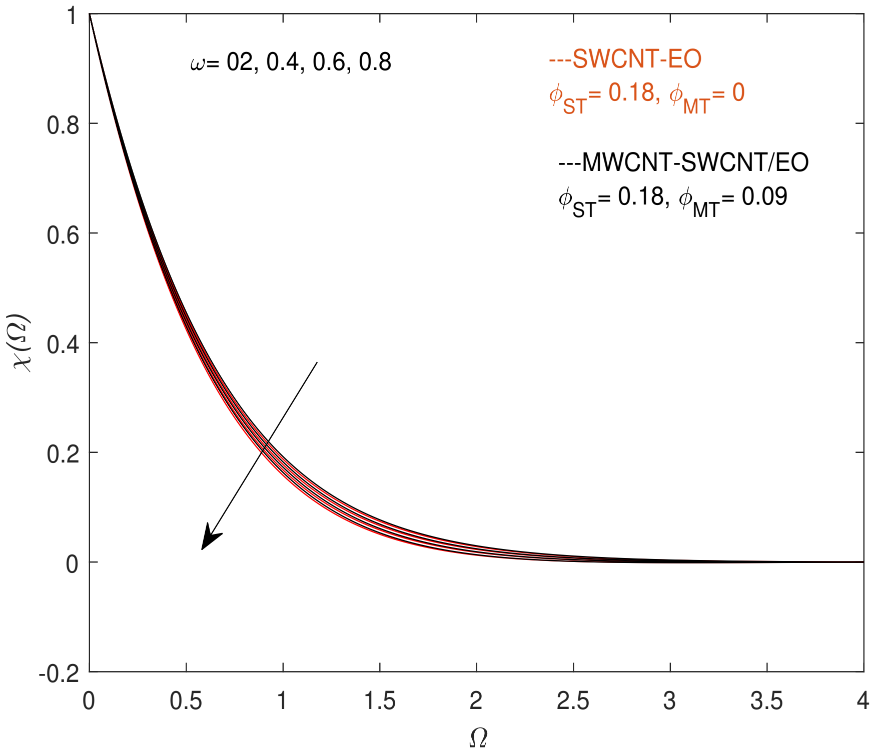

FIGURE 4.4: Impact of Motile against ω

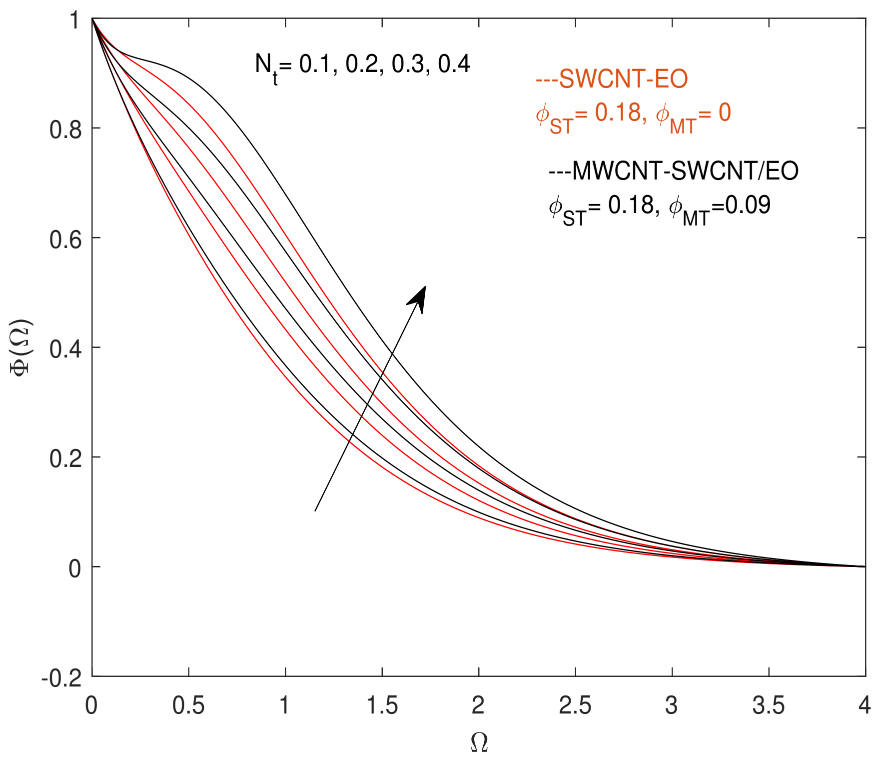

FIGURE 4.5: Impact of concentration against N_t

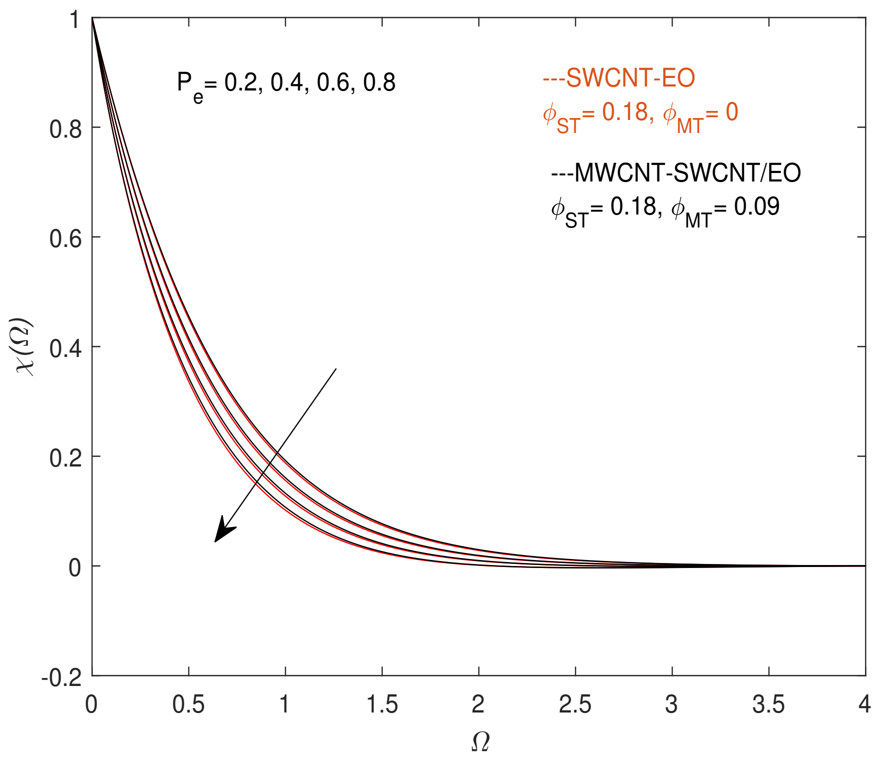

FIGURE 4.6: Impact of Motile against P_e

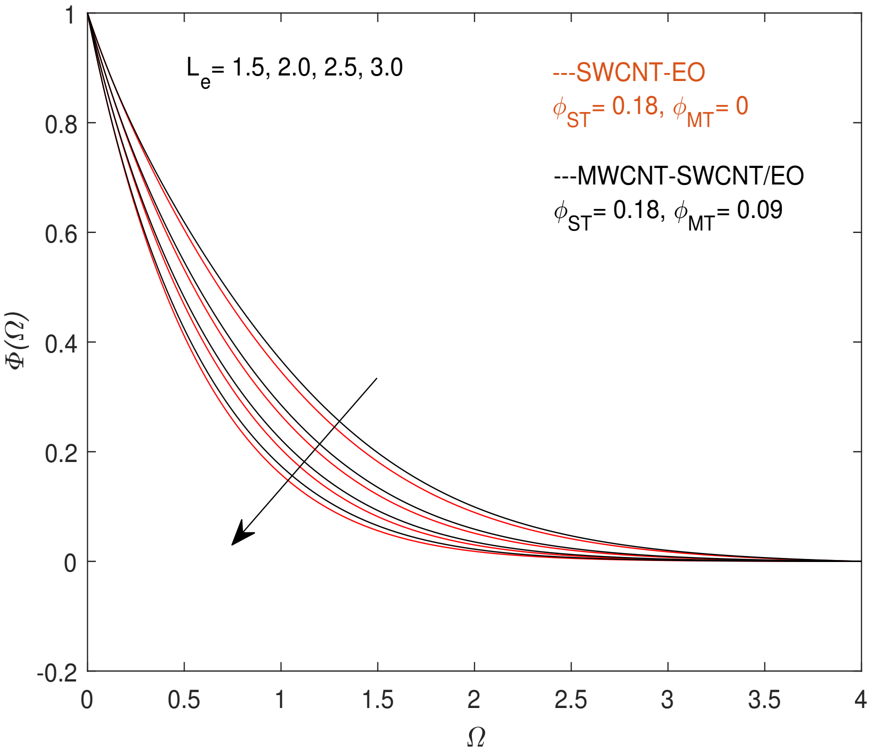

FIGURE 4.7: Impact of concentration against $\mathcal{L}_e$

Chapter 5

Conclusion

In this work, article of Jamshed et al. [23] is reviewed and the work is extended with the effect of chemical reaction, bio convection lewis number, brownian motion and thermophoresis. First of all, momentum, energy concentration and motile microorganism equations are converted into the ODEs by using similarity transformations. The transformed ODEs have a numerical solution that has been found using the shooting technique. Using different values of the physical parameters, the results are given in the form of tables and graphs. Some important observation about the flow problem are stated here to conclude the whole research.

i. Increased value of A_1^* reduce the viscosity which inturns reduce resistance while increasing fluid velocity

ii. In comparison to SWCNT/EO nanofluid, the hybrid nanofluid moves slowly across the porous medium. Due to the porous medium K_ς the flow is slowed down and surface needs more time to absorb the heat.

iii. Increasing the value of velocity slip variable A_ς velocity, temperature and entropy profile decreases.

iv. By increasing values of B_ς, the entropy profile N_G is increased. The Brinkman number (B_ς) are used to depicts the heat generated by viscous properties as viscous properties increase the generated heat. Ability of such viscous properties enhanced heat that promotes entropy generation in system.

v. Increased values of A_1^* and A_2^* reduce the skin friction for MWCNT with base fluid EO.

vi. By increasing values of Biot number H_ς, Nusselt number also increases for MWCNT-SWCNT/EO.

vii. As the values of chemical reaction parameter γ increases the concentration profile decreases. MWCNT-SWCNT/EO hybrid nanofluid have higher concentration profile than SWCNT-EO nanofluid.

viii. By increasing value of bioconvection lewis number $\mathcal{L}_b$ motile microorganism profile decrease.

Bibliography

[1] T. Aziz, A. Fatima, C. Khalique, and F. Mahomed, "Prandtl's boundary layer equation for two-dimensional flow: exact solutions via the simplest equation method," *Mathematical Problems in Engineering*, vol. 2013, 2013.

[2] M. Hussain, A. Ghaffar, A. Ali, A. Shahzad, K. S. Nisar, M. Alharthi, and W. Jamshed, "MHD thermal boundary layer flow of a Casson fluid over a penetrable stretching wedge in the existence of nonlinear radiation and convective boundary condition," *Alexandria Engineering Journal*, vol. 60, no. 6, pp. 5473–5483, 2021.

[3] H. Abedi, S. Sarkar, and H. Johansson, "Numerical modelling of neutral atmospheric boundary layer flow through heterogeneous forest canopies in complex terrain (a case study of a swedish wind farm)," *Renewable Energy*, vol. 180, pp. 806–828, 2021.

[4] Z. Long, L. Liu, S. Yang, L. Feng, and L. Zheng, "Analysis of marangoni boundary layer flow and heat transfer with novel constitution relationships," *International Communications in Heat and Mass Transfer*, vol. 127, p. 105523, 2021.

[5] H. Hanif, "A computational approach for boundary layer flow and heat transfer of fractional Maxwell fluid," *Mathematics and Computers in Simulation*, vol. 191, pp. 1–13, 2022.

[6] A. Ali, M. Awais, A. Al-Zubaidi, S. Saleem, and D. K. Marwat, "Hartmann boundary layer in peristaltic flow for viscoelastic fluid: Existence," *Ain Shams Engineering Journal*, vol. 13, no. 2, p. 101555, 2022.

[7] S. Suresh, K. Venkitaraj, P. Selvakumar, and M. Chandrasekar, "Synthesis of $Al2O3 - Cu$/water hybrid nanofluids using two step method and its thermo physical properties," *Colloids and Surfaces A: Physicochemical and Engineering Aspects*, vol. 388, no. 1-3, pp. 41–48, 2011.

[8] Ç. Yıldız, M. Arıcı, and H. Karabay, "Comparison of a theoretical and experimental thermal conductivity model on the heat transfer performance of $Al2O3 - SiO2$/water hybrid-nanofluid," *International Journal of Heat and Mass Transfer*, vol. 140, pp. 598–605, 2019.

[9] I. Waini, A. Ishak, and I. Pop, "Flow and heat transfer along a permeable stretching/shrinking curved surface in a hybrid nanofluid," *Physica Scripta*, vol. 94, no. 10, p. 105219, 2019.

[10] M. A. Qureshi, S. Hussain, and M. A. Sadiq, "Numerical simulations of MHD mixed convection of hybrid nanofluid flow in a horizontal channel with cavity: Impact on heat transfer and hydrodynamic forces," *Case Studies in Thermal Engineering*, vol. 27, p. 101321, 2021.

[11] F. Mabood and A. Akinshilo, "Stability analysis and heat transfer of hybrid $Cu - Al2O3/H2O$ nanofluids transport over a stretching surface," *International Communications in Heat and Mass Transfer*, vol. 123, p. 105215, 2021.

[12] A. Dogonchi and D. Ganji, "Impact of Cattaneo-Christov heat flux on MHD nanofluid flow and heat transfer between parallel plates considering thermal radiation effect," *Journal of the Taiwan Institute of Chemical Engineers*, vol. 80, pp. 52–63, 2017.

[13] N. Muhammad, S. Nadeem, and T. Mustafa, "Squeezed flow of a nanofluid with Cattaneo–Christov heat and mass fluxes," *Results in Physics*, vol. 7, pp. 862–869, 2017.

[14] H. Waqas, T. Muhammad, S. Noreen, U. Farooq, and M. Alghamdi, "Cattaneo-Christov heat flux and entropy generation on hybrid nanofluid flow in a nozzle of rocket engine with melting heat transfer," *Case Studies in Thermal Engineering*, vol. 28, p. 101504, 2021.

[15] S.-R. Yan, D. Toghraie, L. A. Abdulkareem, A. Alizadeh, P. Barnoon, and M. Afrand, "The rheological behavior of $MWCNTs - Zno$/water–ethylene glycol hybrid non-newtonian nanofluid by using of an experimental investigation," *Journal of Materials Research and Technology*, vol. 9, no. 4, pp. 8401–8406, 2020.

[16] M. H. Esfe, S. Esfandeh, M. H. Kamyab, and D. Toghraie, "Analysis of rheological behavior of $MWCNT - Al2O3$ (10: 90)/5w50 hybrid non-newtonian nanofluid with considering viscosity as a three-variable function," *Journal of Molecular Liquids*, vol. 341, p. 117375, 2021.

[17] J. Madhukesh, R. N. Kumar, R. P. Gowda, B. Prasannakumara, G. Ramesh, M. I. Khan, S. U. Khan, and Y.-M. Chu, "Numerical simulation of $AA7072 - AA7075$/water-based hybrid nanofluid flow over a curved stretching sheet with newtonian heating: A non-fourier heat flux model approach," *Journal of Molecular Liquids*, vol. 335, p. 116103, 2021.

[18] A. Hussain, M. Malik, M. Awais, T. Salahuddin, and S. Bilal, "Computational and physical aspects of MHD Prandtl-Eyring fluid flow analysis over a stretching sheet," *Neural Computing and Applications*, vol. 31, no. 1, pp. 425–433, 2019.

[19] Y.-M. Li, M. I. Khan, S. A. Khan, S. U. Khan, Z. Shah, and P. Kumam, "An assessment of the mathematical model for estimating of entropy optimized viscous fluid flow towards a rotating cone surface," *Scientific Reports*, vol. 11, no. 1, pp. 1–15, 2021.

[20] R. R. Sahoo, "Thermo-hydraulic characteristics of radiator with various shape nanoparticle-based ternary hybrid nanofluid," *Powder technology*, vol. 370, pp. 19–28, 2020.

[21] U. Rashid, H. Liang, H. Ahmad, M. Abbas, A. Iqbal, and Y. Hamed, "Study of ($Ag\ and\ TiO2$)/water nanoparticles shape effect on heat transfer and hybrid nanofluid flow toward stretching shrinking horizontal cylinder," *Results in Physics*, vol. 21, p. 103812, 2021.

[22] S. A. A. Shah, N. A. Ahammad, E. M. T. E. Din, F. Gamaoun, A. U. Awan, and B. Ali, "Bio-convection effects on Prandtl hybrid nanofluid flow with chemical reaction and motile microorganism over a stretching sheet," *Nanomaterials*, vol. 12, no. 13, p. 2174, 2022.

[23] W. Jamshed, D. Baleanu, N. A. A. M. Nasir, F. Shahzad, K. S. Nisar, M. Shoaib, S. Ahmad, and K. A. Ismail, "The improved thermal efficiency of Prandtl-Eyring hybrid nanofluid via classical keller box technique," *Scientific reports*, vol. 11, no. 1, pp. 1–24, 2021.

[24] Y. Cengel and J. Cimbala, *Ebook: Fluid Mechanics Fundamentals and Applications (SI units).* McGraw Hill, 2013.

[25] R. Bansal, *A Textbook of Fluid Mechanics and Hydraulic Machines:(in SI Units).* Laxmi Publications, Ltd., 2005.

[26] S. K. Das, S. U. Choi, W. Yu, and T. Pradeep, *Nanofluids: science and technology.* John Wiley & Sons, 2007.

[27] H. M. Ali, *Hybrid nanofluids for convection heat transfer.* Academic Press, 2020.

[28] S. S. Molokov, R. Moreau, and H. K. Moffatt, *Magnetohydrodynamics: Historical evolution and trends*, vol. 80. Springer Science & Business Media, 2007.

[29] C. Kothandaraman, *Fundamentals of heat and mass transfer.* New Age International, 2006.

[30] M. A. Qureshi, "A case study of MHD driven Prandtl-Eyring hybrid nanofluid flow over a stretching sheet with thermal jump conditions," *Case Studies in Thermal Engineering*, vol. 28, p. 101581, 2021.

[31] J. N. Reddy and D. K. Gartling, *The finite element method in heat transfer and fluid dynamics.* CRC press, 2010.

[32] J. Kunes, *Dimensionless physical quantities in science and engineering.* Elsevier, 2012.

[33] B. Lautrup, *Physics of continuous matter: exotic and everyday phenomena in the macroscopic world*. CRC press, 2011.

[34] K. S. Mekheimer and S. F. Ramadan, "New insight into gyrotactic microorganisms for bio-thermal convection of Prandtl nanofluid over a stretching/shrinking permeable sheet," *SN Applied Sciences*, vol. 2, no. 3, pp. 1–11, 2020.

[35] A. Aziz, W. Jamshed, and T. Aziz, "Mathematical model for thermal and entropy analysis of thermal solar collectors by using Maxwell nanofluids with slip conditions, thermal radiation and variable thermal conductivity," *Open Physics*, vol. 16, no. 1, pp. 123–136, 2018.

[36] A. U. Yahya, N. Salamat, W.-H. Huang, I. Siddique, S. Abdal, and S. Hussain, "Thermal charactristics for the flow of Williamson hybrid nanofluid ($mos2 + zno$) based with engine oil over a streched sheet," *Case Studies in Thermal Engineering*, vol. 26, p. 101196, 2021.